STATE OF WASHINGTON

Daniel J. Evans, Governor

DEPARTMENT OF ECOLOGY

John A. Biggs, Director

Water-Supply Bulletin 40

DIGITAL-MODEL STUDY OF GROUND-WATER HYDROLOGY, COLUMBIA BASIN IRRIGATION PROJECT AREA, WASHINGTON

By

H. H. Tanaka, A. J. Hansen, Jr., and J. A. Skrivan

Prepared in cooperation with

U. S. GEOLOGICAL SURVEY

1974

STATE OF WASHINGTON

Daniel J. Evans, Governor

DEPARTMENT OF ECOLOGY

John A. Biggs, Director

Water-Supply Bulletin 40

DIGITAL-MODEL STUDY OF GROUND-WATER HYDROLOGY, COLUMBIA BASIN IRRIGATION PROJECT AREA, WASHINGTON

By

H. H. Tanaka, A. J. Hansen, Jr., and J. A. Skrivan

Prepared in cooperation with

U. S. GEOLOGICAL SURVEY

1974

CONTENTS

	Page
Abstract	1
Introduction	2
Purpose and scope	2
Previous investigations	2
Acknowledgments	3
Physical features and geographic provinces	5
Climate	6
Geologic setting	6
Yakima Basalt	6
Unconsolidated deposits	9
Ringold Formation	10
Glaciofluvial deposits	10
The aquifer system	10
Hydraulic characteristics	10
Yakima Basalt	10
Unconsolidated deposits	12
Ringold Formation	12
Glaciofluvial deposits	12
Physical and hydrologic boundaries	12
Yakima Basalt (lower aquifer)	12
Unconsolidated deposits (upper aquifer)	12
Internal boundaries	13
Head distribution before irrigation	13
Upper aquifer	13
Lower aquifer	13
Head distribution since irrigation	13
Upper aquifer	13
Lower aquifer	13
The digital model	14
Method of analysis	16
Mathematical description	20
Steady-state analysis	20
Boundary conditions	23
Recharge from precipitation	23
Discharge by evapotranspiration	23
Vertical flow between aquifers	23
Quincy model	24
Special boundary conditions	24
Lakes	24
Streams	24
Springs	24
Lateral flow in the upper aquifer	24
Lateral flow in the lower aquifer	24
Results	25
Head maps of the upper and lower aquifers	25
Inflow and outflow	25
Pasco model	25
Special boundary conditions	25
Streams	25
Lateral flow in the upper aquifer	25
Lateral flow in the lower aquifer	25
Results	25
Head maps of the upper and lower aquifers	25
Inflow and outflow	26

Royal model . . . 28
Special boundary conditions . . . 29
No flow . . . 29
Streams . . . 29
Lateral flow in the lower aquifer . . . 30
Results . . . 30
Head map in the lower aquifer . . . 30
Inflow and outflow . . . 31
Transient models . . . 31
Manmade stresses . . . 31
Recharge from irrigation . . . 32
Expansion of saturated areas . . . 32
Recharge from canal and lateral leakage . . . 32
Discharge by wasteways and drains . . . 36
Increased discharge by evapotranspiration . . . 39
Discharge by pumping wells . . . 40
Quincy model . . . 40
Special boundary condition . . . 40
Potholes Reservoir . . . 40
Results . . . 40
Head maps of the upper and lower aquifers . . . 40
Change in aquifer storage . . . 40
Pasco model . . . 41
Special boundary condition . . . 41
Scooteney Reservoir . . . 41
Results . . . 42
Head maps of the upper and lower aquifers . . . 42
Change in aquifer storage . . . 42
Royal model . . . 44
Results . . . 44
Head maps of the upper and lower aquifers . . . 44
Change in aquifer storage . . . 45
Summary and conclusions . . . 47
References cited . . . 60

ILLUSTRATIONS

Page

FIGURES 1-5. Maps showing:
- 1. Location of study area . . . 2
- 2. Physiographic features in the study area . . . 4
- 3. Topography of the Columbia Basin Irrigation Project area . . . 5
- 4. Precipitation in the study area . . . 7
- 5. Generalized geology and typical section of the study area . . . 9

6. Diagrammatic section of the upper and lower aquifers . . . 12

7-10. Maps showing:
- 7. Preirrigation head in upper aquifer . . . 14
- 8. Preirrigation head in lower aquifer . . . 15
- 9. Head in the upper aquifer in 1963 . . . 16
- 10. Head in the upper aquifer in 1968 . . . 17

11. Hydrographs of selected wells in the upper and lower aquifers . . . 18
12. Map showing head in the lower aquifer in 1963 . . . 19
13. Map showing head in the lower aquifer in 1968 . . . 21
14. Map showing outlines of the Quincy, Pasco, and Royal model areas . . . 22

15-19. Maps showing preirrigation computed and measured heads:
- 15. In the upper aquifer of the Quincy model . . . 26
- 16. In the lower aquifer of the Quincy model . . . 27
- 17. In the upper aquifer of the Pasco model . . . 28
- 18. In the lower aquifer of the Pasco model . . . 29
- 19. In the lower aquifer of the Royal model . . . 30

20. Map showing irrigation blocks and first-year water application . . . 33
21. Map showing main canals and wasteways . . . 34
22. Map of laterals and wasteways in Block 75 . . . 35

23-26. Graphs showing:
- 23. Relation of seepage rate to wetted perimeter of canals and laterals . . . 36
- 24. Leakage from canals and laterals . . . 37
- 25. Relation of drainage from tile drains and wasteways to depth to water . . . 38
- 26. Relation of evapotranspiration rate to depth to water . . . 39

27. Hydrograph of Potholes Reservoir . . . 41
28. Map showing computed and measured heads in the upper aquifer of the Quincy model in 1968 . . . 42
29. Map showing computed and measured heads in the lower aquifer of the Quincy model in 1968 . . . 43
30. Graph showing cumulative storage increase in the upper and lower aquifers of the Quincy model . . . 44
31. Graph showing relationship of water storage versus time of the Quincy model aquifers . . . 45

32-35. Maps showing:
- 32. Distribution of water added to storage in the upper aquifer of the Quincy model, 1952-68 . . . 46
- 33. Distribution of water added to storage in the lower aquifer of the Quincy model, 1952-68 . . . 47
- 34. Computed and measured heads in the upper aquifer of the Pasco model in 1968 . . . 48
- 35. Computed and measured heads in the lower aquifer of the Pasco model in 1968 . . . 49

36. Graph showing cumulative storage increase in the upper and lower aquifers of the Pasco model . . . 50
37. Graph showing relationship of water storage versus time of the Pasco model aquifers . . . 51

FIGURES 38-41. Maps showing:
38 Distribution of water added to storage in the upper aquifer of the Pasco model, 1952-68 52
39. Distribution of water added to storage in the lower aquifer of the Pasco model, 1952-68 53
40. Computed and measured heads in the upper aquifer of the Royal model in 1968 54
41. Computed and measured heads in the lower aquifer of the Royal model in 1968 55
42. Graph showing cumulative storage increase in the upper and lower aquifers of the Pasco model 56
43. Graph showing relationship of water storage versus time for the Royal model aquifers 57
44. Map showing distribution of water added to storage in the upper aquifer of the Royal model, 1952-68 58
45. Map showing distribution of water added to storage in the lower aquifer of the Royal model, 1952-68 59

TABLES

Pages

TABLE 1. Major stratigraphic units and their water-yielding characteristics 8
2. Transmissivity of basalt based on specific-capacity test of selected wells in project area 11
3. Hydraulic conductivity and storage coefficient of Ringold Formation and glaciofluvial deposits in the Hanford area 11
4. Quantity of water applied on irrigated acres during the period 1952-67 32

DIGITAL-MODEL STUDY OF GROUND-WATER HYDROLOGY, COLUMBIA BASIN IRRIGATION PROJECT AREA, WASHINGTON

By H. H. Tanaka, A. J. Hansen, Jr., and J. A. Skrivan

ABSTRACT

Since 1952 water diverted from the Columbia River at Grand Coulee Dam has been used to irrigate parts of the Columbia Basin Irrigation Project area in eastern Washington, and as a result ground-water levels generally have risen in the area. The rapid increases in ground-water inflow, outflow, and storage from irrigation have created a need for a better understanding of the ground-water system before and after the start of irrigation to establish guidelines necessary for management of the area's ground-water resource. Data and information from previous geologic and hydrologic studies were used as a basis for quantitative analyses of ground-water inflow and outflow by means of digital computer models representing three major areas—Quincy Basin, Pasco Basin, and Royal Slope.

The digital computer models were designed to simulate the hydraulic-head response to natural or man-made stresses in the two-aquifer system underlying the area. The two-aquifer system is described as an unconfined upper aquifer (clay, silt, sand, and gravel in varying amounts) overlying a confined lower aquifer (basalt), separated by a leaky confining layer. The steady-state model analyzes conditions before irrigation (1952) when inflow and outflow to the aquifer system were essentially in balance and the transient model analyzes conditions during the first 16 years of irrigation (1952-67), when rapid hydrologic changes were taking place in the aquifer system.

Data required for the steady-state simulation of the hydrologic system included transmissivity of the lower aquifer, hydraulic conductivity of the upper aquifer, vertical permeability of the confining layer, recharge from rainfall, and special boundary conditions. The steady-state analysis simulated the measured pre-irrigation heads in both aquifers after the initial hydraulic characteristics and natural boundary conditions of the aquifers simulated in the model had been adjusted. Steady-state digital computations show that, for the Quincy model, annual inflow and outflow from both aquifers totaled 105,000 acre-feet, and average annual recharge from precipitation to both aquifers was 11,000 acre-feet; for the Pasco model, inflow and outflow from both aquifers totaled 28,700 acre-feet, and average annual recharge from precipitation to both aquifers was 5,200 acre-feet; for the Royal model, annual inflow and outflow from the lower aquifer totaled 14,800 acre-feet and average annual recharge from precipitation to the lower aquifer was 1,300 acre-feet.

Additional data required for the transient analysis included recharge from irrigation and from leakage from canals and laterals, discharge from wasteways and drains, from evapotranspiration, and from pumpage by wells, and special boundary conditions. The transient analysis for the period 1952-68 simulated heads for 1958, 1963, and 1968 for both aquifers after adjustments had been made for all the artificial hydrologic stresses and special boundary conditions associated with irrigation simulated in the model. Results of the transient analysis indicate that the cumulative storage of water between 1952-68 for the Quincy model was about 2.7 million acre-feet in the upper aquifer and about 29 thousand acre-feet in the lower aquifer; for the Pasco model it was about 3.8 million acre-feet in the upper aquifer and about 23 thousand acre-feet in the lower aquifer; and for the Royal model it was about 750 thousand acre-feet in the upper aquifer and about 14 thousand acre-feet in the lower aquifer.

INTRODUCTION

Purpose and Scope

The area of this report covers about 3,600 square miles in east-central Washington (fig. 1). The boundaries correspond roughly to the boundaries of the U.S. Bureau of Reclamation's Columbia Basin Irrigation Project (CBIP) in parts of Grant, Adams, and Franklin Counties, Washington.

Since 1952 water diverted from the Columbia River at Grand Coulee Dam has been used to irrigate parts of the CBIP and, as a result, ground-water levels generally have risen in the project area. The rapid increase in ground-water inflow, outflow, and storage from irrigation created a need for a better understanding of the ground-water system before and after the start of irrigation to establish necessary guidelines to manage the ground-water resource by the State of Washington. This study uses the data and information from previous geologic and hydrologic studies as a basis for a mathematical model, designed for use with a digital computer, to simulate the ground-water flow system under pre-irrigation conditions and the relation between past irrigation and past water levels in the project area. Once past water levels could reasonably be simulated with known input stresses, it would be possible to simulate future water levels with proposed stresses on the digital-computer model.

Previous Investigations

The first detailed investigation of the ground-water resources of a part of the project area was made by Schwennesen and Meinzer (1918). Earlier reports by others were mainly reconnaissance in nature. The report by Schwennesen and Meinzer describes the geologic units and their water-bearing properties, and includes a small-scale contour map of the water table in the Quincy Basin. In 1940 the U.S. Geological Survey, in cooperation with the State of Washington Department of Conservation, Division of Water Resources, began a ground-water investigation in the CBIP area. Data obtained during the period 1939-42 were compiled and assembled in three reports. The first report (Taylor, 1941) presents a summary of ground-water conditions in the project area, the second report (Taylor, 1944) contains water-level data collected through 1942, and the third report (Taylor, 1948) compiles the basic hydrologic data collected to 1947 and describes the geology and water-bearing char-

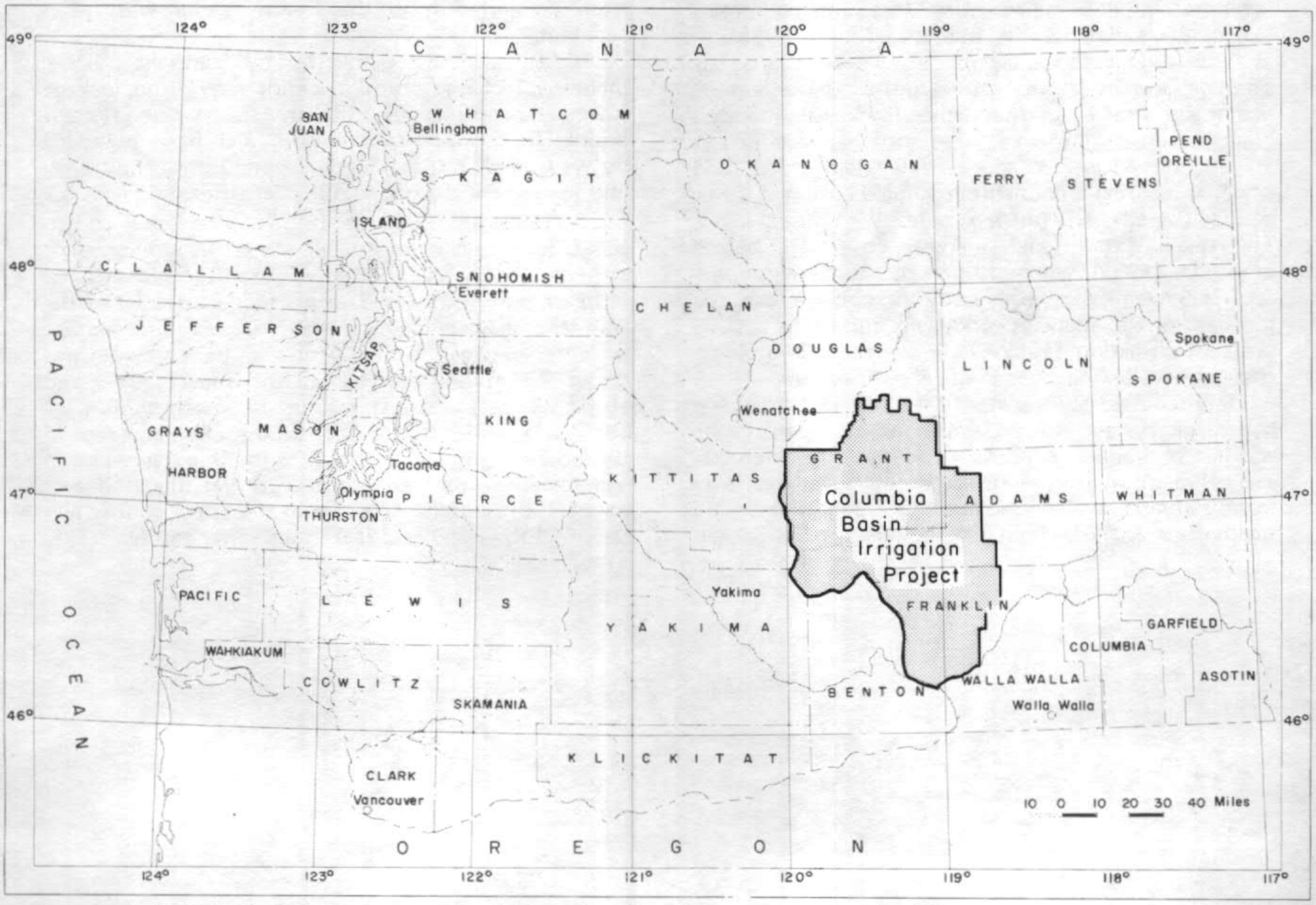

FIGURE 1.—Location of study area.

acteristics of the principal rock units in the project area. The first complete reconnaissance geologic map of the project area accompanies the third report. A report by Mundorff and others (1952) tabulates all well data collected since Taylor's reports, describes the occurrence and movement of ground water in relation to the geologic structural features in the project area, and includes water-table and basalt-surface contour maps of the Quincy Basin. A report by Walters and Grolier (1960) tabulates all well data and lists hydrographs and drillers' logs of selected wells in the project area. A geologic map and sections by Grolier and Bingham (1971) show the details of the structures and stratigraphy of the study area.

Acknowledgments

Acknowledgment is made of the cooperation and assistance of the U.S. Bureau of Reclamation, Ephrata, Washington, for providing the engineering and hydrologic data on irrigation in the Columbia Basin Irrigation Project area. P. A. Eddy, of the Washington Department of Ecology, assisted in the compilation and analysis of data from 1968 to 1970. Programming specialists of the U.S. Geological Survey provided invaluable technical assistance during the formulation and analysis of the digital models.

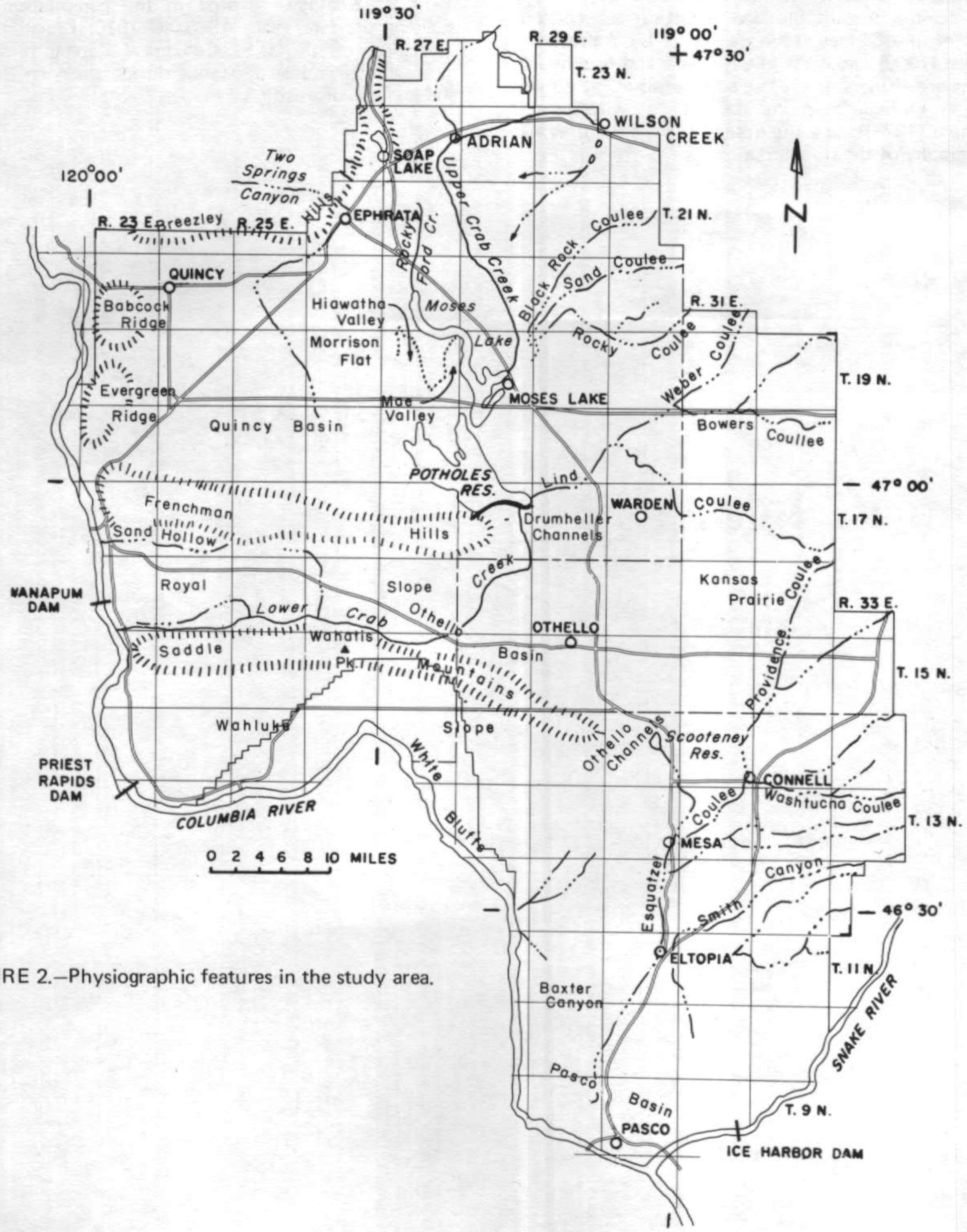

FIGURE 2.—Physiographic features in the study area.

The physiographic features (fig. 2) of the CBIP area include several broad, east-west trending synclinal basins and anticlinal ridges, transected in some areas by stream channels, flat-bottomed coulees and scabland tracts. These erosional features are products of erosion by glacial melt-water rivers and floods during the Pleistocene Epoch (Bretz, 1930). Land-surface altitudes range from about 350 feet near Pasco to about 2,700 feet at Wahatis Peak on Saddle Mountains (figs. 2 and 3).

The eastern part of the area is a loess-mantled upland that in places has been dissected into many flat-bottomed coulees whose floors merge with the basins and plains to the west. The western and southern parts of the area include several broad basins and plains. Among these are the glaciofluvial gravel plain in the Quincy and Pasco Basins, the largely dune-covered lacustrine plain in the Quincy Basin, and the plains formed of the Ringold formation in the Othello and Pasco Basins.

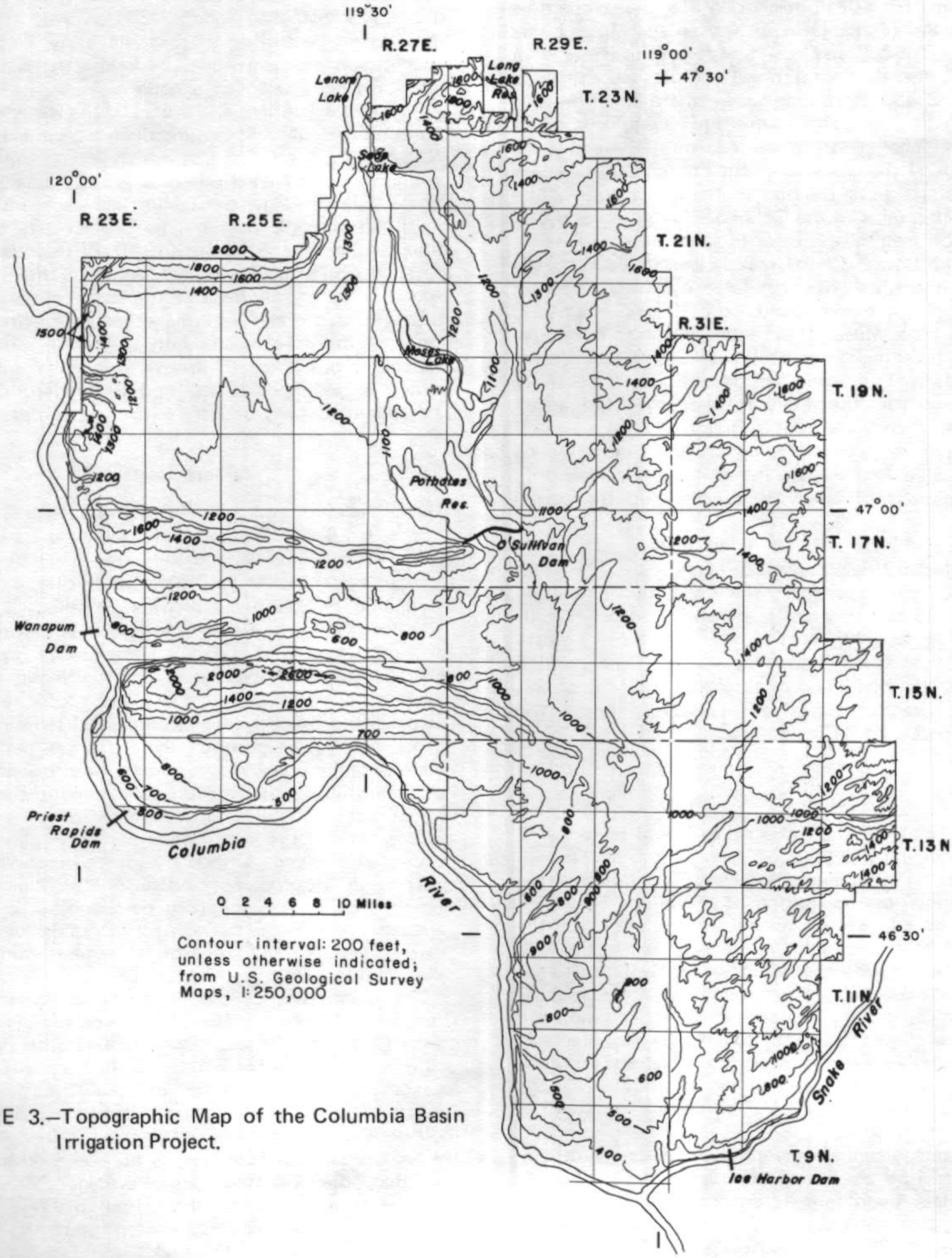

FIGURE 3.–Topographic Map of the Columbia Basin Irrigation Project.

The Quincy Basin in the northwestern part of the study area (fig. 2) is drained by Lower Crab Creek. The creek flows generally westward into the basin from the northeastern boundary of the project area to Adrian, where it continues in a southeasterly direction to Moses Lake. This reach of the stream is known as Upper Crab Creek. The flow of Crab Creek upstream from Wilson Creek is perennial, but below Wilson Creek it disappears into the gravels and the flow was intermittent to Moses Lake before 1952. Since then, return flow from CBIP irrigation water caused the flow to become perennial between Adrian and Moses Lake.

Before 1952, Crab Creek flowed southeasterly from an outlet near the southern end of Moses Lake through a scabland and sand-dune area, where the flow was augmented by discharge from springs along Drumheller Channels. The creek continued southerly about 15 miles around the east end of the Frenchman Hills, and then westerly along the base of the north slope of the Saddle Mountains to the Columbia River near Beverly. This reach from Moses Lake to the Columbia River is known as Lower Crab Creek. Flow in Lower Crab Creek, although slightly regulated by water levels on Moses Lake, was perennial before 1952. Since 1952, overflow from Moses Lake enters Potholes Reservoir, and the perennial flow of Lower Crab Creek downstream from O'Sullivan Dam depends almost entirely on seepage from the reservoir, discharge from wasteways, and return flow from irrigation.

All other streams, including those in Lind, Bowers, and Esquatzel Coulees, are intermittent and flow only during periods of heavy rain or during the spring runoff.

Moses Lake is about 14 miles long and from one-quarter to three-quarters of a mile wide. The north half of the lake is relatively shallow, with a maximum depth of 38 feet near the south end (Wolcott, 1964). In addition to flow from Upper Crab Creek, Moses Lake receives water from Rocky Ford Creek, which flows into the north end of the lake. The flow of this stream is supplied almost entirely by springs at the head of Rocky Ford Creek, in sec. 6, T. 21 N., R. 27 E.

CLIMATE

The climate of the project area is arid to semiarid. Average annual precipitation ranges from less than 6 inches to a little over 10 inches, and most of the precipitation occurs during the winter. The areal distribution of average annual precipitation for the period of record at nine stations is shown in figure 4. Precipitation during the winter generally falls as light rain or as snow which may accumulate as much as 12 inches on the ground. Chinook winds are common and cause rapid snowmelt; this in turn results in appreciable surface runoff when the ground is frozen. The mean annual temperatures recorded in the study area range from 9°C (Celsius) or 48.4°F at Moses Lake to 12°C (54.5°F) at Wahluke.

The average annual evaporation (Kohler and others, 1951, pls. 1-5) as measured from a U.S. Weather Bureau Class A pan, ranges from about 50 to 70 inches. Lake evaporation is about 70 percent of the Class A pan values, or 35 to 50 inches. About 80 percent of this evaporation occurs during the period May through October.

GEOLOGIC SETTING

The major geologic events that influenced the lithologic and structural control of ground water in the project area were (1) the extrusion of basaltic lavas in the Miocene and early Pliocene Epochs, (2) tectonic deformation of the basalt flows during the Pliocene and early Pleistocene Epochs, (3) lacustrine, fluviatile, and eolian deposition during the early Pleistocene Epoch, and (4) glaciofluvial erosion and deposition during the late Pleistocene Epoch.

The major stratigraphic units and the water-yielding characteristics of wells tapping them are summarized in table 1. Structural features which exert control on ground-water movement in the project area are discussed later in the description of each model. A simplified geologic map of the project area adapted from Grolier and Bingham (1971) differentiates the gravel deposits in the upper aquifers (fig. 5). This separation is shown because the hydraulic characteristics between gravel and the other sediments in the upper aquifer are significantly different. The areas mapped as basalt are arbitrarily assigned a thin overburden of sediment (20 ft or less) to permit lateral hydraulic continuity over the entire model area.

Yakima Basalt

The Yakima Basalt of the Columbia River Group is a thick sequence of basalt flows which underlies the entire project area. Generally, the basalt is quite permeable and, under favorable conditions, is capable of yielding large quantities of water to wells.

Water occurs mostly in the tabular zone along the tops and bottoms of individual flows. The flow tops generally are permeable because of their highly jointed nature, the presence of cinders and rubble, and the existence of vesicular cavities connected by joints and cracks. The lower parts of the flows are permeable where irregular openings are present, or in places where lava deposited in water forms a characteristic pillowlike broken zone. Many of these pillow zones are continuous over large areas and are very permeable. Connected openings formed by joints, cracks, broken zones, and incomplete closure of the rough and irregular surface of one flow over another create a permeable zone along the contact favorable for lateral movement of water. A zone of this type is commonly called an interflow zone.

The thicknesses of individual basalt flows range from 20 to 100 feet in the project area. Mundorff and others (1952, p. 10) and Newcomb and others (1970, p. 22) reported that basalt flows in the nearby Hanford area range in thickness generally from 10 to 150 feet. Results of geophysical logging in a well near Hanford indicate that basalt flows between 1,000 and 10,000 feet below land surface average 68 feet in thickness, and that the interflow zones average 22 feet in thickness (Raymond and Tillson, 1968, p. 22).

The massive central part between interflow zones is less permeable because the rock usually is dense, and the movement of water mainly is restricted to vertical flow through joints and cracks formed as a result of rock shrinkage during the cooling process, or as a result of later tectonic stress. The degree of hydraulic connection between interflow zones can vary considerably, depending on the density of the basalt and the size of the openings in the joint and crack system. Usually the vertical joints and cracks in the center of the basalt flow are narrow and become tighter with depth because increased pressure from the weight of the overlying rock tends to close them.

In places, the basalt flows are interbedded with fine-grained sedimentary material of low permeability deposited during the period between successive flows. These interbeds, like the dense central part of basalt flows, retard the vertical movement of water between interflow zones, and perch or confine water in the interflow zone. The net result is many separate,

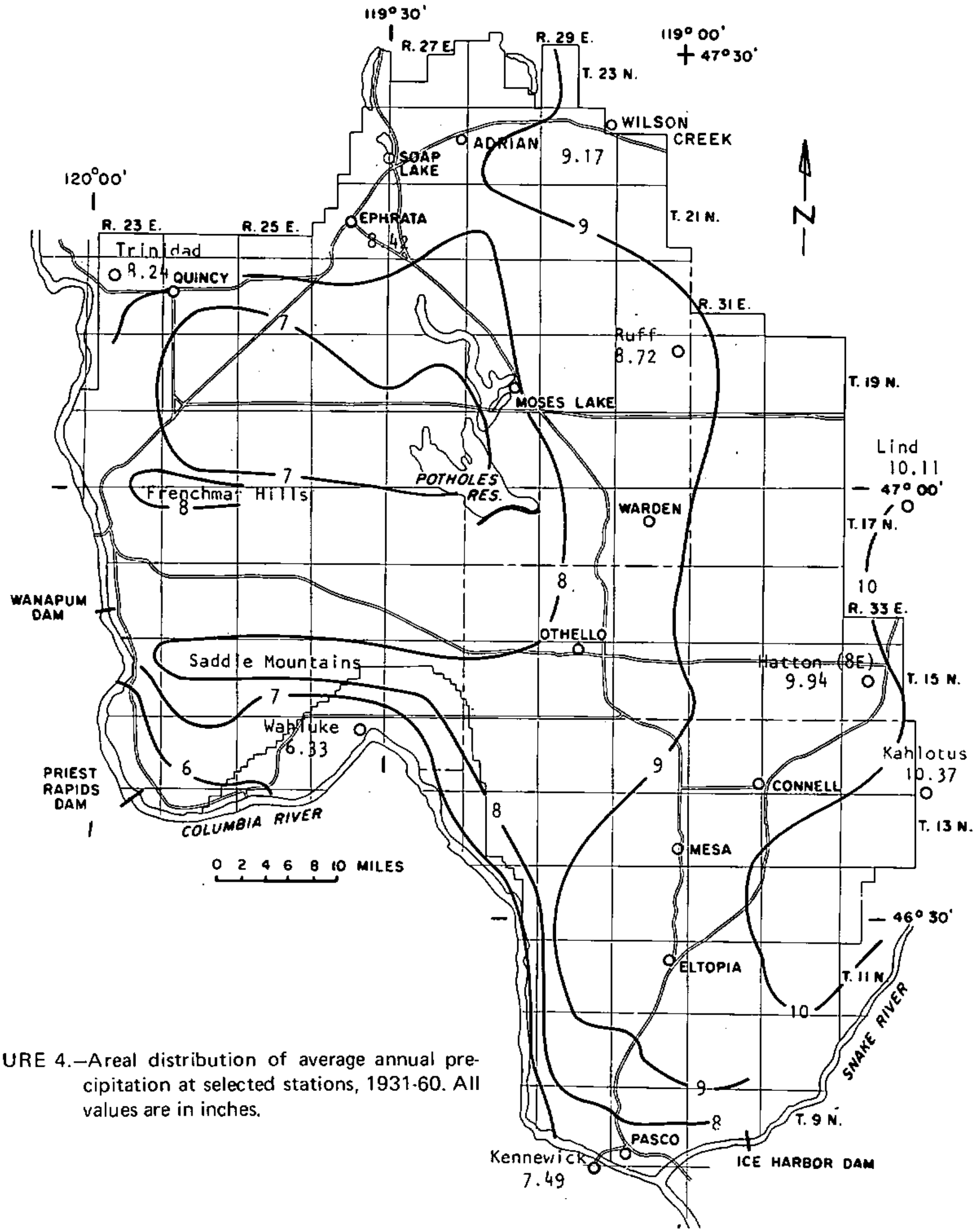

FIGURE 4.—Areal distribution of average annual precipitation at selected stations, 1931-60. All values are in inches.

TABLE 1.—Major stratigraphic units and their water-yielding characteristics

System	Series	Formation	Member, unit or lithology	Maximum thickness	Water-bearing characteristics of wells	Aquifer designation used in this report
Quarternary	Pleistocene	Glaciofluvial deposits	Gravel and sand	225	Yields from 100 to over 1,000 gpm can be expected.	Upper aquifer
		Ringold Formation	Sand and silt Conglomerate Clay	100 200 500	Yields vary from small (10 gpm) to large (1,000 gpm) depending on amount of silt or cementation. Specific capacities range from less than 1 to 75 gpm per foot of draw-down. Sand strata in clays may yield small amounts of water to wells.	
Tertiary	Pliocene or Miocene	Ellensberg Formation	Beverly Member (sand, clay, conglomerate, pumicite)	400	Hydraulic conductivity generally is low. Specific capacities range from less than 1 to 34 gpm per foot of drawdown.	
	Miocene	Yakima Basalt	Saddle Mountains Member Priest Rapids Member Roza Member Frenchman Springs Member Vantage Sandstone Member Lower Basalt	 200 200 375 35 1,000+	Well yields range from 1 to 2,400 gpm, with specific capacities from less than 1 to 712 gpm per foot of drawdown. Generally yields can be obtained from the lower basalt in wells penetrating below the Vantage Sandsone Member.	Lower aquifer

semiconfined, leaky aquifers with a different hydrostatic head in each interflow zone. The head measured in a basalt well is dependent, for the most part, on the depth of the well because the water level in the well reflects the composite head of the interflow zones penetrated by the well.

Unconsolidated Deposits

Lying above the basalt are unconsolidated sedimentary deposits consisting of stratified clay, silt, sand, and gravel. The material includes the Ringold Formation, glaciofluvial deposits, and loessal (wind-carried)

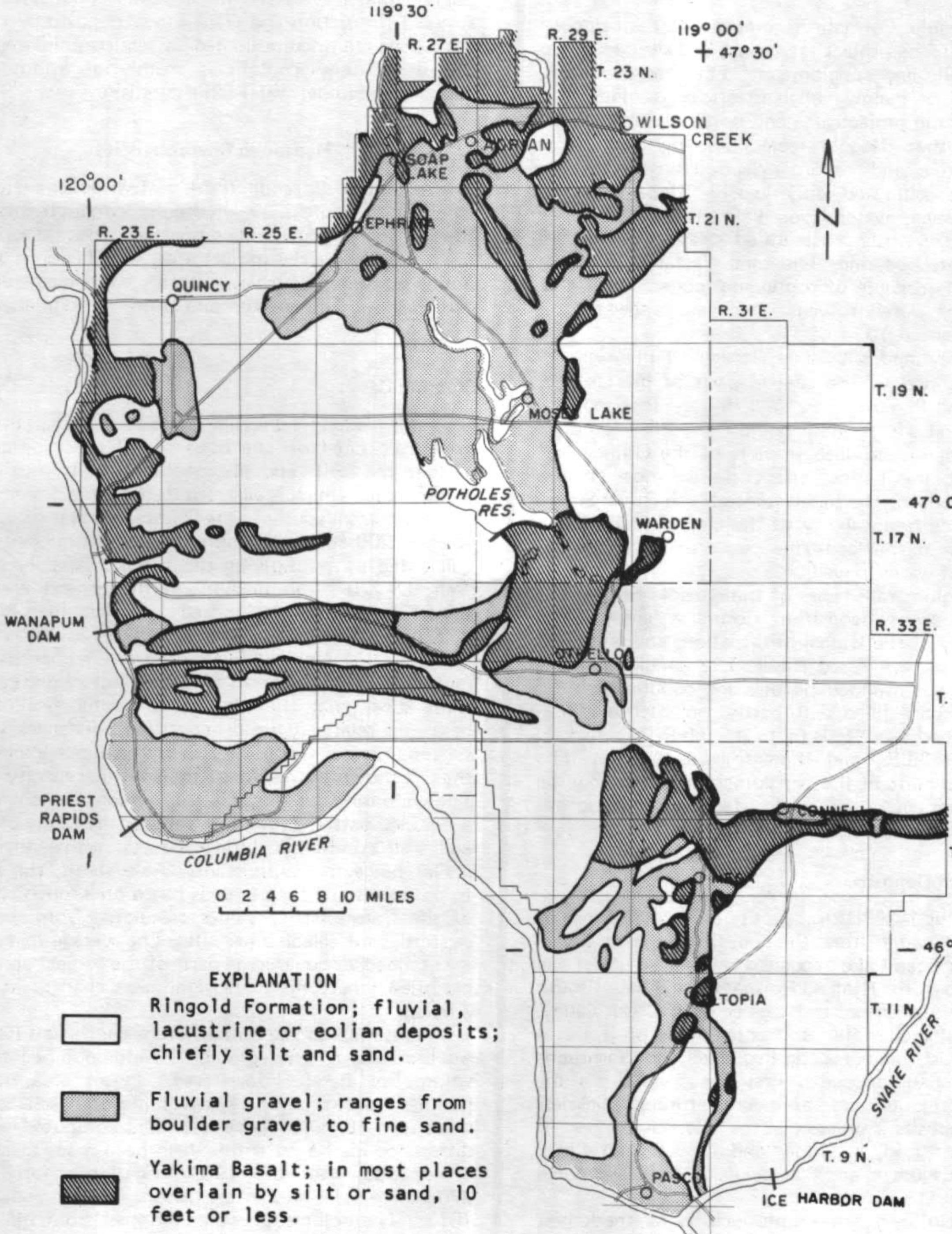

FIGURE 5.–Generalized geology of the study area. After Grolier and Bingham (1972).

deposits. Loess consisting mainly of silt and very fine sand are widespread over the project area, but is unimportant hydrologically because it usually is deposited as a relatively thin surface mantle, generally above the water table.

Ringold Formation

The Ringold Formation comprises three principal lithofacies in the project area: sand and silt, laminated clay and silt, and conglomerate. The sand-silt facies, believed to be mainly eolian in origin, is widespread throughout the project area and usually is interbedded with the other Ringold facies. The permeability is relatively low, and, before irrigation began, the deposits were saturated only locally. Since irrigation began, however, water levels have risen and in large areas the previously unsaturated sand-silt facies has become water bearing. The sand-silt facies in these areas now is capable of producing moderate to large quantities of water to wells. Thickness ranges from a few feet to about 100 feet.

The clay and silt facies, lacustrine in origin, is largely confined to the central parts of the Quincy, Othello, and Pasco Basins. Well drillers' logs indicate that clay and silt of the Ringold Formation comprise the material in the deepest parts of the Quincy and Pasco structural basins, and comprise most of the material overlying the basalt beneath the Royal Slope. Although the permeability of the clay and silt is low, sand strata in the lacustrine facies may yield small quantities of water to wells.

The conglomerate facies of the Ringold Formation, formed by stream deposition, occurs as lenses in the silt and clay of the Ringold Formation, and is limited to a part of the Pasco Basin. The conglomerate is formed of well-rounded pebbles and cobbles with the interstitial space filled with partly cemented medium- to fine-grained sand. It is more than 180 feet thick in T. 11 N., R. 29 E., and thins toward the east. The uncemented parts of the conglomerate facies form the best aquifers where they yield adequate domestic and small irrigation supplies.

Glaciofluvial Deposits

During the late Pleistocene Epoch large volumes of glacial melt water from the mouth of Lower Grand Coulee near Soap Lake deposited well-sorted gravel and sand on top of the Ringold Formation and basalt south and west along Upper and Lower Crab Creek valley. Also, glacial melt water that entered the project area from the east, mainly along Esquatzel and Washtucna Coulees (fig. 2) deposited gravel and sand on the Ringold Formation and basalt. The saturated thickness of these deposits is greatest in the northeastern part of the Quincy Basin, in Upper and Lower Crab Creek valleys, in Esquatzel and Washtucna Coulees, and north of Pasco.

The glaciofluvial gravels produce by far the largest yields of water. Wells that tap glaciofluvial gravels have the highest specific capacities in the project area. High yields can be expected from properly constructed wells wherever a substantial saturated thickness of gravel or coarse sand is found.

THE AQUIFER SYSTEM

Two principal aquifer systems are considered in this report: the basalt, herein denoted as the lower aquifer, and the unconsolidated deposits overlying the basalt, which are herein denoted as the upper aquifer.

The basalt is consolidated and water it contains is mainly under pressure or artesian conditions. The Ringold Formation and glaciofluvial deposits overlying the basalt are unconsolidated to semiconsolidated and the water they contain is mainly at atmospheric pressure and under water-table conditions.

Hydraulic Characteristics

The initial determinations of hydraulic characteristics—of transmissivity, hydraulic conductivity, and storage—were based on aquifer and specific-capacity tests in and near the project area. Modifications of the initial estimates of characteristics were made during verification of the steady- and transient-state analyses.

Yakima Basalt

Transmissivity values for the Yakima Basalt initially were calculated on the basis of 13 specific-capacity tests in the CBIP, and 342 specific-capacity tests in the Odessa area, which is adjacent to the project area. (The average transmissivity in the Odessa area was calculated to be 3,200 ft^2/day.) Approximate transmissivity was calculated by multiplying the specific capacity of the well by 270. Transmissivity in the project area obtained in this manner ranged from less than 500 to 7,400 ft^2/day and averaged about 2,600 ft^2/day (table 2). Geologic information from numerous well logs as well as inspection of basalt flows along canyon walls show that the physical characteristics of the basalt are relatively uniform over large distances, which suggests greater uniformity in hydraulic characteristic than is shown by results of the specific-capacity tests. The wide range in transmissivity which occurs without a distinct pattern, probably reflects the range of field and well conditions during the test rather than the actual range in transmissivity. As a result, the initial transmissivity of the basalt is based on a rough average of the transmissivity values calculated from specific-capacities for selected test sites. The average value then is extended to cover large parts of the project area, but modified where there are significant changes in head gradient.

An estimate of the initial storage coefficient is based on the ratio of the volume of water pumped to the volume of basalt "dewatered" in an area heavily pumped for irrigation. The volume of basalt aquifer dewatered, 6.7×10^6 acre-feet, was computed as the difference in the potentiometric head maps measured before and after the 1967 irrigation season in a 276-square-mile area near Odessa (Luzier and Burt, 1973). The volume of water pumped from the same area during 1967 was 1.7×10^4 acre-feet, as calculated from electrical-power consumption at each well. The storage coefficient is the ratio of the volume pumped to the volume of aquifer dewatered and was computed to be 2.5×10^{-3}.

TABLE 2.—Transmissivity of basalt based on specific-capacity test of selected wells in project area

Well number	Depth (ft)	Basalt penetrated (ft)	Yield (gpm)	Drawdown (ft)	Hours pumped	Specific capacity (gpm/ft)	Transmissivity GPD/ft	Transmissivity ft²/day
11/30-11C	614	576	280	33	24	8.5	17,000	2,300
12/29-28F	699	249	54	62	48	.9	1,800	240
14/30-8G	371	355	55	40	24	1.4	2,800	380
-10P	433	430	25	5	24	5.0	10,000	1,400
15/28-24L	389	139	18	6	24	3.0	6,000	800
16/25-6M	850	832	49	15	26	3.2	6,400	860
17/31-8R	155	110	10	9	24	1.1	2,200	300
19/28-13J	568	496	1,050	51	24	20.5	41,000	5,500
-27H	1,045	948	610	55	12	11.1	22,200	3,000
20/24-10E	153	103	1,600	58	72	27.5	55,000	7,400
-10P	184	124	750	68	72	11.0	22,000	3,000
20/25-7A	150	89	2,000	80	96	25	50,000	6,700
-7C	182	131	1,000	113	72	8.8	17,600	2,400
							254,000	34,280
					Average transmissivity =		19,500	2,600

TABLE 3.—Hydraulic conductivity and storage coefficient of Ringold Formation and glaciofluvial deposits in the Hanford area (after Bierschenk, 1959)

Aquifer tested	Well no.[1]	conductivity (gpd/ft²)	Hydraulic conductivity (rounded; ft/day)	Storage coefficient
Glaciofluvial sand and gravel	699-55-50	66,700	8,900	0.20
	-24-33	64,500	8,600	......
	-31-30	53,500	7,100	......
	-65-50	13,700	1,800	......
	-62-43	12,700	1,700	.06
Undifferentiated glaciofluvial sand and gravel, with some Ringold Formation sand and gravel	699-42-12	5,000	670	......
	-14-27	2,400	330	......
	-77-54	4,900	650	......
	-20-20	1,200	160	......
	-40-24	1,400	190	......
	-33-56	1,700	230	......
	-31-53	900	120	.06
	-26-15	1,500	200	......
	199-F7-1	3,900	520	......
Ringold Formation sand and gravel with undifferentiated thin silty beds	699-2-3	575	80	......
	-58-19	500	70	......
	-8-17	490	65	......
	-35-9	420	55	......
	-71-52	600	80	......
	-17-5	190	25	......
	-8-32	105	15	......
	-S12-3	50	5	......
Conglomerate	699-1-8	450	60	......
	199-K-10	400	50	......
	699-47-35	150	20	......
Clay	699-40-33	10	1	......

[1]Well numbers from Bierschenk (1959).

Unconsolidated Deposits

Ringold Formation

Hydraulic-conductivity values were based on results from 12 aquifer and six specific-capacity tests near Hanford (table 3). Hydraulic conductivity ranged from 1 to 80 feet per day, and an overall initial value of 40 feet per day is used for the conductivity of the Ringold Formation. The initial storage coefficient or specific yield is assumed to be 0.1 since data on specific yield of the Ringold Formation are not available.

Glaciofluvial Deposits

Hydraulic conductivity values were based on 14 aquifer tests near Hanford (table 3). An initial value of 1,600 feet per day was used for the conductivity of the glaciofluvial deposits. The initial storage coefficient was based on the specific yield determined from two aquifer tests near Hanford (table 3). An initial value of 0.15 was used for the storage coefficient of the glaciofluvial deposits.

Physical and Hydrologic Boundaries

Yakima Basalt (Lower Aquifer)

The entire project area is underlain by Yakima Basalt. To the west and south, the Columbia and Snake Rivers are natural discharge boundaries for the basalt aquifers. The Beezley Hills along the northwest border is a natural recharge boundary for the basalt because it is formed by a monoclinal fold in the basalt that dips toward the Quincy Basin. Crab Creek, along the northeast border is a natural discharge boundary. The east border forms a recharge boundary since the land and basalt surface gain in elevation to create a gentle gradient toward the project area. The Frenchman Hills and Saddle Mountains, both formed by anticlinal folds, retard the lateral movement of water in basalt in the interior of the project area.

Unconsolidated Deposits (Upper Aquifer)

Before irrigation began, the saturated parts of the upper aquifer were limited in size to topographically

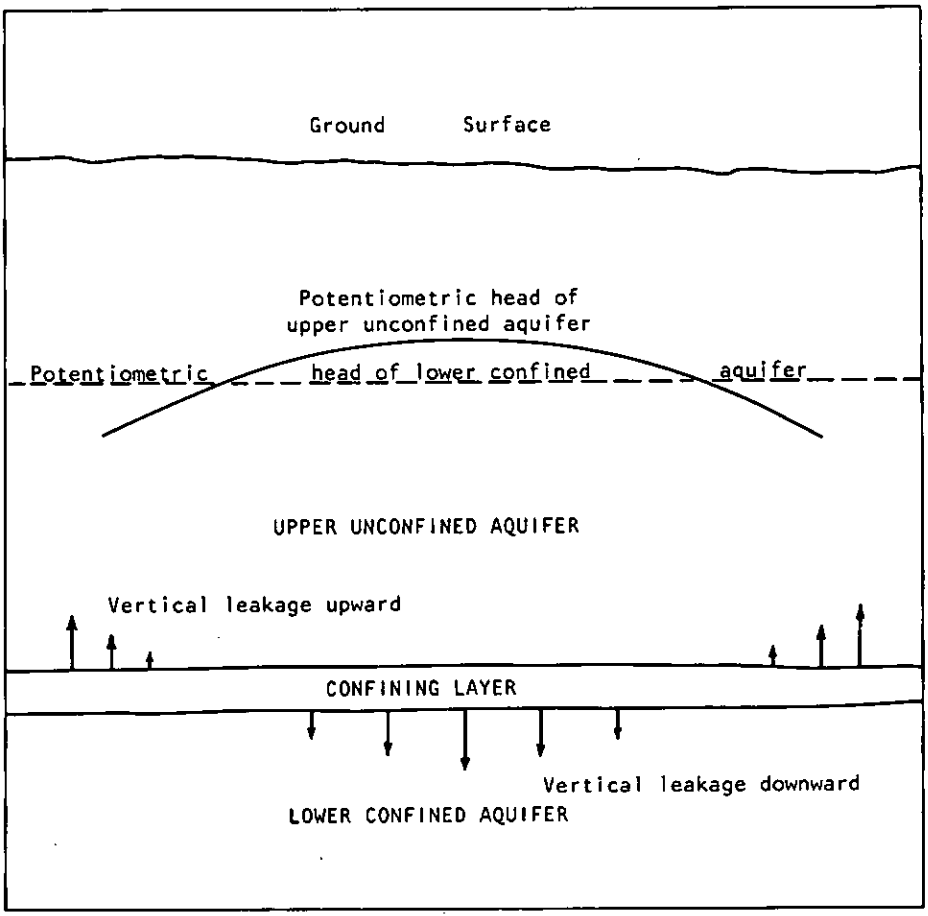

FIGURE 6.—Diagrammatic section showing the hydraulic relation of the upper and lower aquifers and the confining layer between the two aquifers.

low areas in basins and along the main drainage systems. The remaining upland areas, although mantled by the unconsolidated deposits, was essentially "dry." After the start of project irrigation, the unconsolidated deposits became saturated where water was applied and the boundary of the saturated area expanded downgradient to join other previously saturated areas or to eventually discharge to streams or lakes.

Internal Boundaries

A diagrammatic section of the upper and lower aquifers is shown in figure 6. The upper aquifer extends from the top of the water table to the top of a confining layer that separates it from the lower aquifer. The lower aquifer extends downward an undetermined depth.

The upper aquifer is at atmospheric pressure—and is considered to be a water-table aquifer. The lower aquifer is artesian and the measured head is usually a composite of heads in several interflow zones penetrated by the well. Water moves between the two aquifers through a confining layer in response to the relative head difference of the two aquifers. If the head of the upper aquifer is higher, water moves from the upper to the lower aquifer; if the head of the lower aquifer is higher, movement of the water is upward.

Head Distribution Before Irrigation

Upper Aquifer

Before irrigation, only a part of the upper aquifer was saturated. The saturated parts were located in topographically low areas such as the central part of the Quincy Basin, the area north of Pasco, Upper and Lower Crab Creek valleys, Esquatzel Coulee, and Lind Coulee. In the remainder of the project area the aquifer was unsaturated. The depth to water generally varied with the elevation of land surface, being about 2 to 20 feet in the low areas such as Drumheller Channels and along main drainage valleys, and from 20 to 200 feet below land surface beneath higher ground.

Heads measured in the upper aquifer, in most places, accurately reflect the position of the water table, and where there was a wide distribution and enough wells, the measurements provided adequate control for construction of contoured head maps. The pre-irrigation water-level measurements show that heads in the upper aquifer remained nearly constant from year to year in most places, with the principal declines occurring locally from irrigation pumping. To construct the pre-irrigation map, heads were averaged where more than one measurement was available in a well, and head contours were modified in the Hiawatha and Mae valley areas west of Moses Lake to adjust for head declines resulting from irrigation pumping there. The pre-irrigation head map of the upper aquifer is shown in figure 7.

Lower Aquifer

Outside the Quincy Basin there were few water-level data for the lower aquifer before 1952. The head map in the Quincy Basin is based on the average of measurements taken between 1916 and 1952, while the head maps for the Pasco and Othello Basins are based on the averages of measurements taken between 1939 and 1952 (fig. 8). Comparison of the potentiometric head in basalt during this interval shows relatively little change from year to year, except in local areas, such as near the town of Quincy, where large quantities of water were being pumped. The potentiometric head in the basalt was modified in those areas to remove the pumping effect in order to approximate the natural or undisturbed head distribution in the basalt.

Heads measured in the lower aquifers are dependent on the thickness of the aquifer penetrated by the measured observation well. In order to minimize the differences in head, the heads used to construct the head maps were restricted to wells that penetrated about the same thickness of the lower aquifer as other wells in the general area. Of the three models, the pre-irrigation contoured head map in the basalt in the Quincy model area is probably more reliable than the contoured head map in the Pasco and Royal model areas because more usable data points for constructing the head map were available.

Head Distribution Since Irrigation

Upper Aquifer

Since irrigation, the saturated area of the upper aquifer expanded in response to recharge to the water table from irrigation. Generally, the saturated area expanded downgradient from the irrigated areas, and, with the steady increase in irrigated acreage each year, saturated unconsolidated deposits now overlie the basalt over most of the project area (figs. 9 and 10).

Water levels in irrigated areas rose on the average about 5-15 feet per year, as indicated by the hydrograph of well 19/25-2 (fig. 11). Water levels in nonirrigated areas rose more slowly, since any significant rise is due to lateral flow from nearby irrigated areas, as indicated by the hydrograph of well 13/30-26. Water levels in gravel aquifers as a rule show relatively little rise because the high permeability of the gravel allows greater lateral flow which prevents a significant water-level buildup in the aquifer.

In all cases where heads were increased in saturated areas or where heads were created in previously unsaturated zones, the amount of leakage between the upper and lower aquifers changed in relation to the head change between the two aquifers. In most cases the initial head buildup in the upper aquifer started or increased leakage downward into the lower aquifer.

Lower Aquifer

In irrigated areas, the buildup of head in the upper aquifer caused or increased leakage through the confining layer to the lower aquifer. The potentiometric head in the lower aquifer responds quickly and strongly to any change in vertical leakage because the storage coefficient is small. In a typical well the potentiometric head rose about 20-40 feet per year in an irrigated area as shown by two hydrographs in figure 11. The contoured head map of the lower aquifer for 1963 and 1968 (figs. 12 and 13) shows substantial head changes during the interval from pre-irrigation to 1963 and less change from 1963 to 1968, indicating that within a relatively short time, heads in the lower aquifer came into approximate balance with ground-water inflow, outflow, and leakage.

THE DIGITAL MODEL

The essence of computer simulation of ground-water flow is a mathematical model or set of equations which describes the flow. However, it is not sufficient merely to develop mathematical equations to duplicate a specific pattern of water-level changes. To be suitable, the model must (1) function within the

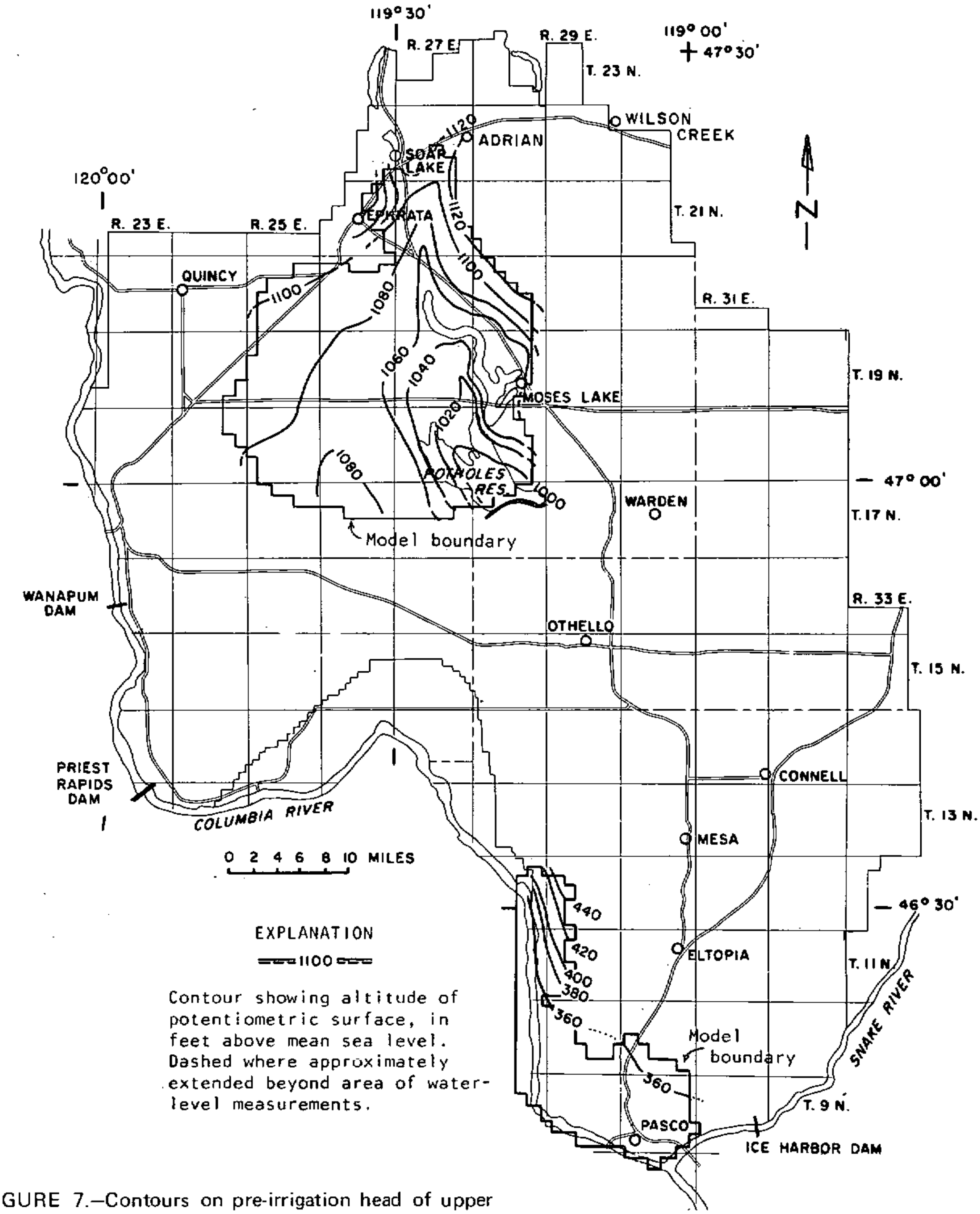

FIGURE 7.—Contours on pre-irrigation head of upper aquifer, inside the outline of the modeled saturated upper aquifer.

constraints of theoretically valid equations of ground-water flow, (2) be based on reasonable simplifying assumptions and technically sound hydrologic information, and (3) utilize model parameters whose values do not exceed reasonable limits.

The digital-computer program developed for this project is designed to simulate the hydraulic-head response to natural or man-made stresses in a two-aquifer system. The real ground-water system, in three dimensions, is simplified to two aquifers in two dimensions coupled by leakage through a confining layer. Simplifying assumptions were made that transformed the complex two-aquifer system into a form which would be adaptable for modeling purposes and still remain representative of the real system. Important assumptions basic to the development of the present model are that (a) the upper and lower aquifers are single layered and separated by a confining layer of

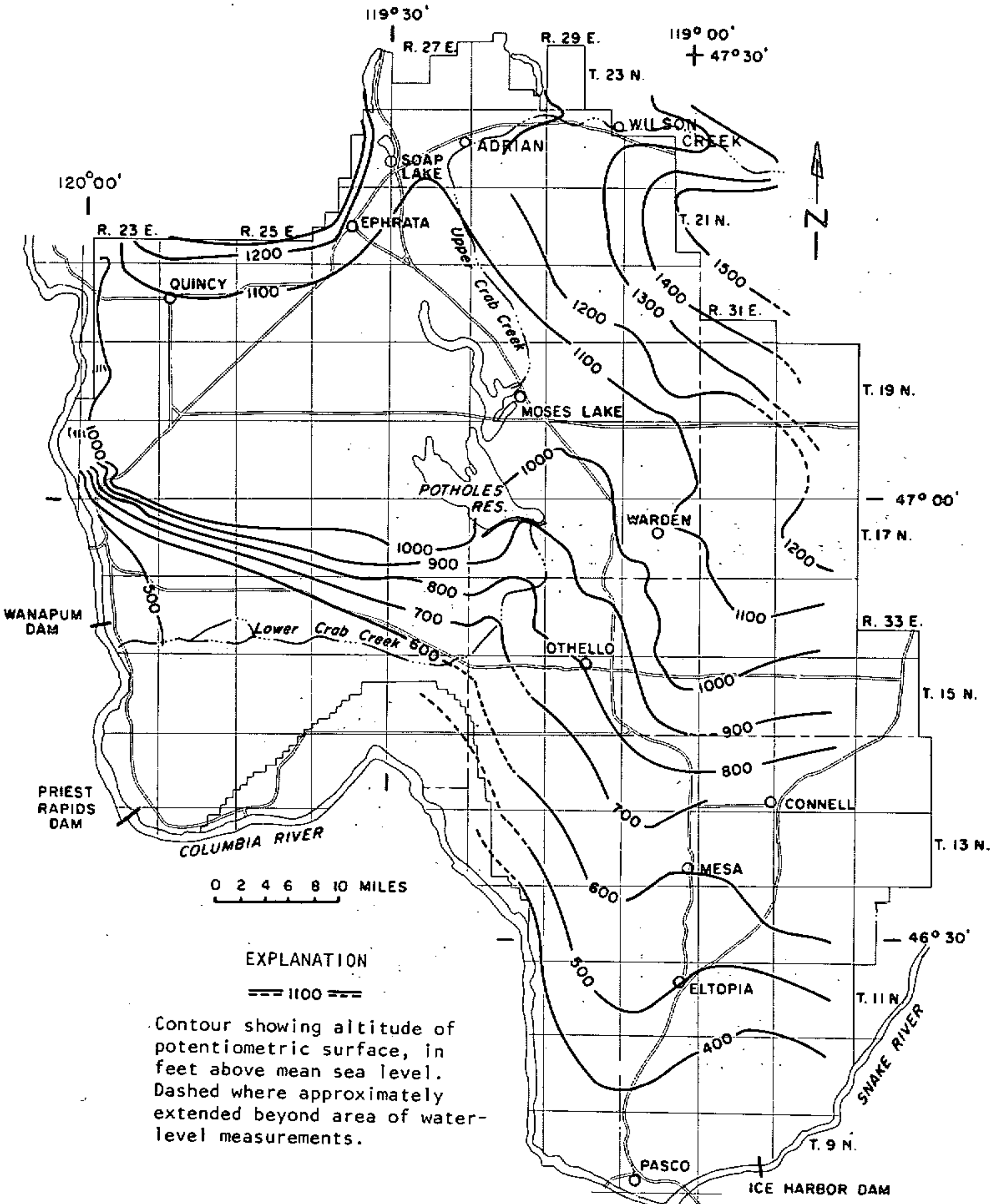

FIGURE 8.—Contours on pre-irrigation heads of the lower aquifer.

uniform thickness, but varying hydraulic conductivity; (b) flow in the aquifers is horizontal; flow in the confining layer is vertical; (c) water is transferred instantly into and out of aquifer storage, with no storage in the confining layer; and (d) the transmissivity of the lower aquifer remains constant.

Method of Analysis

Basic data on water-level measurements, aquifer characteristics, and natural or artificial recharge and discharge are compiled to define the problem and develop a general concept of the hydrologic system.

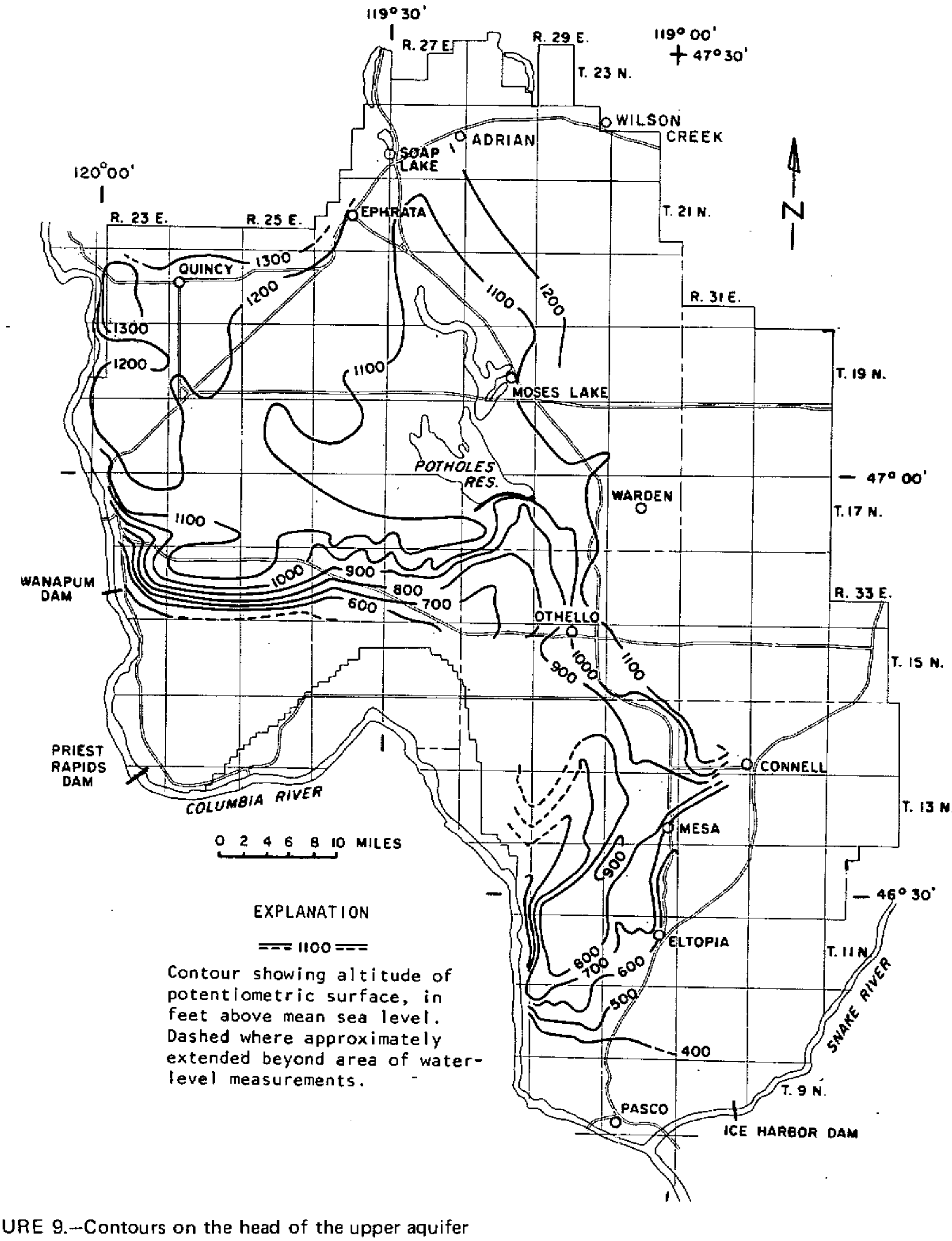

FIGURE 9.--Contours on the head of the upper aquifer in 1963.

Then the data must be evaluated quantitatively and incorporated into the digital model which is constructed to simulate the prototype system as closely as possible.

Analysis by the digital model is done in two parts—steady-state and transient. The steady-state model analyzes conditions before 1952 (pre-irrigation) when, except for local pumping, the total aquifer system may have been essentially undisturbed and in balance. The initial estimates for aquifer characteristics and natural stresses on the system are adjusted by trial and error to obtain a reasonable fit between measured and computed heads. In steady-state analysis, adjustments are made in the transmission characteristics of the aquifer, natural boundary conditions, and natural ground-water inflow and outflow until reasonable

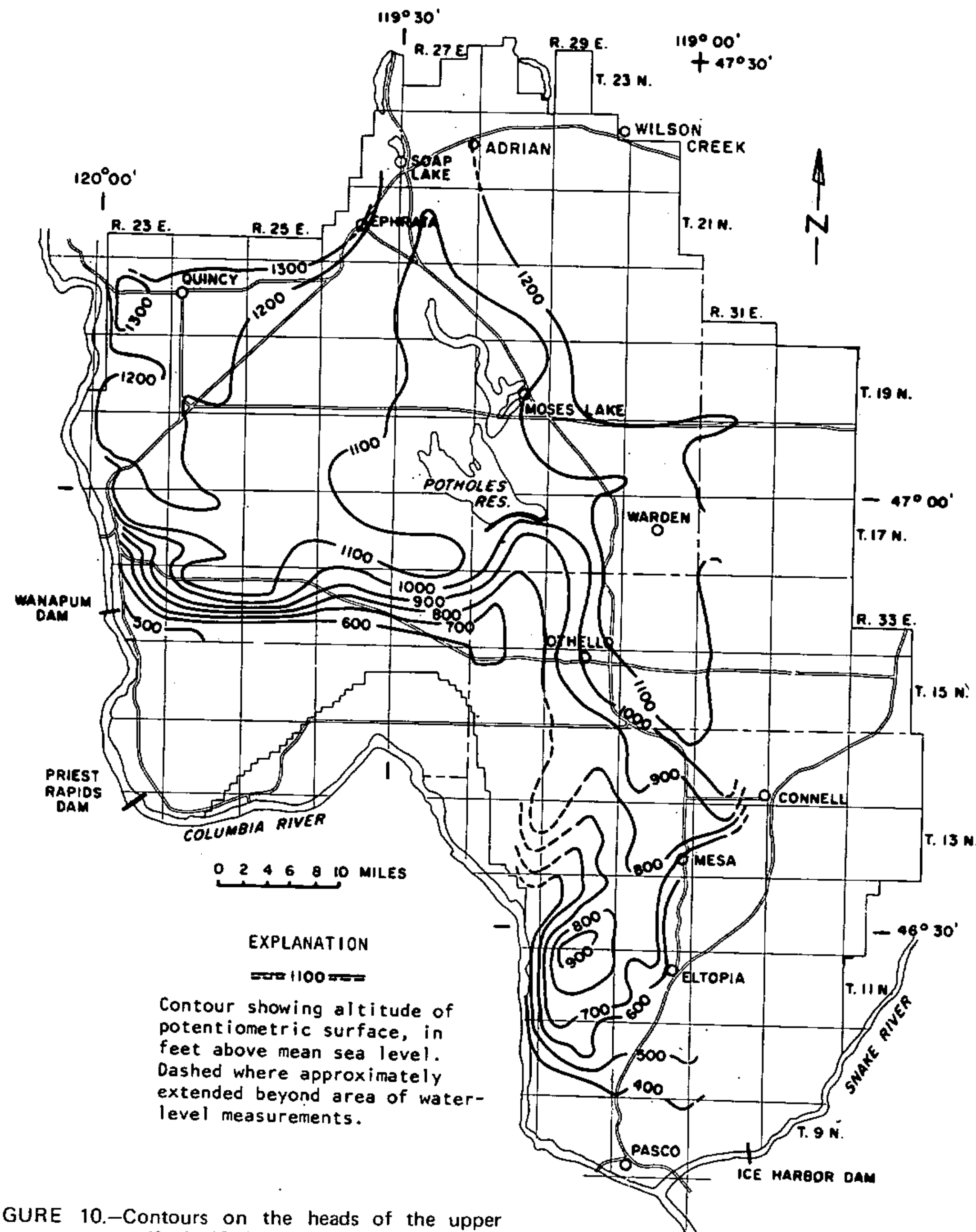

FIGURE 10.—Contours on the heads of the upper aquifer in 1968.

values for these parameters are determined. This provides the initial condition for the transient analysis. The transient model analyzes conditions after 1952 (post-irrigation) when the total hydrologic effect of the imported irrigation water was superimposed on the initial undisturbed conditions. During transient analysis, the aquifer characteristics not determined during steady-state analysis, and the initial estimate values of the artificial stresses imposed on the system by irrigation are adjusted to obtain a reasonable fit between measured and computed head. Transient analysis also determines the ground-water inflow and outflow, storage, and head in both aquifers with time.

The digital model's role as a predictive device is based on the premise that if past conditions can be simulated in the model, then, within limits, so can future conditions. In this study, water-level changes in response to irrigation during a 16-year historical period

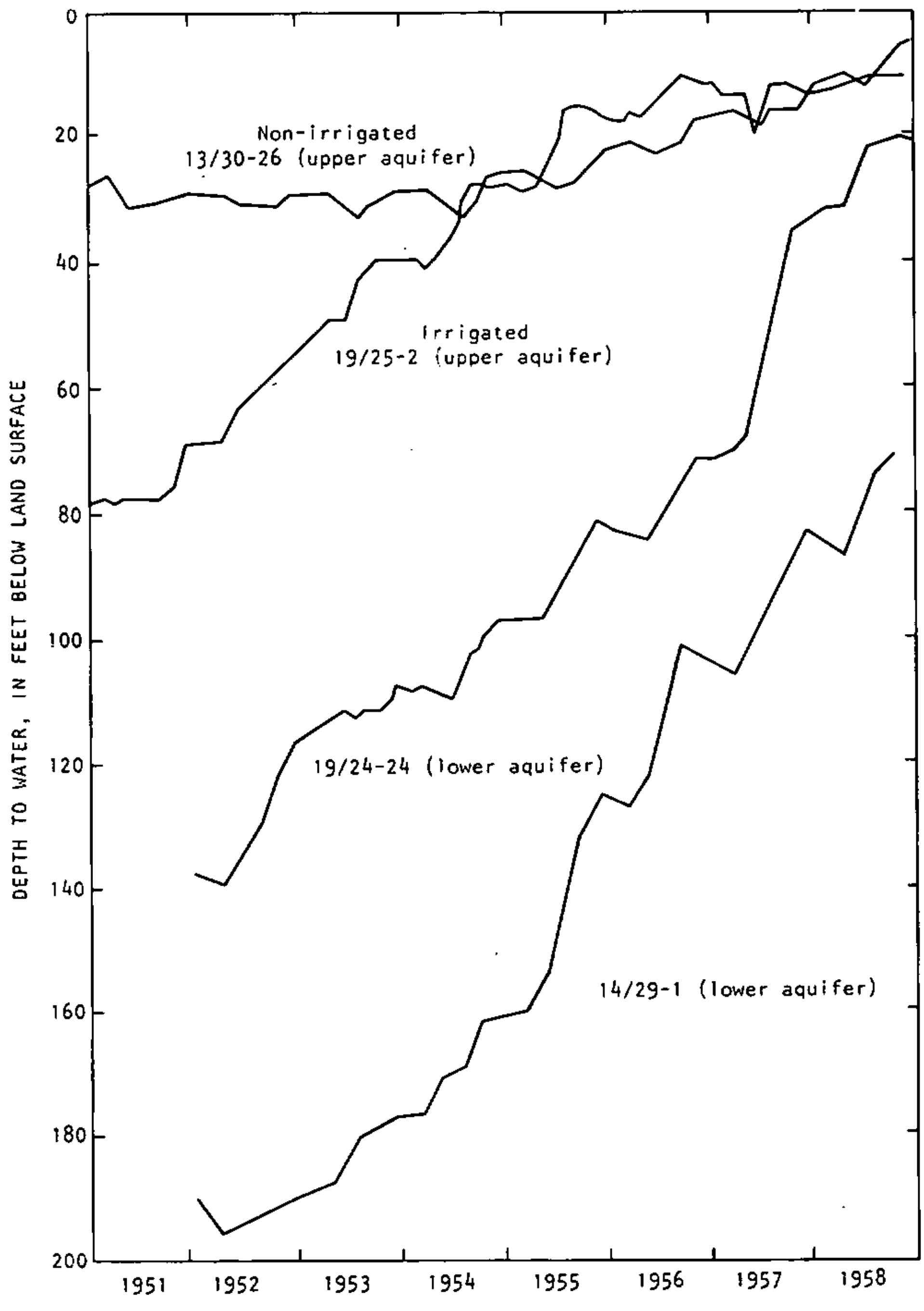

FIGURE 11.—Hydrograph of selected wells tapping the upper and lower aquifers.

were simulated, after which it is assumed that the model will react to hypothetical stresses in approximately the same manner and degree as the real system.

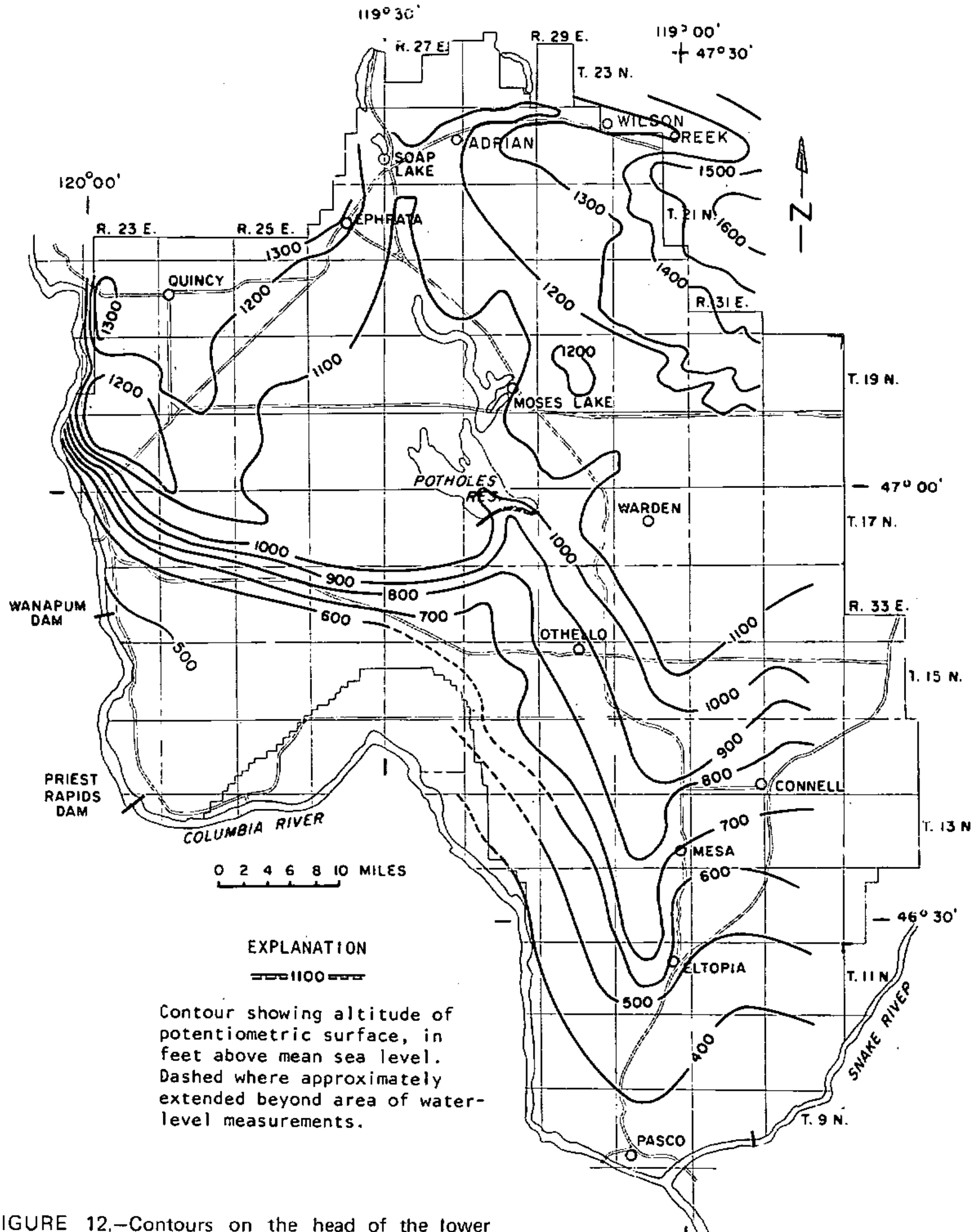

FIGURE 12.—Contours on the head of the lower aquifer in 1963.

Mathematical Description

The equation for transient ground-water flow in the upper aquifer is

$$\frac{\partial}{\partial x}\left(Kb\frac{\partial h}{\partial x}\right)+\frac{\partial}{\partial y}\left(Kb\frac{\partial h}{\partial y}\right)=S^u\frac{\partial h}{\partial t}-Q^u+\frac{K_{cl}}{M_{cl}}(h-H)$$

where

h = water-table head in the upper aquifer, in feet
K = permeability of the upper aquifer, in feet per day
b = h minus bottom of the upper aquifer (saturated thickness of the upper aquifer), in feet
S^u = specific yield of the upper aquifer (dimensionless)
Q^u = injection or withdrawal rate in the upper aquifer, in cubic feet per day
K_{cl} = vertical permeability of the confining layer, in feet per day
M_{cl} = thickness of the confining layer, in feet
H = potentiometric head in the lower aquifer, in feet
x, y = rectangular coordinates, in feet
t = time, in days

The corresponding equation for transient ground-water flow in the lower aquifer is

$$\frac{\partial}{\partial x}\left(T\frac{\partial H}{\partial x}\right)+\frac{\partial}{\partial y}\left(T\frac{\partial H}{\partial y}\right)=S^L\frac{\partial H}{\partial t}-Q^L-\frac{K_{cl}}{M_{cl}}(h-H)$$

where

T = transmissivity of the lower aquifer, in feet squared per day
S^L = storage coefficient of the lower aquifer (dimensionless)
Q^L = injection or withdrawal rate in the lower aquifer, in cubic feet per day

The direction of the vertical leakage through the confining layer is dependent on the relative position of the heads of the two aquifers, and the magnitude of the leakage is dependent on the vertical permeability and thickness of the confining layer (fig. 6).

The method of solution of equations 1 and 2 involves finite-difference approximations. In general, each aquifer is represented as a two-dimensional mesh of elements with each element representing 1 square mile. At the center of the element is a node which is the hypothetical point where average data values are given. Calculations are desired for both heads at each node as a function of time; for example, heads are calculated at each node at 30 days, then 60 days, and continuing in steps of 30 days to the end of the run.

If heads in one aquifer are known, then heads in the other aquifer can be calculated by the method of Pinder and Bredehoeft (1968, p. 1073-1079). This algorithm is called the alternating-direction implicit procedure (ADIP) in which the heads can be calculated on the basis of estimates of the aquifer parameters. In general, the heads depend on lateral flow, upward or downward leakage through the confining layer, change in quantity of ground water in storage, and the quantity of applied water or pumping. The leakage term, $\frac{K_{cl}}{M_{cl}}(h-H)$ involves unknown heads in both aquifers and the ADIP procedure cannot be applied directly for the solution of equation 1 or 2. The method developed for solving these equations simultaneously is very similar to that used by Bredehoeft and Pinder (1970) and involves an iterative solution. The procedure is very similar to that used by Bredehoeft and Pinder (1970) and involves an iterative solution. The procedure is as follows: (1) at a given step in time, use the iterative ADIP (modified ADIP using iteration parameters generally more accurate than ADIP) to calculate heads in the upper aquifer, using the last calculated heads of the lower aquifer; (2) use iterative ADIP to calculate heads in the lower aquifer, using the just-calculated heads in the upper aquifer; (3) repeat the two steps until the heads in both aquifers have changed insignificantly from the last calculated values; and (4) advance the time and repeat the whole procedure. Bredehoeft and Pinder (1970) show favorable comparisons of this method with theoretical solutions.

Steady-State Analysis

"Steady state" is a hypothetical condition where flow and hydraulic head in a ground-water system are constant; i.e., the hydraulic head does not change with time. In most ground-water systems, a true steady-state condition is never reached because heads are constantly changing in response to seasonal differences in recharge and discharge and the ground-water flow is fluctuating correspondingly. Steady state in the ground-water system, however, can be approximated on the basis of long-term average head. The steady-state head maps (figs. 7 and 8) were compiled from averages of heads measured in observation wells over periods as long as 36 years prior to the application of water from the CBIP. These long-term average heads have been adjusted in places to remove the effects of large pumping wells, so the contours on the head map are assumed to represent an approximately balanced condition of inflow and outflow in the aquifers.

The three parts of the CBIP area considered for the model studies are in the Quincy and Pasco Basins and on the Royal Slope (fig. 14); the models are referred to herein as the Quincy, Pasco, and Royal models. The model divisions were made because a single, large model with the desired array of nodes would have required excessive storage and computation time on the computer. Where possible, the common boundary between models was selected along natural boundaries that separate the three subbasins.

Information necessary for the simulation includes initial hydraulic conductivity of the upper aquifer, initial transmissivity of the lower aquifer, vertical hydraulic conductivity of the confining layer, elevation at the top of the lower aquifer, measured heads in the upper aquifer, measured heads in the lower aquifer, infiltration percentage, precipitation minus evapotranspiration, constant-boundary conditions in the upper aquifer, and boundary conditions in the lower aquifer. Other input data required for computation include model and nodal dimensions, number of iterations, and the desired output information. The input data are similar for each model area except the Royal model which is a single-aquifer model.

The net inflow and outflow of water that enters and leaves both aquifers is computed in the program. This is done by cumulating the net vertical flow at each node and the lateral flow at each constant-head-boundary node. Vertical flow includes recharge by precipitation and ground-water discharge by evapotranspiration. Lateral flow at constant-head-boundary nodes provides ground-water recharge or discharge other than precipitation and evapotranspiration. Values derived for each model are included in the summary sections of the three separate models.

The model computes with the initial data, including known and estimated values. As the computed heads deviate from the defined steady-state heads, the estimated values are revised and adjusted until the computed heads approximate the measured (or estimated) steady-state levels.

The steady-state model is verified by matching

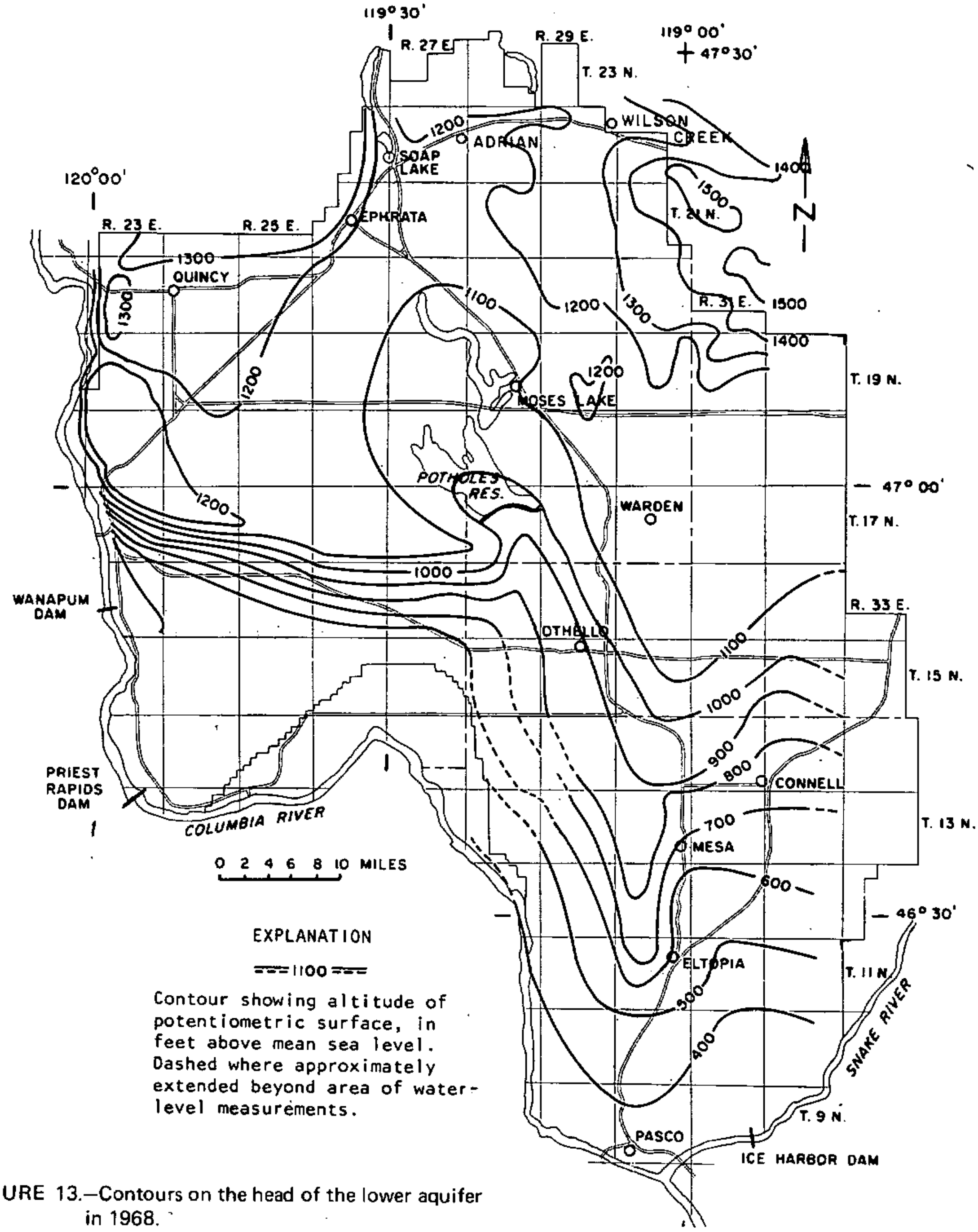

FIGURE 13.—Contours on the head of the lower aquifer in 1968.

computed to measured heads in both the upper and lower aquifers as closely as possible. Heads were matched primarily by adjusting the permeability of the upper aquifer and the transmissivity of the lower aquifer. Other adjustments include rainfall infiltration and evapotranspiration. The head response is unique only in terms of the values that are used to define the aquifer and boundary conditions in the model. Because it is possible to duplicate the head response in the model by adjusting different combinations of values, the adjustments were restricted to values that are considered reasonable and within the limits of what is generally known about the actual aquifer and boundary conditions. Repeated adjustments of data were necessary in order to isolate the effects of each data change on water levels in both aquifers, and these changes are combined to achieve an approximate fit of the measured and computed head-contour maps. Once the heads in both aquifers are reasonably matched, all input data sets and parameters are considered verified.

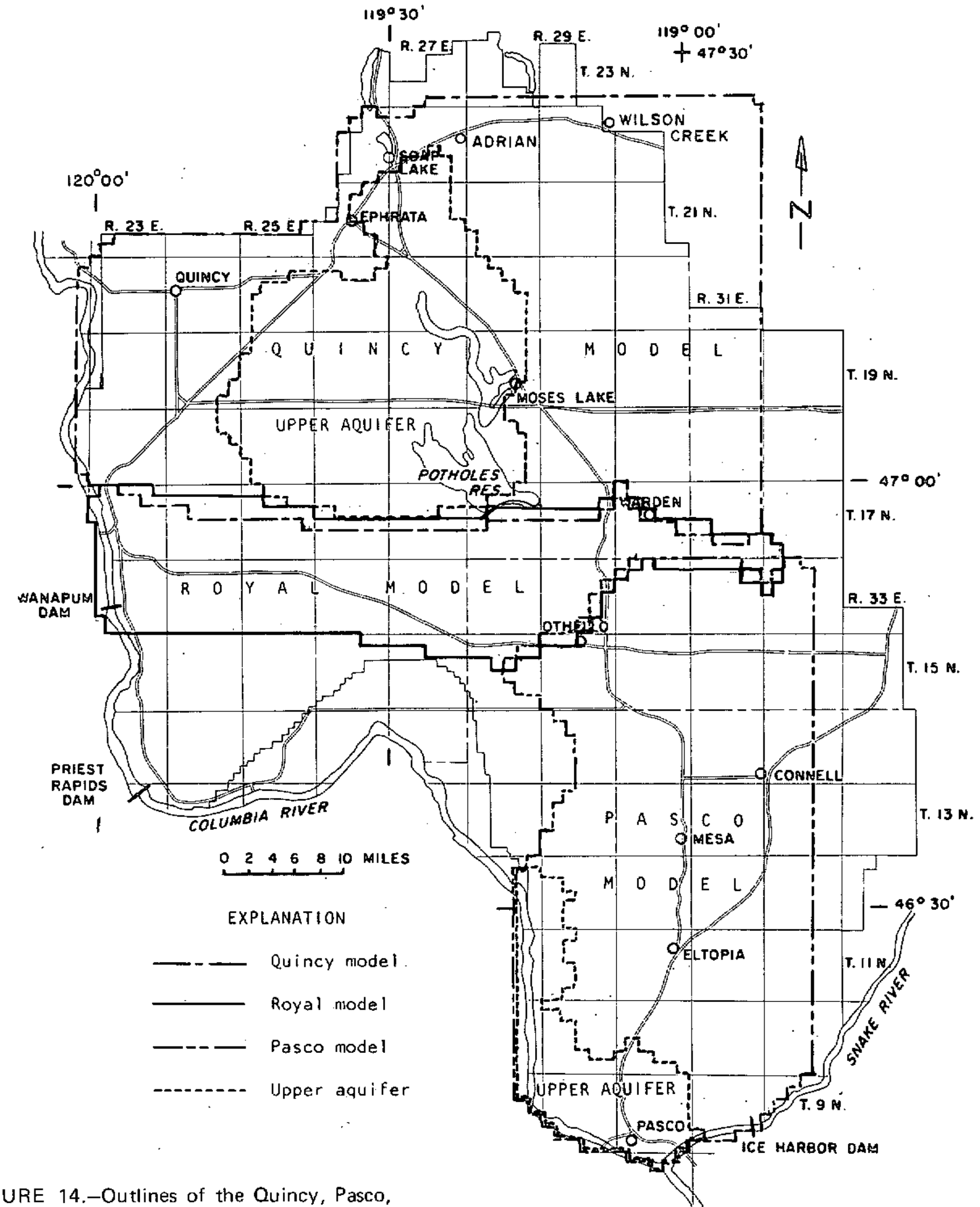

FIGURE 14.—Outlines of the Quincy, Pasco, and Royal model areas.

Boundary Conditions

Natural boundary conditions due to geologic or hydrologic influence are simulated as discussed below.

Impermeable boundaries are simulated by assigning zero hydraulic conductivity to nodes representing a no-flow boundary. Hydraulic boundaries such as lakes and streams are assigned constant-head boundaries. Lateral-inflow and outflow boundaries on the aquifer perimeter are simulated as constant-head boundaries. The amount of inflow and outflow can be computed at these boundaries. Vertical flow into and out of the aquifer, as recharge from precipitation and discharge from evapotranspiration, is simulated as constant flow into or out of the node. Vertical flow between aquifers is a function of the head difference between the two aquifers and the vertical hydraulic conductivity of the confining layer.

Natural boundary conditions such as recharge from precipitation and discharge by evapotranspiration—and in the Quincy and Pasco models the vertical flow between the upper and lower aquifer—are simulated in the same manner in all three models. Other natural boundary conditions, such as the flow into and out of lakes, streams, springs, and from the perimeter of the model, are unique to each model, and are treated as special boundary conditions in the separate discussion of the individual models.

Recharge from precipitation

Average annual precipitation ranges from 6 to 10 inches in the project area. Recharge from precipitation generally occurs during the winter months, as nearly half the annual precipitation falls during winter when evapotranspiration is negligible. During the remainder of the year, nearly all precipitation is evapotranspired from the soil zone. Precipitation during the winter generally falls as light rain or as snow which may accumulate as much as 12 inches on the ground. Relatively warm winds are common during the winters and cause rapid snowmelt; when the ground is frozen, this results in appreciable surface runoff, but otherwise the snowmelt recharges the ground-water reservoir.

Precipitation represented for each node in the model was estimated to the nearest one-half inch on the basis of the precipitation map (fig. 4). Precipitation considered effective for ground-water recharge is assumed to fall only during the months of November, December, January, and February when evapotranspiration loss is small. The percentage of the annual precipitation that falls during each of these four months was averaged from several weather stations in the project area, and was used to compute the effective annual precipitation on the precipitation map.

Potential evapotranspiration for nonirrigated areas was computed by the Blaney-Criddle method (Blaney and Criddle, 1950) for November, December, January, and February, and subtracted from the precipitation amount for the corresponding month. Annual values (precipitation minus evapotranspiration) are assigned to each node in the model.

Ground-water recharge occurs only after the moisture requirements of the soil zone have been satisfied. Fine-grained soils retain more water so less is available for recharge, while coarse-grained soils retain less water and allow greater recharge to the water table. From interpretation of soil maps, the model area was differentiated into fine-, medium-, and coarse-grained surficial soil areas to correspond to areas of slow, moderate, and rapid infiltration capability. These areas were arbitrarily assigned an infiltration factor to represent differences in the infiltration and potential runoff capability of the soil. The initial infiltration factors assigned to each node in the model are 10, 20, and 30 percent of effective annual precipitation, with the smallest percent assigned to soils with slow infiltration capacity. Adjustment of these estimated values necessary to achieve a match between observed and computed heads resulted in a range of 5 to 15 percent.

Recharge by precipitation is simulated in the model as the difference between precipitation and evapotranspiration during the four winter months multiplied by the infiltration factor.

Discharge by evapotranspiration

When the water table is near land surface, water is discharged to the atmosphere by a combination of evaporation from the capillary fringe above the water table and transpiration by plants from the capillary fringe or from the water table. Ground-water control by evapotranspiration therefore is determined not only by climatic conditions, but also by water-table depth. Where the water table is shallow the capillary fringe will be at or near land surface, and the evapotranspiration rate will be high. As the water table is lowered, the evapotranspiration rate decreases until a depth is reached where no ground-water evapotranspiration takes place.

Before project irrigation began, maximum ground-water discharge by evapotranspiration occurred in areas of a naturally shallow water table, such as Upper and Lower Crab Creek valleys, lower Lind Coulee, Drumheller Channels, and in part of the area later inundated by Potholes Reservoir (fig. 2). In the model nodes representing these areas, a vertical upward flow, based on the annual evapotranspiration rate computed by the Blaney-Criddle method, simulates discharge of ground water from the upper aquifer. The amount discharged at any particular node is adjusted for the area of that node underlain by the shallow water table.

Vertical flow between aquifers

As represented in the model, the upper and lower aquifers are coupled by vertical flow through a confining layer, arbitrarily designated as the upper 1 foot of the basalt. The rate of vertical flow depends on the head relation between the upper and lower aquifer and the vertical hydraulic conductivity of the confining layer.

In the absence of reliable field data on the vertical hydraulic conductivity of basalt in the project area, several hydraulic conductivity values were estimated indirectly by analysis of the head response in basalt to application of known amounts of irrigation water, and these values were tested as model parameters. After repeated trials on the model, comparing different values of hydraulic conductivities to head response in the upper and lower aquifers, an average value of 0.00002 foot per day (within a range of 0.000001 foot/day to 0.000037 foot/day) gave computed heads that were similar in response to measured heads in both aquifers.

Quincy Model

The Quincy Basin is bounded on the north by the Beezley Hills and part of upper Crab Creek; on the south by Frenchman Hills and Lind Coulee; on the east by a westward sloping basalt surface, and on the west by the Columbia River. The Quincy model comprises a rectangular grid of 36 by 55 nodes with a node spacing representing 1 mile. The lower aquifer, represented by about 1,600 nodes, underlies the entire model area. The initial boundary of the saturated zone in the upper aquifer (before irrigation) was established at the inner perimeter nodes (fig. 14). Actually, the upper aquifer is more extensive, but in the model the perimeter nodes are located where the initial saturated zone was estimated to be at least 5 feet thick. The maps of measured pre-irrigation heads for the upper and lower aquifers are shown in figures 7 and 8.

Special boundary conditions

Lakes—Moses Lake (fig. 2) is a discharge area for much of the surface and ground water in the Quincy Basin lying to the north, east, and west of the lake. The water in Moses Lake is kept at a constant elevation of 1,040 feet by a control dam near the southern end of the lake. Excess water spills over the control dam into Drumheller Channels and Lower Crab Creek, to discharge eventually to the Columbia River near Beverly.

In the model, the nodes representing Moses Lake are held constant at 1,040-foot elevation which allows up-gradient nodes in the upper aquifer to discharge into the lake.

Streams—Crab Creek and its principal eastern tributaries, Lind and Bowers Coulees, constitute the main drainage system in the Quincy Basin. The records from a gaging station near Moses Lake indicate that, before 1952, surface flow of upper Crab Creek occurred only during spring floods. Lind and Bowers Coulees had intermittent flows only during periods of heavy rain or during the spring runoff.

The basalt-aquifer-head map indicates that water in the aquifer discharges into Crab Creek between Adrian and the east boundary of the model area (fig. 8). In the model, heads representing Crab Creek in the basalt aquifer are held constant and equal to heads in Crab Creek between these two points to provide a line discharge for the basalt aquifer.

The upper-aquifer-head map indicates that Crab Creek, from Adrian to Moses Lake, was a constant recharge source to the upper aquifer. The supply of ground water in Crab Creek is provided by subsurface flow from Adrian, and by ground-water seepage from upgradient sources east of the channel. In the model, the heads in the upper-aquifer nodes representing Crab Creek between Adrian and Moses Lake are held constant to provide a recharge source at the boundary of the upper aquifer.

Springs—The mean discharge of Rocky Ford Springs (fig. 2) during 1942-52 was 69.5 cubic feet per second (Washington Division of Water Resources, 1955, p. 570). In the model, the head on the node representing the spring location is held constant at 1,075 feet, which is the land-surface elevation at the mouth of the spring. The constant-head node becomes a discharge node for the adjacent upgradient nodes to the north, east, and west.

The discharge of Drumheller Springs and other seeps in the area now occupied by Potholes Reservoir represented by ground-water discharge from the topographically lowest area of the Quincy Basin. The annual discharge was estimated by Schewennessen and Meinzer (1918, p. 154) to be 23,500 acre-feet in 1913. Taylor (1948) estimated the annual discharge from a number of springs in the Drumheller channels and Lind Coulee to be 18,000 acre-feet. Drumheller Springs are simulated in the model by a constant ground-water discharge flux out of the upper aquifer from several nodes. The annual total flux out, which represents discharge from springs and increased evaporation from seep areas, is equivalent to 15,000 acre-feet. Smaller springs that occur in the Quincy Basin are neglected.

Lateral flow in the upper aquifer—The available historical water-level data indicate that before 1952 the saturated zone of the upper aquifer occupied only the structurally deep central part of the Quincy Basin (fig. 7). In the model, the heads inside the perimeter of the upper aquifer are maintained by lateral inflow from adjacent upgradient nodes. In the steady-state analysis, the heads on the perimeter nodes are kept constant and equal to the pre-irrigation measured heads to allow constant lateral flow of water into the saturated area.

The natural discharge area for the Quincy Basin is Moses Lake and the Lower Crab Creek channel. Appropriate constant heads were assigned to nodes that represent Moses Lake and the natural-discharge points on the model boundary. This simulates lateral flow out of the upper aquifer.

Lateral flow in the lower aquifer—Heads along the entire boundary of the modeled area were made equal to measured pre-irrigation heads, and were held constant during the steady-state analysis. This simulates steady-state lateral flow into and out of the lower aquifer.

The top of the basalt generally is higher than the center of the Quincy Basin on all sides except at the east end of the Frenchman Hills, the natural drainage outlet from the basin. As a result, the potentiometric heads in the basalt, influenced by the structure of the basin and greater altitude of the basalt, generally are higher at the modeled boundaries, especially to the north and east, causing lateral flow into the basin. Along the western margin of the basin, the head in the basalt is more than 500 feet higher than the level of the Columbia River, creating a discharge boundary. In the model, very small transmissivity values in nodes adjacent to the river control the large head difference and restrict lateral flow to nodes representing the river. On the south side of the basin, the head difference in basalt between the Quincy Basin and Royal Slope is more than 200 feet in places. This difference indicates that the Frenchman Hills anticline impedes the southward movement of water. The constant heads on the south boundary of the Quincy model represent lower heads in the Royal Slope. In the model, head differences between the Quincy Basin and Royal Slope are controlled by assigning small transmissivity values in the Frenchman Hills. This permits only a small ground-water outflow along the southern boundary of the Quincy Basin.

Results

Head maps of the upper and lower aquifers—Contours of the verified steady-state computed heads in the upper and lower aquifers in the Quincy Basin are superimposed on manually drawn contours of the measured heads for comparison (figs. 15 and 16).

Generally the simulated and measured contours for the upper aquifer are in agreement; the maximum difference between the computed and measured head is 15 feet. In most areas the difference is less than 5 feet.

The computed and measured contours of the lower aquifer are substantially in agreement. Because of sparser data and the composite nature of the input heads, precise agreement was not forced. The maximum difference between the computed and measured head is 80 feet. Over most of the model area the difference is less than 15 feet.

Inflow and outflow—Analysis of the steady-state ground-water balance in the Quincy model indicates that, for the upper aquifer in the Quincy basin, about 70,000 acre-feet per year of water entered by lateral inflow and 65,000 acre-feet per year left by lateral outflow. Of the total yearly inflow, Crab Creek contributed about 37,000 acre-feet, Two Springs Canyon (fig. 2) east of Ephrata contributed about 6,000 acre-feet, and about 27,000 acre-feet entered the upper aquifer from the perimeter. Of the total yearly outflow, about 56,000 acre-feet was the combined discharge into Moses Lake and discharge of Rocky Ford Springs, about 2,000 acre-feet left the southern boundary of the modeled area at the channel of Crab Creek, about 3,000 acre-feet flowed into Soap Lake, and the remainder flowed out of the model permimeter at other places. For the lower aquifer, about 24,000 acre-feet entered and 40,000 acre-feet left the modeled-area boundary annually. More than 5,000 acre-feet moved from the upper to the lower aquifers, and the net recharge to both aquifers from precipitation (precipitation minus evapotranspiration) was more than 11,000 acre-feet per year.

The combined steady-state inflow and outflow of ground water from both aquifers were equal at 105,000 acre-feet per year. Although the model derives the quantitative values shown with apparent precision, the reliability of the values can only be judged in terms of how well the model simulates the real system. Since most of the input data in the model were estimated from limited data, solutions derived from the model are only approximate.

Pasco Model

The Pasco model is bounded on the north by the topographic high ground adjacent to Drumheller Channels; on the south by the Columbia and Snake Rivers; on the east by a west and south sloping basalt surface, and on the west by high ground, partly formed as a southward extension of the Saddle Mountains, and by the Columbia River. The Pasco model (fig. 14) comprises a rectangular grid of 50 by 25 nodes with a node spacing representing 1 mile. The lower aquifer, which underlies the entire modeled area, is represented by about 1,000 nodes. The upper aquifer before irrigation began was superimposed on the lower aquifer and as modeled is assumed to occupy the area within the inner perimeter nodes on the basis of a few head measurements. The upper aquifer probably occupies a larger area than that represented within the model outline because the perimeter nodes are those representative of a saturated section estimated to be at least 10 feet thick. The measured pre-irrigation head maps for the upper and lower aquifers are shown in figures 7 and 8.

Special boundary conditions

Streams—Esquatzel Coulee, the principal surface drainageway represented in the Pasco model, enters Pasco basin from the east, trends southwesterly to about the center of the modeled area, and then due south to end in a closed depression north of Pasco (fig. 2). Before irrigation, flow in Esquatzel Coulee occurred intermittently and only for short duration after unusually heavy rain or during snowmelt runoff. Esquatzel Coulee is not simulated as a line recharge or discharge source for either the upper or lower aquifers in the steady-state model. The coulee is simulated by appropriate ground elevations and permeability values to become a line discharge for the upper aquifer and a line recharge source for the lower aquifer during the transient-state analysis.

Lateral flow in the upper aquifer—Available water-level data indicate that only a part of the upper aquifer north of Pasco and along the Columbia River was saturated before irrigation began in 1952 (fig. 7). In the model representation of that saturated area under steady-state conditions, the heads on the perimeter nodes of the upper aquifer between the Columbia and Snake Rivers are constant and were made equal to the pre-irrigation measured head to maintain the heads in the upper aquifer by lateral inflow. The constant heads on the nodes representing the long-term average water level of the Columbia and Snake Rivers are line discharge nodes for the upper aquifer.

Lateral flow in the lower aquifer—In accordance with the map of measured heads (fig. 8), water in the lower aquifer entered the modeled area, principally from the north and northeast and discharged into the Snake and Columbia Rivers to the south and southwest. Heads in the lower aquifer along the entire perimeter of the model were set equal to the pre-irrigation heads and held constant during the steady-state analysis.

Results

Head map of the upper and lower aquifers—The contours of the verified computed heads in the upper and lower aquifers are superimposed on contours of the measured heads for comparison (fig. 17 and 18).

Generally the simulated and measured contours for the upper aquifer are in agreement. The maximum difference between the computed and measured head in a nodal area is 10 feet. Over most of the area the difference is less than 3 feet.

The computed and measured contours in the lower aquifer generally are in agreement. The maximum difference between computed and measured heads at the nodes is 28 feet, and over most of the model area is less than 10 feet.

Inflow and outflow—Analysis of the steady-state balance in the Pasco model indicates about 9,000 acre-ft/yr entered and 9,800 acre-ft/yr left the upper aquifers by lateral flow. For the lower aquifer about 14,500 acre-ft/yr entered and 18,900 acre-ft/yr left by lateral flow. About 400 acre-ft/yr moved vertically

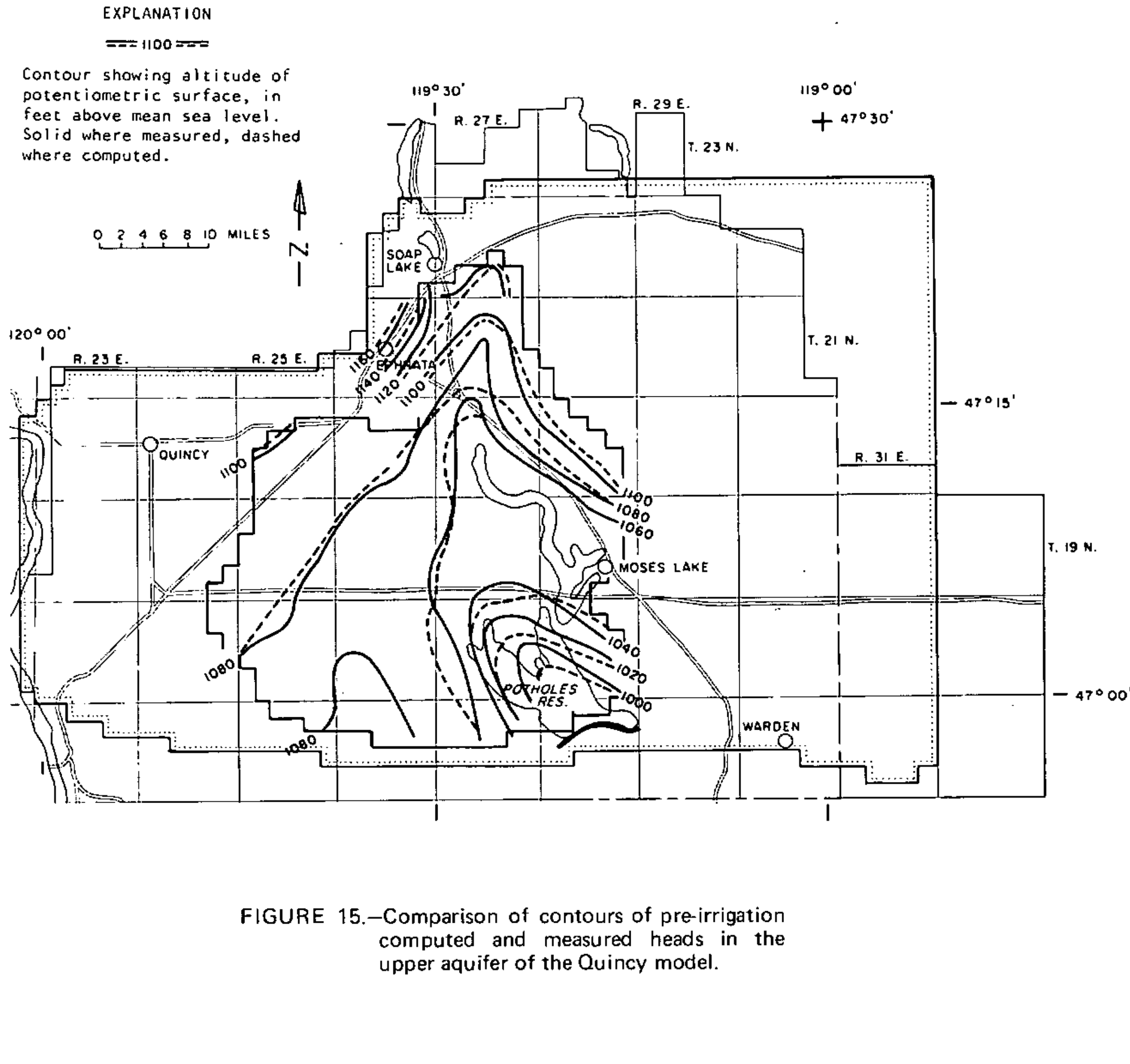

FIGURE 15.—Comparison of contours of pre-irrigation computed and measured heads in the upper aquifer of the Quincy model.

from the upper to the lower aquifer. Net recharge from precipitation was about 5,200 acre-ft/yr to the upper and lower aquifers. The combined steady-state inflow and outflow of ground water from both aquifers was 28,700 acre-ft/yr.

Only a few wells in the Pasco model area have been drilled very deeply into the lower aquifer, and these wells are widely spaced. For these reasons water-level measurements in deeper wells were very limited, and the manually contoured and simulated heads in the model probably are only rough approximations of the actual head conditions in the Pasco model area. As a result, the computed inflow and outflow figures, in part based on actual head conditions in the model, also are rough approximations.

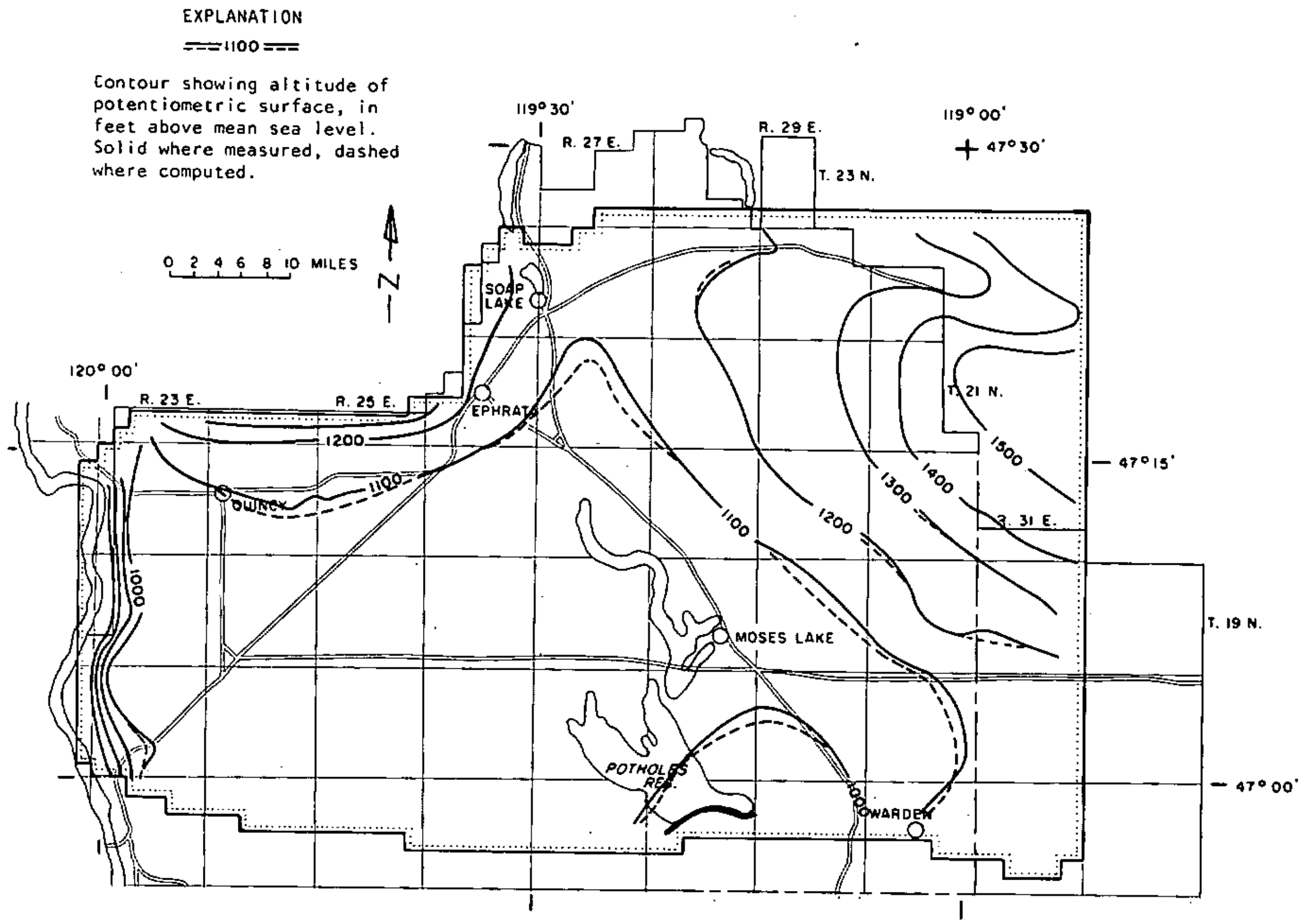

FIGURE 16.–Comparison of contours of pre-irrigation computed and measured heads in the lower aquifer of the Quincy model.

Royal Model

The Royal Slope is bounded on the north by Frenchman Hills and Lind Coulee; on the south by Saddle Mountains and the topographic high ground adjacent to Drumheller Channels; on the east by a westward-sloping basalt surface, and on the west by the Columbia River.

The Royal model (fig. 14) comprises a rectangular grid of 16 by 57 nodes with a node spacing representing 1 mile. The aquifer within the model is represented by about 500 nodes. The Royal model is analyzed as a single aquifer model under steady-state conditions only because available data indicated the upper aquifer was essentially "dry" before irrigation, except along the lower reach of Crab Creek channel. The measured pre-irrigation head map for the lower aquifer is shown in figure 8.

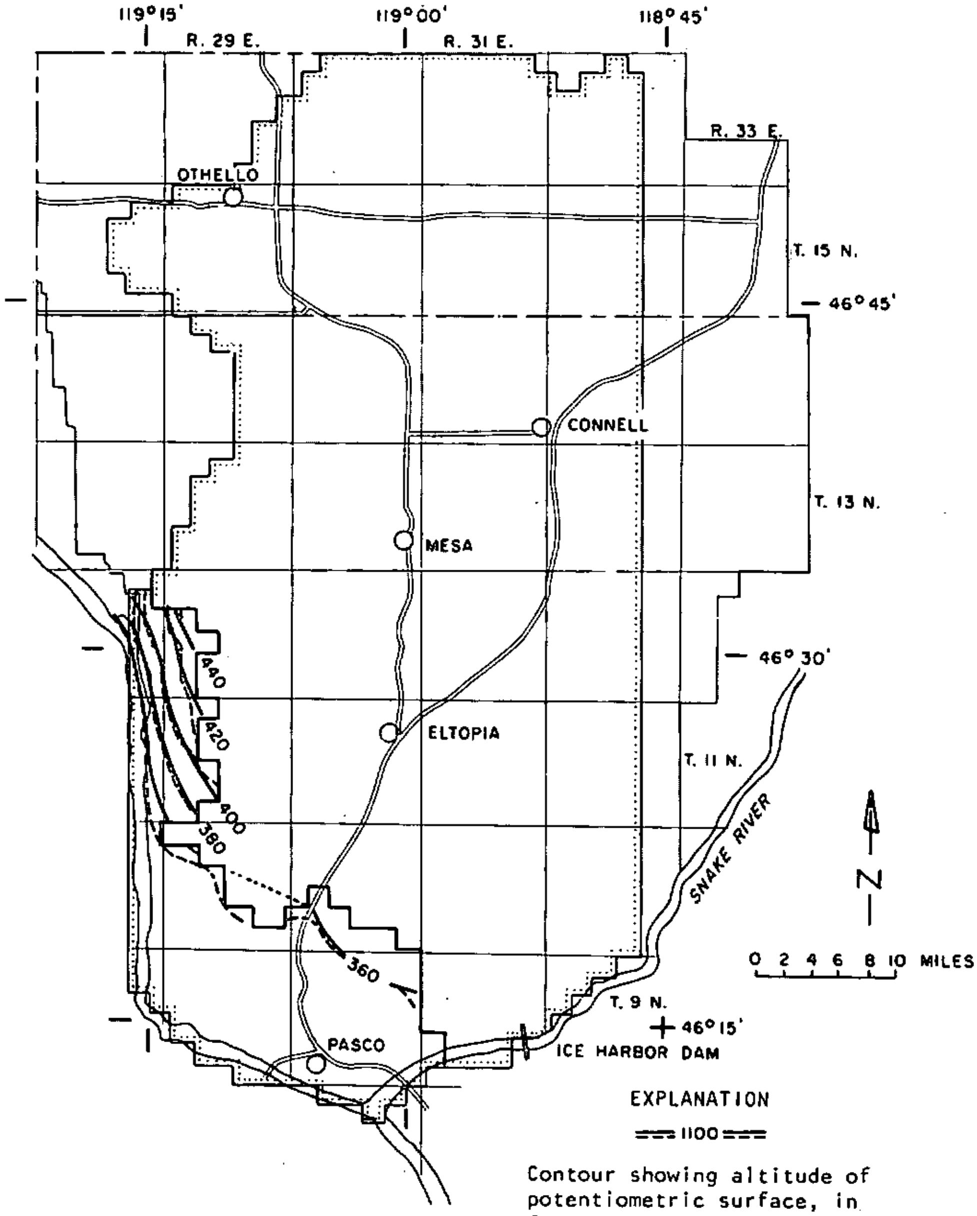

FIGURE 17.—Comparison of contours of pre-irrigation computed and measured heads in the upper aquifer of the Pasco model.

Special boundary conditions

No flow—The Saddle Mountains, a steeply folded, anticlinal structure of basalt, faulted along the strike, is modeled as a barrier to the movement of water. Nodes along the south model boundary that represent Saddle Mountain have zero transmissivities to simulate no-flow conditions.

Streams—Crab Creek is the principal surface drainage for the Royal model. Crab Creek enters from the north, flows southwest through Drumheller Channels until it reaches the valley north of Saddle Mountain, where the flow is due westward to the Columbia River near Beverly. The 10-year (1942-53) average discharge of Crab Creek near Warden was about 40 cfs, and

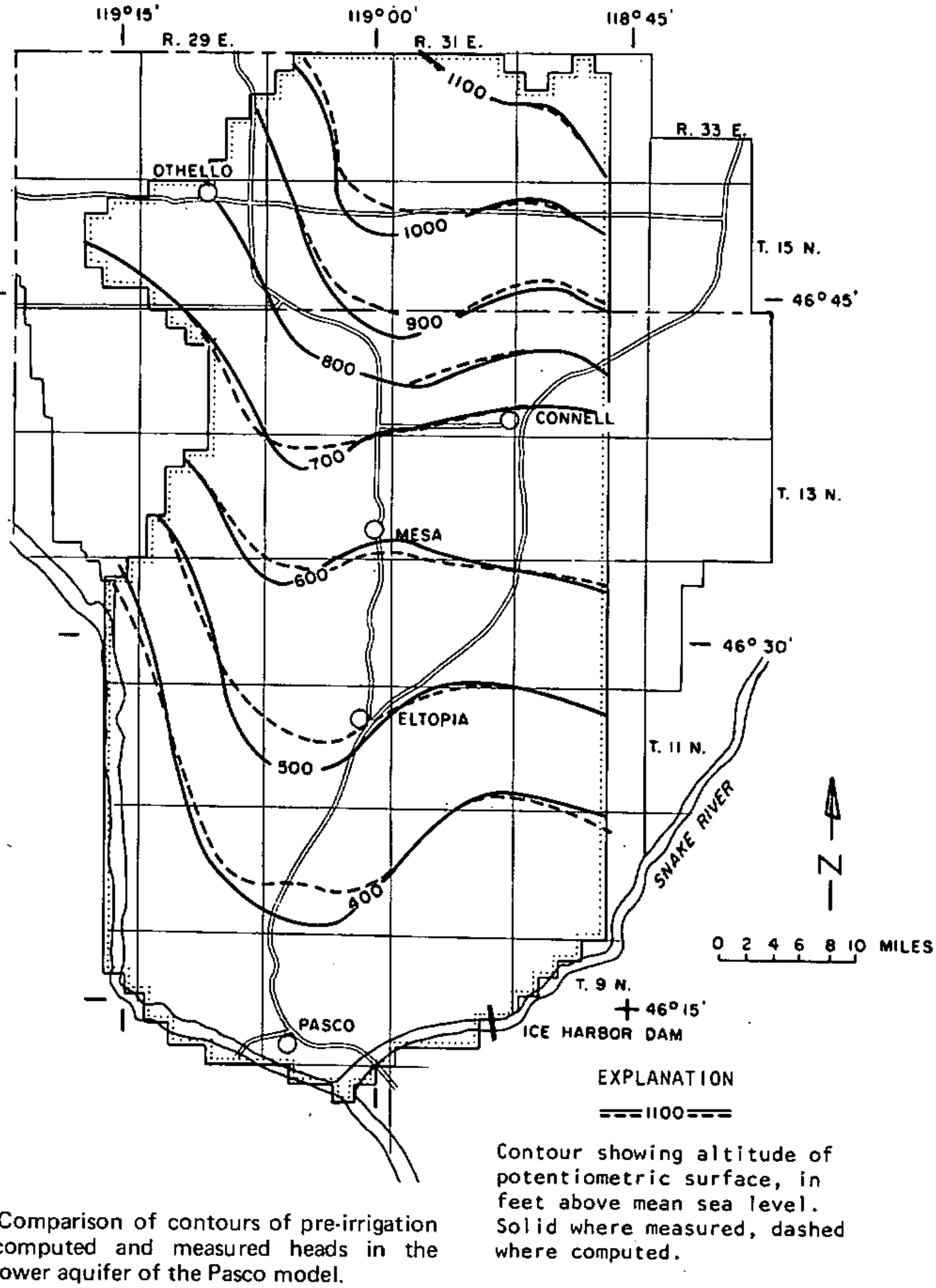

FIGURE 18.—Comparison of contours of pre-irrigation computed and measured heads in the lower aquifer of the Pasco model.

consisted of overflow from Moses Lake augmented by spring flow from Drumheller Channels.

Crab Creek is represented in the model by constant-head nodes, since the pre-irrigation head map indicates that the creek is a line discharge for the lower aquifer.

Lateral flow in the lower aquifer—In accordance with the map showing measured heads, water in the basalt enters the model from the north and northeast and discharges into Crab Creek and the Columbia River at the west boundary (fig. 8).

Results

Head map of the lower aquifer—Contours of the verified computed heads in the lower aquifer are superimposed on contours of the measured heads for comparison (fig. 19).

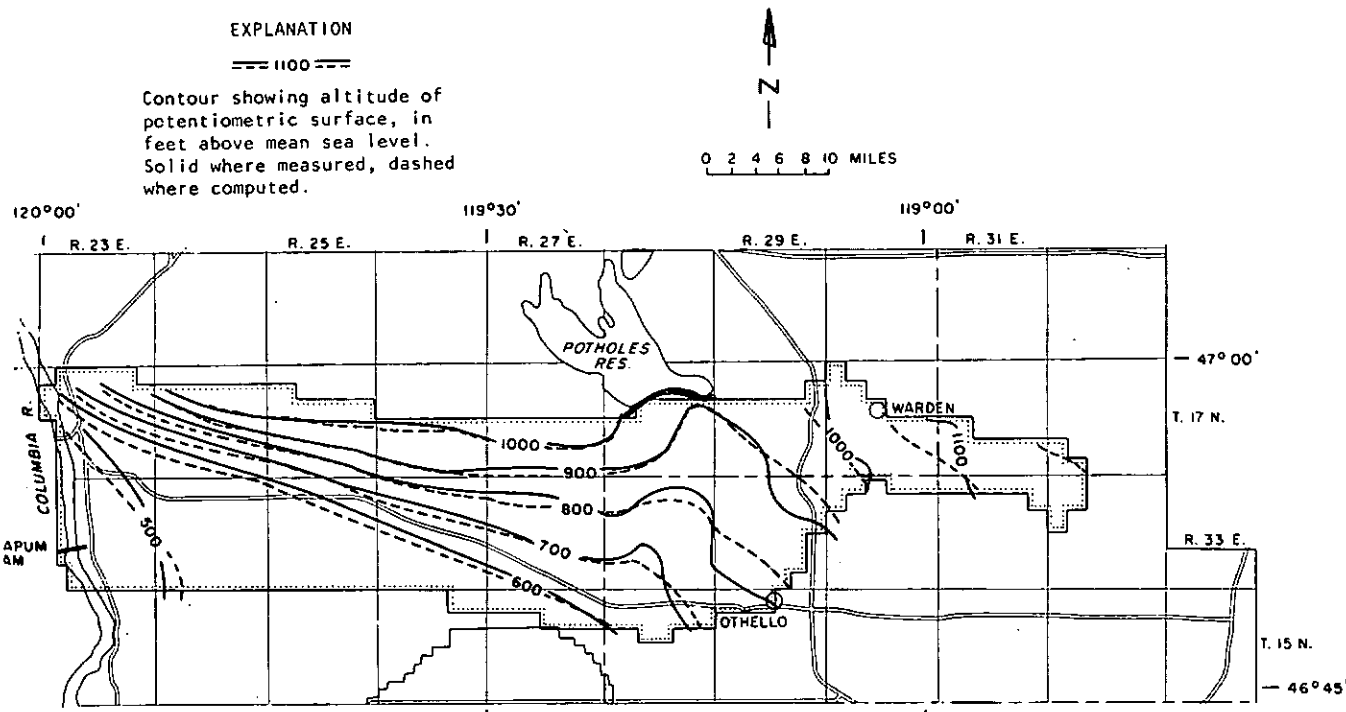

FIGURE 19.—Comparison of contours of pre-irrigation computed and measured heads in the lower aquifer of the Royal model.

The contour interval is 100 feet. The computed and measured contours generally are in agreement, although the reliability of the computed and measured contours is questionable because water-level measurements over most of the model area are not adequate for good control and almost totally lacking in the western part of the area. The maximum difference between computed and measured heads at a node is 28 feet, and over most of the model is about 10 feet.

Inflow and outflow—Analysis of the steady-state balance in the Royal model indicates about 13,500 acre-ft/yr entered and 14,800 acre-ft/yr left the lower aquifer by lateral flow. Net recharge from precipitation was about 1,300 acre-ft/yr to the lower aquifer.

No assurance is given of the reliability of the flow figures computed in the model because the flow computations are based on heads that may not reflect the actual pre-irrigation heads that may not reflect the actual pre-irrigation heads in the west half of the Royal model area where water-level control was not available.

Transient Models

The transient models were derived from the steady-state models by adding simulated storage to both aquifers and including time as an added dimension. All model parameters and natural boundary conditions verified during the steady-state analysis are the initial conditions for the transient models.

A modification was necessary to permit transition from steady to transient analysis in the Quincy and Pasco models by replacing the constant heads on the perimeter nodes of the upper aquifer (except along the Columbia and Snake Rivers in the Pasco model) with either a constant recharge or discharge flow equal to the net rate of flow into or out of the constant head nodes under steady-state conditions. This modification maintains heads initially at and inside the perimeter nodes of the upper aquifer at their steady-state conditions, and allows the heads on the perimeter nodes to fluctuate independently during transient analysis.

Data from the verified steady-state model are used as input data for transient analysis of the three models. These data include verified hydraulic conductivity of the upper aquifer, verified transmissivity of the lower aquifer, elevation at the top of the lower aquifer, infiltration from precipitation, and the verified steady-state heads in both aquifers, with the exception of the Royal model where the upper aquifer was not saturated under steady-state conditions. Additional data necessary for transient analysis that were transferred to appropriate nodes in the model include storage coefficients in the upper and lower aquifers, ground elevation, yearly irrigation-water application, percentage recharge of irrigation water, canal and lateral length, pumpage from the upper and lower aquifers, reservoir hydrograph, and constant heads in the upper and lower aquifers.

Other model parameters required are the initial time, the time step, total length of the simulation period, number of iterations, critical water-table depths (above which maximum evapotranspiration occurs and below which no evapotranspiration occurs), maximum yearly evapotranspiration rate, depth above which maximum drainage from wasteways and drains occurs, maximum drainage rate of wasteways and drains, applied water factor, leakage factors for lined and unlined canals and laterals, saturated thickness to activate surrounding nonsaturated nodes, and initial saturated thickness applied to nonsaturated nodes.

The increase in head in both aquifers indicates the cumulative increase in aquifer storage as a result of the addition of water during the irrigation season. To convert the increase in head in terms of aquifer storage, the difference in head at each node between any designated period is multiplied by the specific yield of the upper aquifer or by the storage coefficient of the lower aquifer, and the change in volume of water stored is cumulated. The small increase in the storage in the lower aquifer compared to the large increase in that of the upper aquifer is due mainly to the relatively small storage coefficient of the lower aquifer which is under artesian pressure.

The transient model was calibrated by matching computed heads to heads measured during 1958 and 1963. Heads were matched primarily by adjusting large artificial stresses such as irrigation and leakage from canals and laterals. Changes also were made in the storage coefficients for both aquifers, and in the hydraulic conductivity outside the nodes of the upper-aquifer perimeter which was not verified during steady-state analysis. Repeated adjustments of individual variable parameters were necessary to isolate the effects of each change on heads in both aquifers. Finally, these changes were combined and further adjustments made to obtain a fit with heads measured in 1958 and 1963.

After the model was calibrated, the analysis was continued through steps representing 5 more years, and the computed and measured heads for 1968 are compared. If the heads were reasonably matched, the model was considered verified; if additional changes were necessary, more emphasis was placed on matching to heads measured in 1968 in order to verify the model over the longest time period.

Man-Made Stresses

Artificial boundary conditions due to man-made stresses are simulated by appropriate head or flow conditions.

Recharge as a result of irrigation and canal and lateral leakage is simulated as a specified vertical flux into the aquifer at each time step. Conversely, discharge from wasteways and drains, evapotranspiration, and pumping are simulated as a specified vertical flux out of the aquifer at each time step. Lateral inflow to and outflow from the model boundary of the lower aquifer are simulated by adjusting heads on the boundary nodes so as to maintain a specified gradient with an adjacent interior node at each time step, to permit the head at the boundary to conform with any hydrologic stress imposed near the boundary.

Artificial stresses, which include recharge from irrigation, expansion of saturated areas, recharge from canal and lateral leakage, discharge from wasteways and drains, increased discharge by evapotranspiration as water levels rise closer to land surface, and discharge by pumping wells, are simulated in the same manner in all three models. Simulation of Potholes and Scooteney Reservoirs (fig. 21), created as part of the irrigation distribution system, are special boundary conditions that apply to only the Quincy and Pasco models, respectively.

Recharge from irrigation

The amount of water delivered yearly to farms in the Columbia Basin Irrigation Project is shown in table 4. Irrigation began in 1952 with 96,000 acre-feet of water applied on 22,000 acres, and water delivery has increased steadily each year to 1.9 million acre-feet applied on 449,000 acres in 1967.

The irrigation blocks, and the first year of water application are shown in figure 20. Records are available on the total irrigated acres of, and the yearly amount of water supplied to, each irrigation block. The number of irrigated acres for each node within the irrigation block was summed, and the amount of water applied to a node was determined as a proportion of its irrigated acres to the total irrigated acres and water applied on the irrigation block.

The amount of water applied to the fields averages more than 4 acre-feet per acre; of this, a part percolates downward to recharge the upper aquifer. The percolation percentages used in this study, adapted from results of unpublished records of drainage investigations by the Bureau of Reclamation in the CBIP, ranged from 19 to 37 percent and were adjusted downward to about 80 percent of the initial values during model verification.

Recharge to the upper aquifer from water applied for irrigation is simulated as the product of the acre-feet applied and the percolation percentage for that node. This amount is applied as a flux to the upper aquifer at each time step during the irrigation season.

Expansion of saturated areas

The area outside the perimeter nodes of the upper aquifer is assumed to be unsaturated at the beginning of transient analysis. As a result of irrigation parts of the area represented by those outside nodes become saturated. In the model, a method was devised to allow the saturated area to expand. Because unsaturated nodes, by definition, have no hydraulic conductivity, the basic model was unable to simulate movement of the water laterally downgradient across the unsaturated nodes. To permit lateral movement to take place from saturated to unsaturated areas, the model was revised to permit expansion when the head reached 2 feet or more at any saturated node. To accomplish this, at each time step the model searches for an unsaturated node whose basalt-surface elevation is equal to or lower than the head in an adjacent saturated node. An unsaturated node that meets the above condition arbitrarily is assigned 1 foot of head. When the head in the newly saturated node equals or exceeds 2 feet, the process is repeated on adjacent unsaturated nodes to continue the expansion of the saturated area.

Recharge from canal and lateral leakage

The extent and type of canals and laterals by which irrigation water is distributed to farms are shown on lateral and lateral-lining maps published by the Bureau of Reclamation for each irrigation block. Only the main canal and wasteway system are shown in figure 21. A typical irrigation block is shown in figure

TABLE 4.—Quantity of water applied on irrgated acres during the period 1952-67

Year	Quantity delivered to farms (acre-ft)	Land irrigated (acres)	Average quantity of water applied per irrigated acre (acre-ft)	New irrigation block number
1952	95,960	21,552	4.4	40, 41, 70, 701, 71, 72
1953	263,894	57,031	4.6	11, 42, 49, 73
1954	450,215	98,233	4.6	12, 15, 43, 74, 75
1955	657,170	148,125	4.4	13, 16, 44, 76, 78
1956	757,270	175,046	4.3	19, 45, 86, 87
1957	821,030	202,006	4.1	14, 18, 421, 47, 89
1958	1,044,810	237,204	4.4	401, 46, 77, 79
1959	1,051,800	265,103	4.0	20, 85
1960	1,209,840	294,242	4.1	82, 881
1961	1,337,360	311,713	4.3	201, 83, 88
1962	1,361,100	342,970	4.0	80
1963	1,494,960	367,091	4.1	23
1964	1,638,270	385,254	4.2	17
1965	1,727,470	407,762	4.2	81, 741
1966	1,867,910	429,229	4.4	(none)
1967	1,902,980	448,698	4.2	21, 48

23 to illustrate the intricate network of lined and unlined canals, laterals, and wasteways which distribute or remove water from individual farms. Using the information from these maps, the length, in miles, for all lined and unlined laterals and wasteways is summed up for each node in the model and leakage factors are applied to estimate both recharge from the distributary system and discharge to the wasteways.

According to the Bureau of Reclamation, canals range in width from 8 to 40 feet. Most main canals are about 30 feet wide and lined with concrete. Branch canals are 15 to 20 feet wide and mostly unlined, or else lined with compacted earth. Laterals range in width from 4 to 12 feet, but most are about 6 feet and unlined. There are 331 miles of canals, of which 170 miles are lined and 161 miles are unlined; 1,231 miles

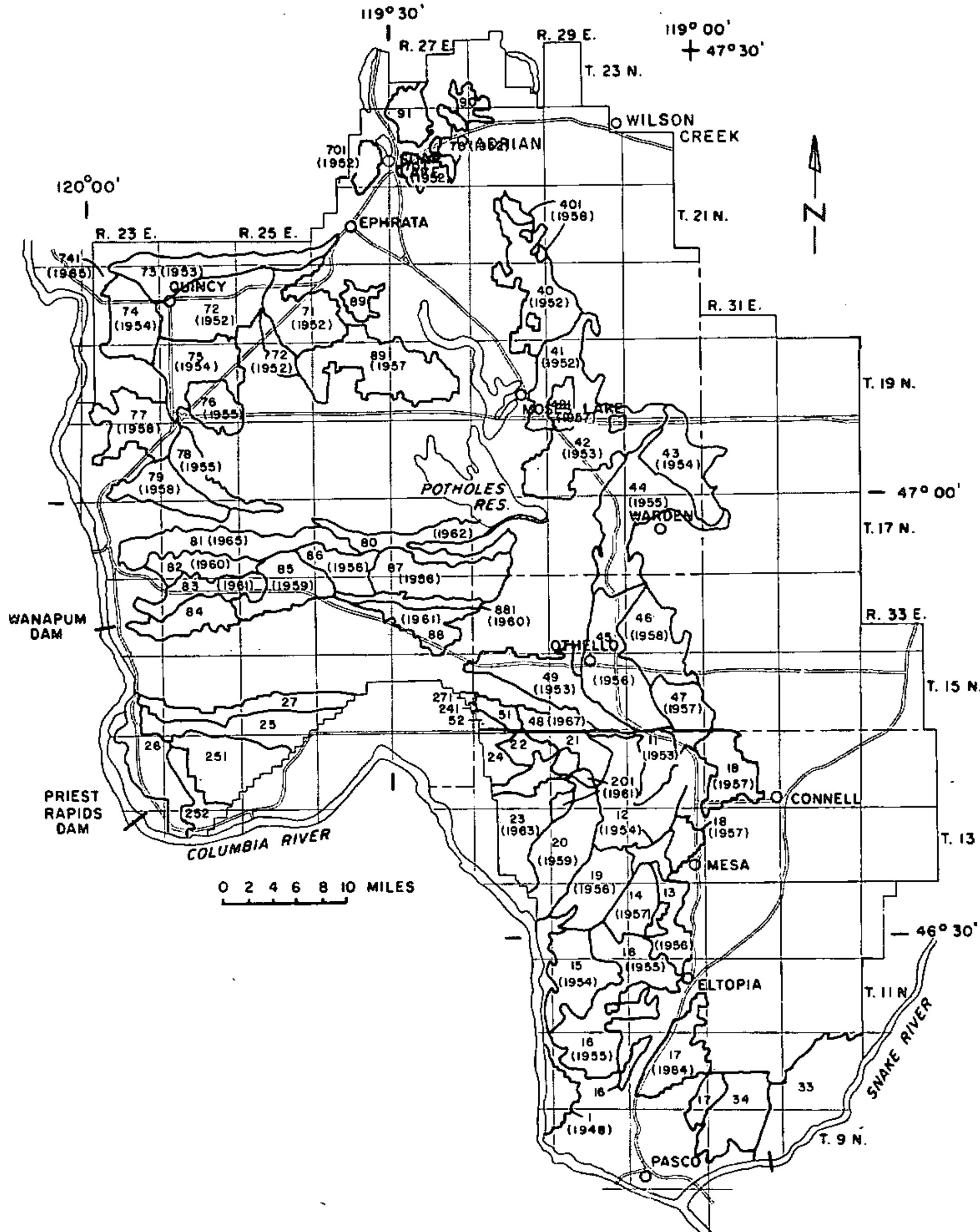

FIGURE 20.—Map showing irrigation blocks and first year of water application. Blocks with no year were undeveloped as of 1967.

of laterals, of which 673 miles are lined and 558 miles are unlined. Lining materials for canals and laterals include concrete, asphaltic concrete, compacted earth, and buried membrane; however, the leakage factor used in this report does not consider the lining material, but only whether the canal and lateral is lined or unlined.

Since 1963, the Bureau of Reclamation conducted yearly ponding tests on canals and laterals after each irrigation season to determine the rate of seepage loss in selected areas of the irrigation-distribution system. The leakage rates observed from ponding tests from 1963 through 1967 (unpublished records) are plotted against the length of the wetted perimeter to determine approximate leakage factors for canals and laterals to use during model simulation (fig. 23). The tests are usually made in locations where excessive leakage is suspected, so leakage factors selected for use in the

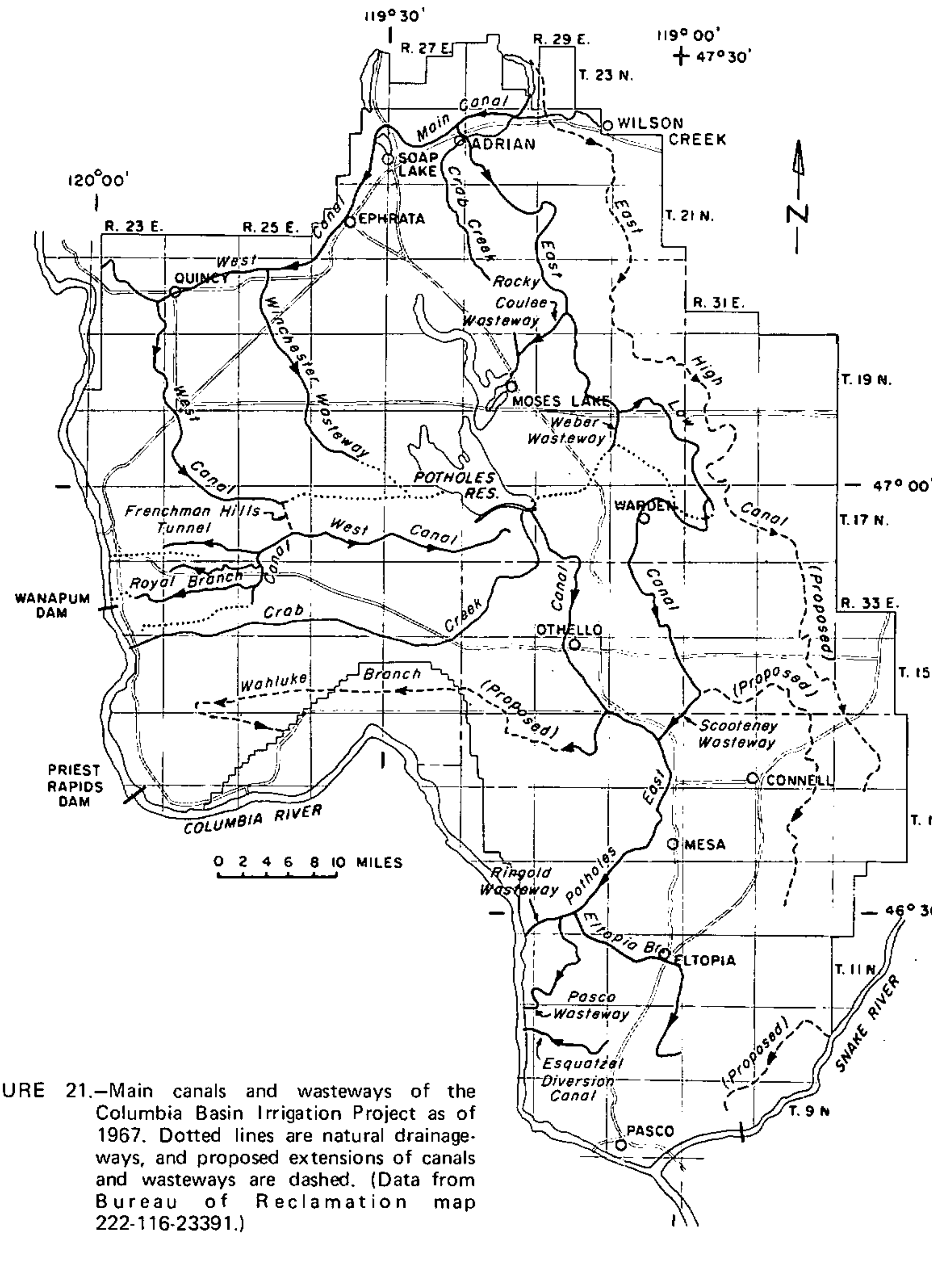

FIGURE 21.—Main canals and wasteways of the Columbia Basin Irrigation Project as of 1967. Dotted lines are natural drainageways, and proposed extensions of canals and wasteways are dashed. (Data from Bureau of Reclamation map 222-116-23391.)

model study were made smaller in value than indicated on the graph in order to represent more closely the average leakage conditions of all canals and laterals during the irrigation season.

Figures from the Bureau of Reclamation's "Monthly Water Distribution" publication for the CBIP show that significant amounts of water leak from canals and laterals (fig. 24). The graph indicates that 48 to 21 percent of the net supply of irrigation water during a year is lost by canal and lateral leakage during transit to farms. The percentage was highest during the initial few years of irrigation, and trended downward to about 20 percent as water levels in the upper aquifer rose near land surface.

Canal and lateral leakage additions to inflow to the ground-water system are simulated as the product of the lengths, in miles, of all canals and laterals in each node area, and the approximate leakage factor

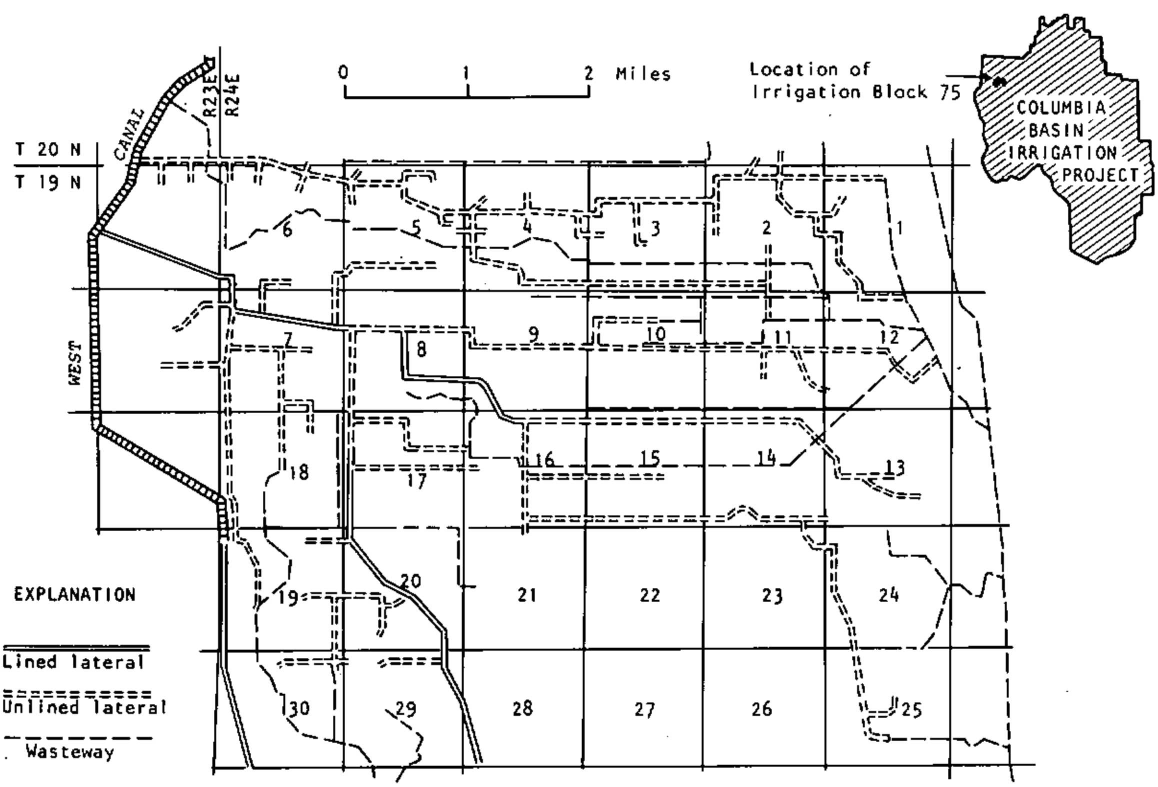

FIGURE 22.—Laterals and wasteways in Irrigation Block 75.

(cfs/mile) for lined or unlined canals or laterals from figure 23. Greater leakage is provided during the first few years of simulation, as suggested by figure 24.

Discharge by wasteways and drains

Wasteways remove excess surface and ground water from the fields by a system of dug channels that augment the natural drainage network of the area. Ground water discharges into the drainage system when the water table rises near land surface and gradients are toward the natural or artificial channels. Wasteways generally are not lined, so initially leakage from the wasteways can recharge the aquifer at places where the water table is lower than the wasteway channel until water levels rise above the level of the wasteways. Consequently, wasteways are sources of

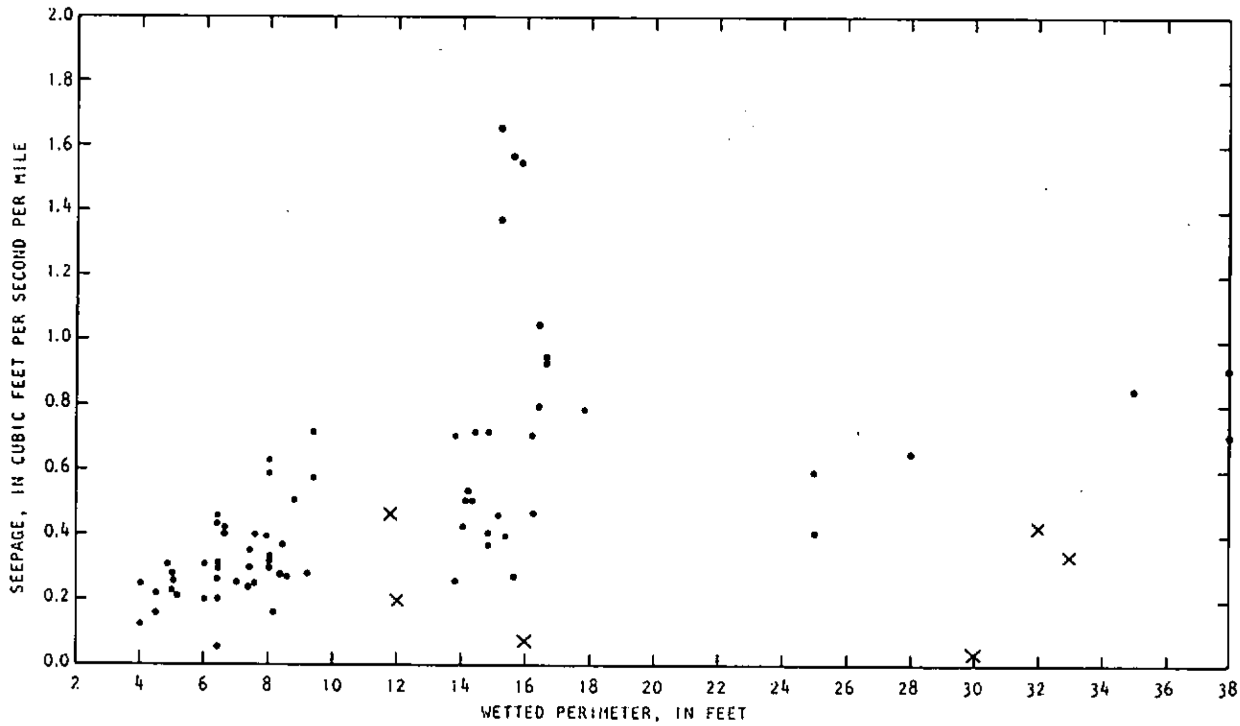

FIGURE 23.—Relation of seepage rate to wetted perimeter of canals and laterals. Crosses indicate lined canals and laterals.

recharge to or discharge from ground water depending on the position of the water table.

Tile drains are part of the artificial drainage system and most are placed 8 feet below land surface to limit the rise of the water table and prevent waterlogging under agricultural land. The amount of drainage possible depends, in part, on the total length of drains in the area. Design yields from tile drains adopted by the Bureau of Reclamation for this project range roughly from 3 to 6×10^{-5} cfs (cubic feet per second) per linear foot of drain. If 2 miles of drainage per square mile is assumed as an overall average for tile drain installation in the Quincy Basin, the amount drainable would be 0.3 to 0.6 cfs per square mile of irrigated area. All discharge from tile drains enters the wasteway system.

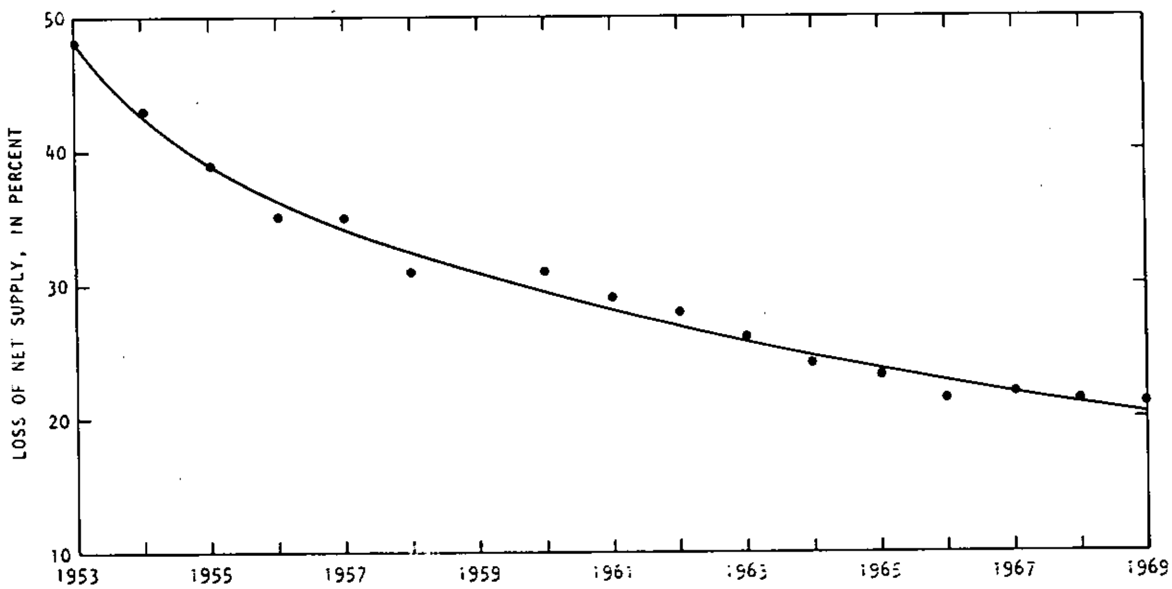

FIGURE 24.—Percentage loss of water from leakage from canals and laterals, 1953-69.

The drainage from wasteways and tile drains is combined for simulation in the model because both function in a similar manner by draining ground water as it approaches land surface. Ground-water discharge by wasteways and tile drains is simulated as a discharge flux that varies inversely with depth to water from land surface. This mode of discharge in the model is restricted to nodal areas that contain laterals or wasteways, since the assumption is made that tile drains are constructed where there are laterals. Discharge is initiated when the head in the upper aquifer is 8 feet or less from land surface, and is increased linearly to a maximum rate of 2 cfs per node when the head rises within 4 feet of the land surface (fig. 25).

During the initial period of irrigation, when the water table was well below land surface, wasteways recharged the upper aquifer in the same manner as laterals. Recharge is simulated for nodal areas with

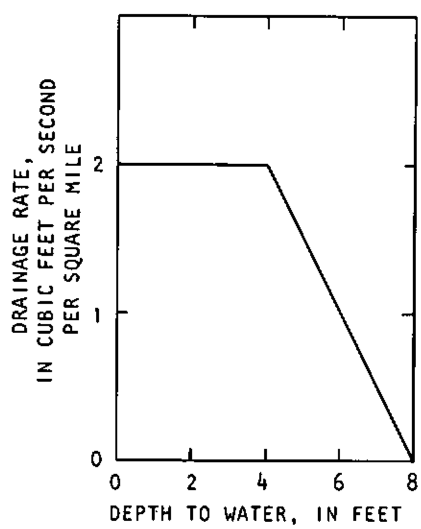

FIGURE 25.—Relation of drainage from tile drains and wasteways to depth to water.

wasteways when the water table is greater than 8 feet below land surface. The amount of recharge from this source to the upper aquifer is the product of the wasteway length, in miles, and the wasteway leakage factor, in cubic feet per second per mile.

Increased discharge by evapotranspiration

The calculated rate of discharge by evapotranspiration is approximated by a linear function of the difference in elevation between land surface and the water table. Discharge by evapotranspiration is based on the assumption that the upward flow of water increases as the water table approaches land surface. Discharge by evapotranspiration is assumed to be zero when the water table is 10 feet from land surface and increases linearly to a maximum rate when the water table is 2 feet or less from land surface (fig. 26). A

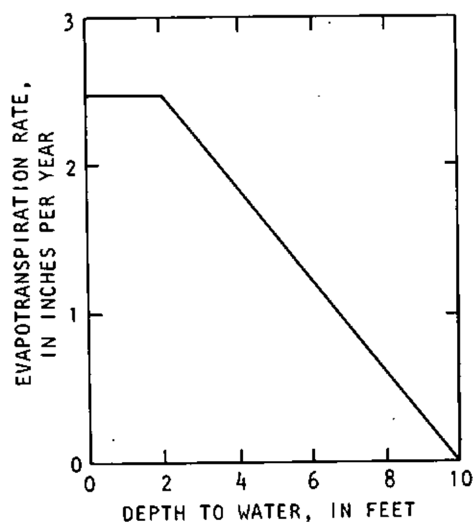

FIGURE 26.—Relation of ground-water-evapotranspiration rate to depth to water.

maximum evapotranspiration rate of 30 inches per year was computed by the Blaney-Criddle method for irrigated areas in the project.

Discharge by pumping wells

A substantial number of wells in the Quincy Basin area are pumped for irrigation, municipal, and industrial supplies. Nearly all municipal and industrial pumpage is from the lower aquifer. Most irrigation wells, before and after project irrigation began, pump water from the lower aquifer, although since 1969 a substantial amount of water has been pumped for irrigation from the upper aquifer by private developers west of Moses Lake. There is no irrigation pumpage of ground water inside the boundaries of the irrigation blocks.

Pumping rates for irrigation are estimates based on available information from well records, previous publications, and inquiry of the irrigators, or are calculated from electrical power consumption derived from meters at the well or furnished by power-supply companies. Industrial and municipal pumping rates are based on information from the well records, previous publications, and data compiled for water-use studies for the State of Washington (Laird and Walters, 1967; Parker, 1971).

Information usually is not available for most wells on the yearly pumpage; therefore, in the models, estimates were made of the average yearly pumpage for 5-year intervals, based on data available during that period. At each 5-year interval the previous estimate is adjusted to conform with any new pumpage data that are available.

Two pumping categories are used in the model: seasonal (irrigation) and yearly (municipal and industrial). Irrigation pumpage is simulated for 6 months of the year to coincide with the irrigation season while municipal and industrial pumpage is used as a constant rate throughout the year.

Quincy Model

Special boundary condition

Potholes Reservoir—Potholes Reservoir was created as a part of the irrigation distribution system with the impoundment of Crab Creek by O'Sullivan Dam in 1952. Potholes Reservoir occupies the topographic low point in the Quincy Basin, so most surplus irrigation water eventually reaches the reservoir, either as surface water or ground-water flow. Potholes serves as a collection reservoir for the Quincy Basin and as a distribution reservoir for most of the irrigated land to the south.

The hydrograph of Potholes Reservoir is shown in figure 27. Subsequent to reaching operating level about 1956, the reservoir stage fluctuated annually about 8 to 18 feet. Land inundated by the reservoir is relatively flat, so large stage fluctuations cause the reservoir to increase or decrease appreciably in size as well as causing changes in the ground water-surface water relation near the reservoir.

The expansion in size of Potholes Reservoir from its beginning in 1952 to its operating size in 1956 is simulated in the model by comparing the stage of the reservoir hydrograph with ground elevation at the nodes in the reservoir area at appropriate 90-day intervals; all nodes where the stage of the reservoir is higher than ground elevation represent the reservoir during that particular time step. In this manner, the reservoir's area was increased at 90-day intervals to its operating size; thereafter, the reservoir area expands and contracts slightly each year relative to the stage of the reservoir.

Results

Head maps of the upper and lower aquifers—Contours of the verified computed heads, after simulating 16 years of irrigation, are superposed on contours of heads measured in 1968 for the upper and lower aquifer for comparison (figs. 28 and 29). As figure 28 shows, the computed and measured contours generally agree for the upper aquifer. The upper aquifer during steady-state analysis is outlined to indicate the extent of lateral expansion of the saturated zone as a result of irrigation.

Contours of the lower aquifer (fig. 29) agree in approximate shape over most of the model but lack agreement in specific areas. Closer conformance of the computed and measured contours in the lower aquifer was not attempted due to head differences mentioned previously.

Change in aquifer storage—The cumulated increase in storage in the upper and lower aquifers after 6, 11, and 16 years of irrigation are plotted (fig. 30). Storage of water in the upper and lower aquifers from 1952 to 1968 increased by 2.7 million acre-feet and 29 thousand acre-feet, respectively.

The net amount of water added to each aquifer is plotted for the intervals 1952-58, 1958-63, and 1963-68 (fig. 31). The graphs show that the amount of water added to storage at each interval became progressively smaller as increasingly larger areas became fully saturated and were unable to store additional water. The net amount of water added to storage in the upper and lower aquifers in the 1963-68 interval is small compared to the total volume added before 1968, indicating there will not be any substantial increase in the amount of water added to storage in the upper and lower aquifers after 1968 under the present irrigation application and pattern.

The increase in storage between 1952-68 in the upper and lower aquifers in the Quincy model is outlined in acre-feet of water per square mile (figs. 32 and 33).

The largest storage increase since 1952 in the upper aquifer is in Tps. 19 and 20 N., Rs. 24 and 25 E., and parts of surrounding townships, where increases of more than 5,000 acre-feet per square mile are indicated (fig. 32). The storage increase in the lower aquifer is much smaller. The largest gain in storage is in T. 20 N., Rs. 23 and 24 E., and parts of surrounding townships where increases over 60 acre-feet per square mile are indicated (fig. 33).

Pasco Model

Special boundary condition

Scooteney Reservoir—Scooteney Reservoir in T. 14 N., R. 30 E., secs. 10 and 15 (fig. 21), was formed in 1953 as part of the irrigation distribution system, and reached operating size in 1954. The water level in the reservoir fluctuates 8 to 12 feet during the irrigation season, but the two nodes representing Scooteney Reservoir in the model are simulated as a constant head equal to the average operating water-level elevation because the reservoir is small and the annual stage fluctuations have little hydrologic effect on the surrounding area.

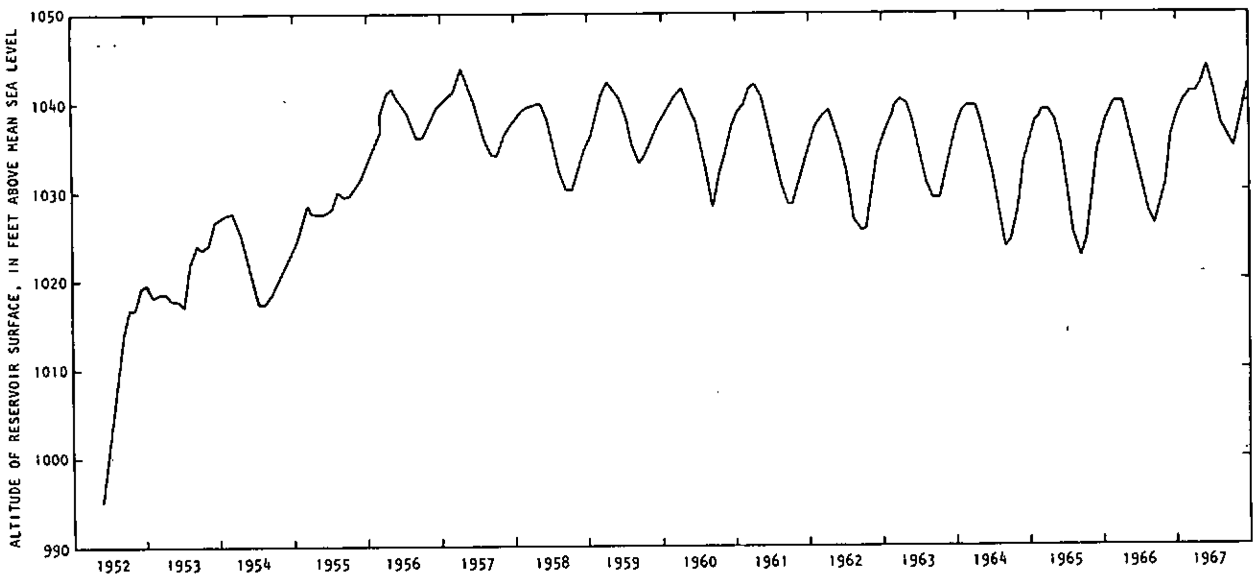

FIGURE 27.—Hydrograph showing fluctuations of surface of Potholes Reservoir, 1952-67.

Results

Head maps of the upper and lower aquifers—Contours of the computed heads, after simulating 16 years of irrigation, are superposed on contours of heads measured in 1968 for the upper and lower aquifers for comparison (figs. 34 and 35). The computed and measured contours of the upper and lower aquifers generally agree in approximate shape and are within a few tens of feet of each other over most of the model area. The computed and measured contours of both aquifers differ most near the model boundary along the Columbia River where the hydraulic gradients are steep. The large differences between the computed and measured heads in this area probably are the result of inadequate and unreliable water-level data.

Change in aquifer storage—The cumulated increase

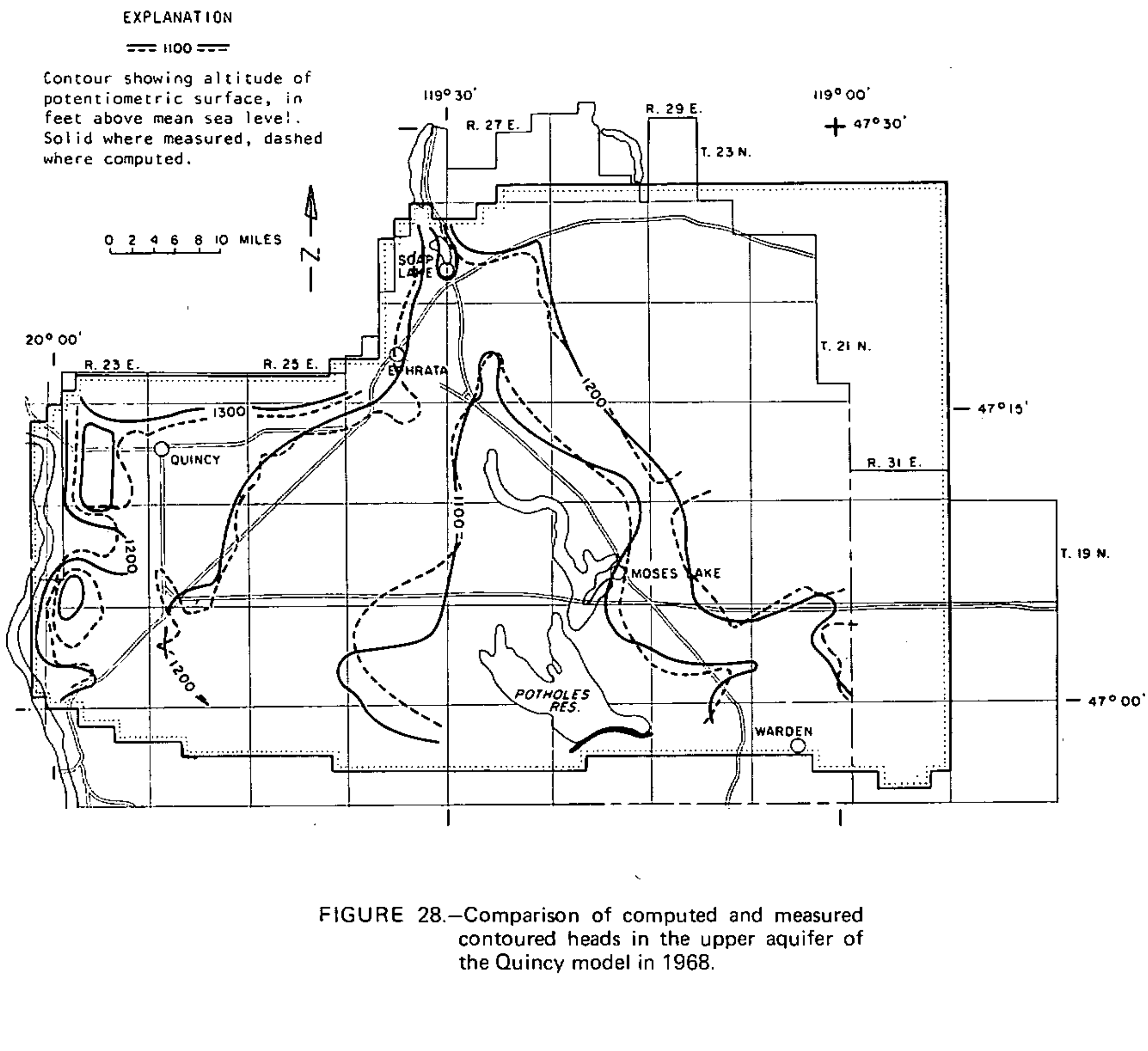

FIGURE 28.—Comparison of computed and measured contoured heads in the upper aquifer of the Quincy model in 1968.

in storage in the upper and lower aquifers after 6, 11, and 16 years of irrigation are plotted (fig. 36). Storage of water in the uper and lower aquifers from 1952 to 1968 increased by 3.8 million acre-feet and 23 thousand acre-feet, respectively.

The net amount of water added to each aquifer is plotted for the intervals 1952-58, 1958-63, and 1963-68 (fig. 37). The graphs indicate that the greatest amount of water added to storage in the upper and lower aquifers occurred in the 5-year interval 1958-63. Even though more land was irrigated in the interval 1963-68, less water was added to storage in both aquifers, indicating that progressively less water will be added to the storage in both aquifers in the future.

The increase in storage between 1952-68 in the upper and lower aquifers in the Pasco model is outlined in acre-feet of water per square mile (figs. 38 and 39).

The largest storage increase since 1952 in the upper

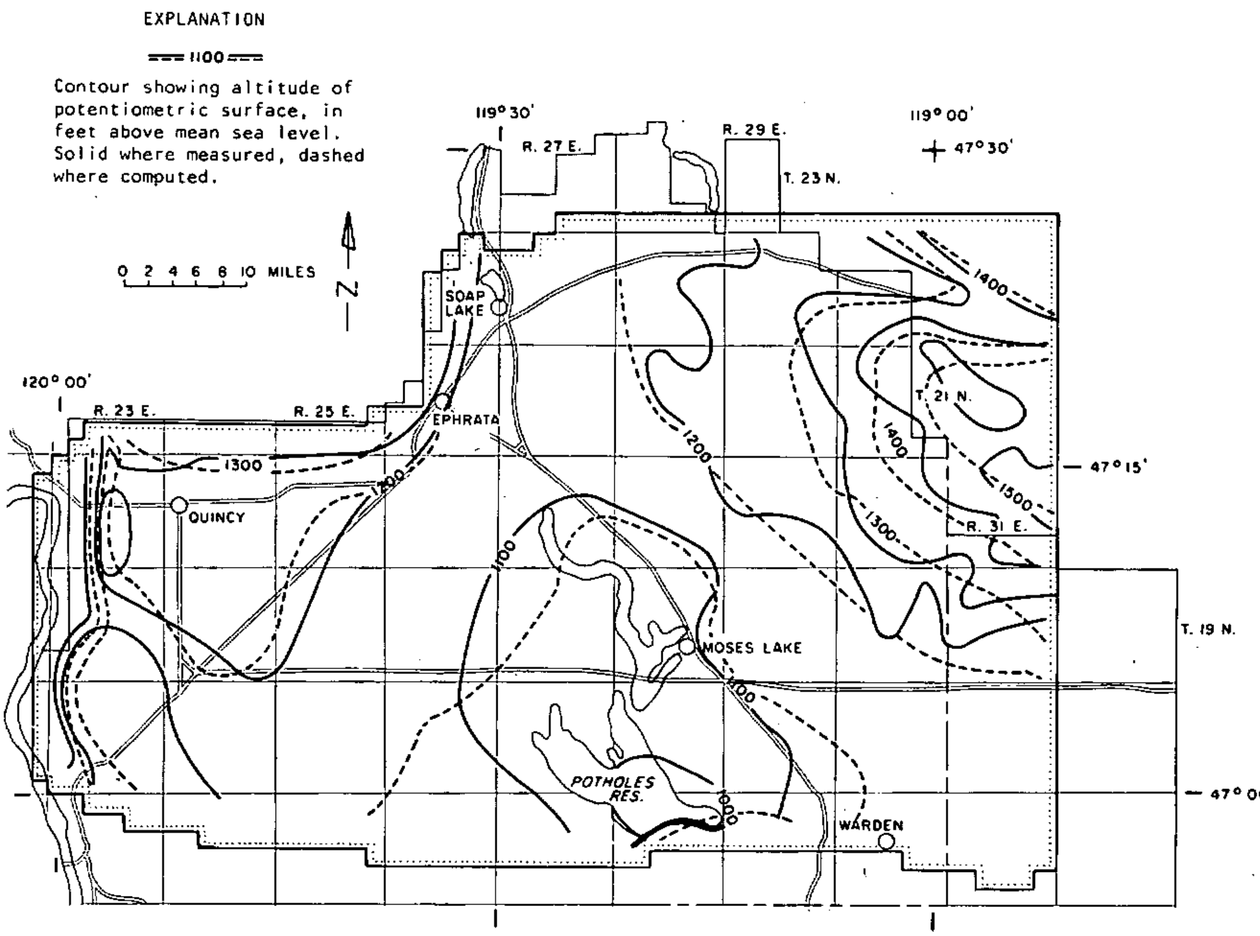

FIGURE 29.–Comparison of computed and measured contoured heads in the lower aquifer of the Quincy model in 1968.

aquifer is in Tps. 11 and 12 N., R. 29 E., and T. 15 N., Rs. 11 and 12 E., where increases exceeding 10,000 acre-feet per square mile are indicated (fig. 38). The storage increase in the lower aquifer is much smaller and more uniform. The area where the storage in the lower aquifer increased between 30 and 60 acre-feet per square mile is outlined in figure 39.

Royal Model

Results

Head maps of the upper and lower aquifers—Contours of the verified computed heads, after simulating 16 years of irrigation, are superposed on contours of heads measured in 1968 for the upper and lower

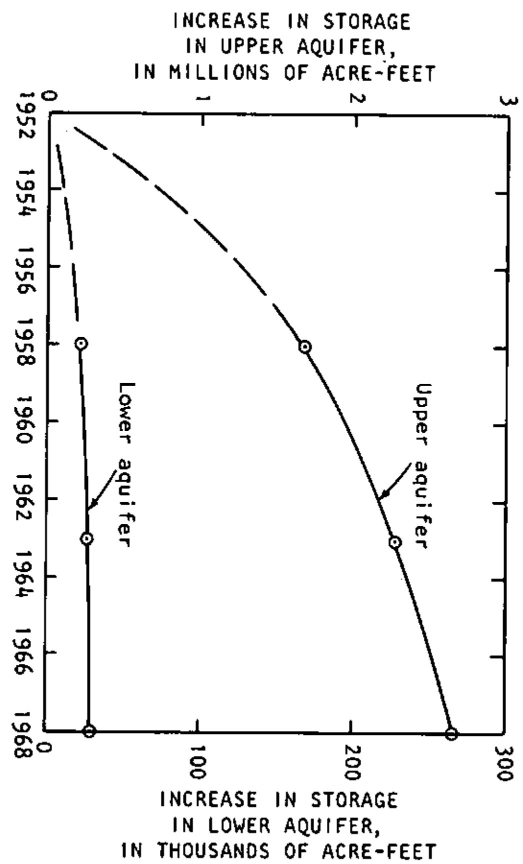

FIGURE 30.—Cumulative increase in storage of water in the upper and lower aquifers in the Quincy model, based on computations for 1958, 1963, and 1968.

aquifer for comparison (figs. 40 and 41). The computed and measured contours in the upper aquifer agree generally over most of the model except near the western margin of the model in Rs. 23 and 24. The lack of agreement probably is due mainly to inaccuracies in the pre-irrigation head map resulting from the lack of water-level control in the western half of the model area. Heads higher than 1,200 feet above sea level in the Frenchman Hills area were computed in the model for the upper and lower aquifers, but the heads were not substantiated because water-level measurements were not available.

Change in aquifer storage—The cumulated increase in storage in the upper and lower aquifers after 6, 11, and 16 years of irrigation are plotted (fig. 42). Storage of water in the upper and lower aquifers from 1952 to 1968 increased by 750 thousand acre-feet and 14 thousand acre-feet, respectively.

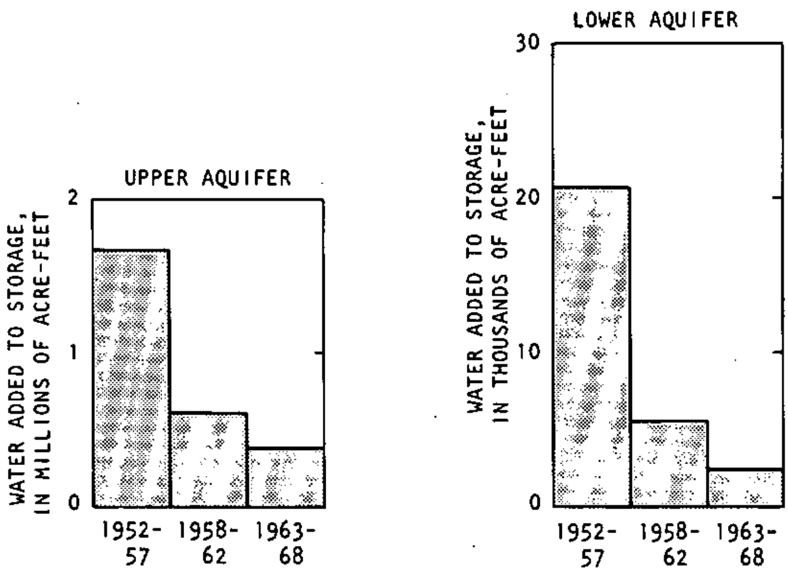

FIGURE 31.—Water added to the upper and lower aquifers of the Quincy model, for the periods 1952-58, 1958-63, and 1963-68.

The net amount of water added to each aquifer is plotted for the intervals 1952-58, 1958-63, and 1963-68 (fig. 43). The graphs show that the amount of water added to storage at each interval became progressively smaller as increasingly larger areas became fully saturated and were unable to store additional water. The net amount of water added to storage in the upper and lower aquifers in the interval 1963-68 is small compared to the total volume added, indicating that irrigation continued after 1968 will not substantially increase the amount of water stored in the upper and lower aquifers.

The increase in storage between 1952-68 in the upper and lower aquifers in the Royal model is outlined in acre-feet of water per square mile (figs. 44 and 45).

The largest storage increase since 1952 in the upper aquifer is in the north half of T. 15 N., R. 28 E., where

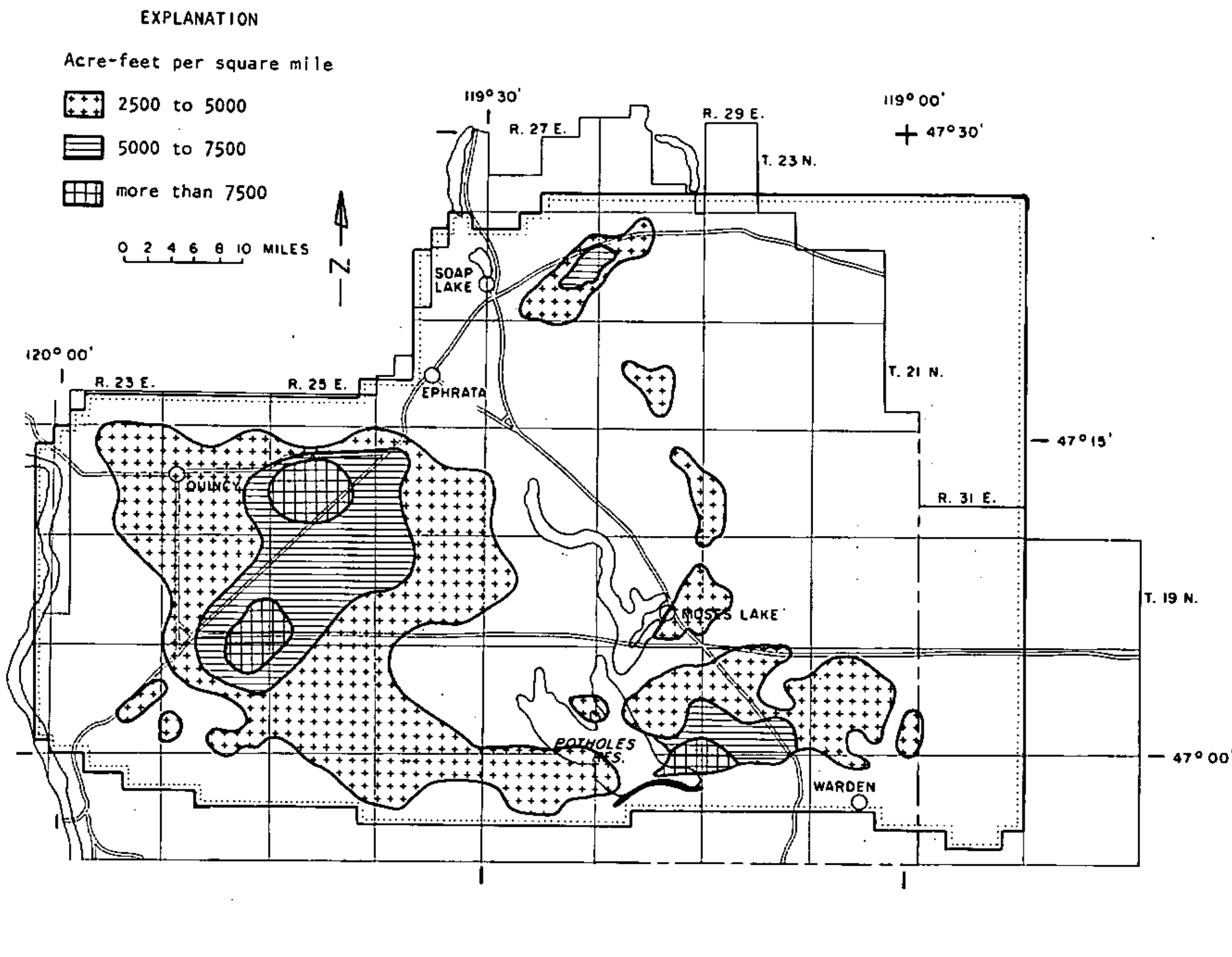

FIGURE 32.—Quantities of water added to storage in the upper aquifer of the Quincy model from 1952 to 1968.

increases of more than 10,000 acre-feet per square mile are indicated. Also, storage in the north half of T. 16 N., Rs. 26 and 27 E., and parts of surrounding townships increased more than 5,000 acre-feet per square mile (fig. 44). The storage increase in the lower aquifer is again much smaller. The largest gain in storage, shaped as an elongated band, is in Tps. 16 and 17 N., Rs. 23 to 27 E., where increases exceeding 60 acre-feet per square mile are indicated (fig. 45).

SUMMARY AND CONCLUSIONS

Three digital computer models were designed to determine the hydrologic conditions before and after irrigation in the Columbia Basin Irrigation Project area, and for possible future use as a tool for ground-water management. The three models were designed using available geologic and hydrologic data, and were considered verified for steady-state and transient con-

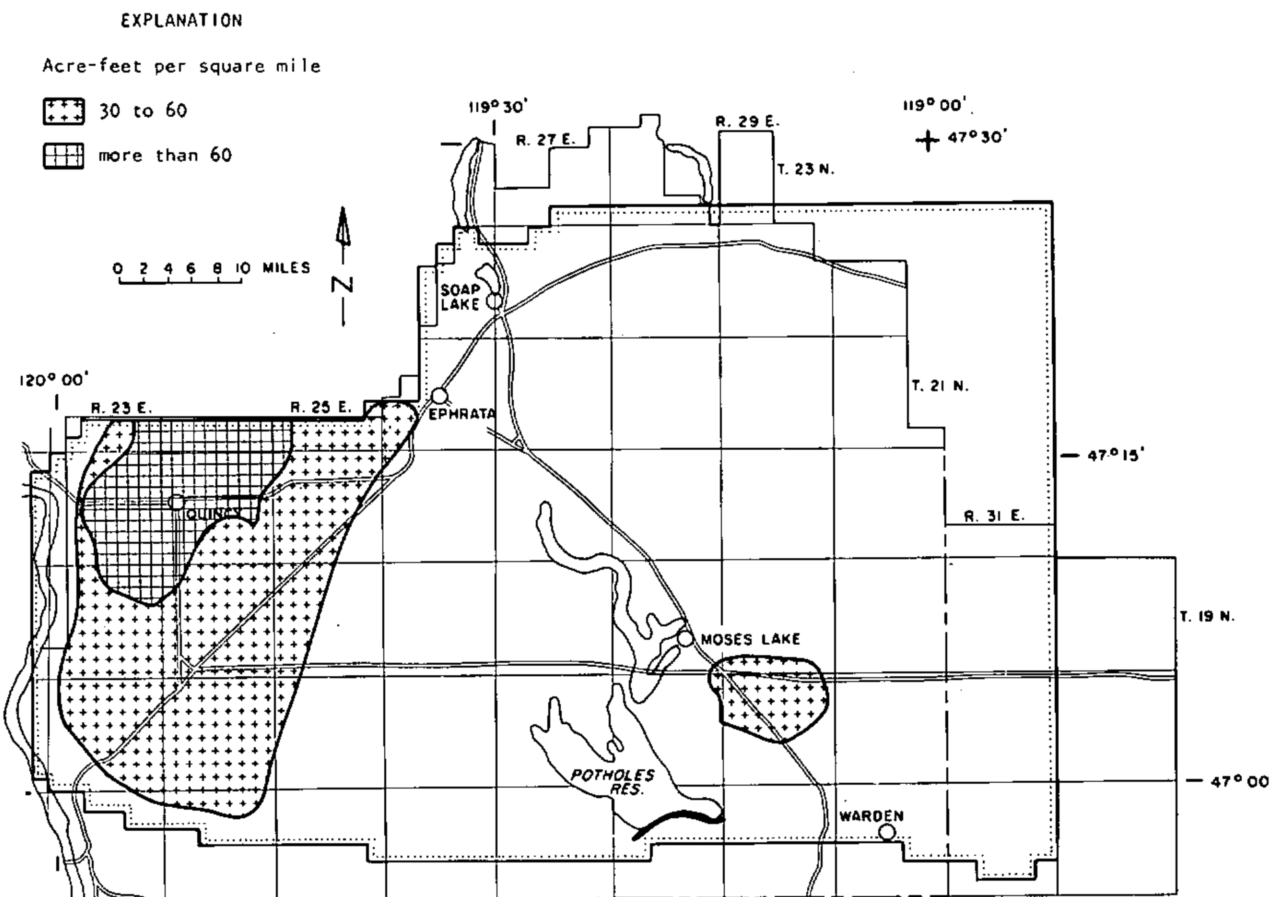

FIGURE 33.—Quantities of water added to storage in the lower aquifer of the Quincy model from 1952 to 1968.

ditions when measured and computed heads were in general agreement. Steady-state analysis verified the transmissivity of the lower aquifer and the hydraulic conductivity of the upper aquifer where saturated before irrigation. Steady-state analysis provides a representation of natural ground-water inflow and outflow from the aquifer system, including recharge from precipitation. For the Quincy model, the combined through-flow of ground water in both the upper and lower aquifers totaled about 105,000 acre-ft/yr. Recharge from precipitation was about 11,000 acre-ft/yr to both aquifers. For the Pasco model, the combined through-flow in both aquifers totaled about 29,000 acre-ft/yr. Recharge from precipitation was about 5,000 acre-ft/yr to both aquifers. For the Royal model, the through-flow of the lower aquifer totaled about 15,000 acre-ft/yr. Recharge from precipitation was about 1,500 acre-ft/yr.

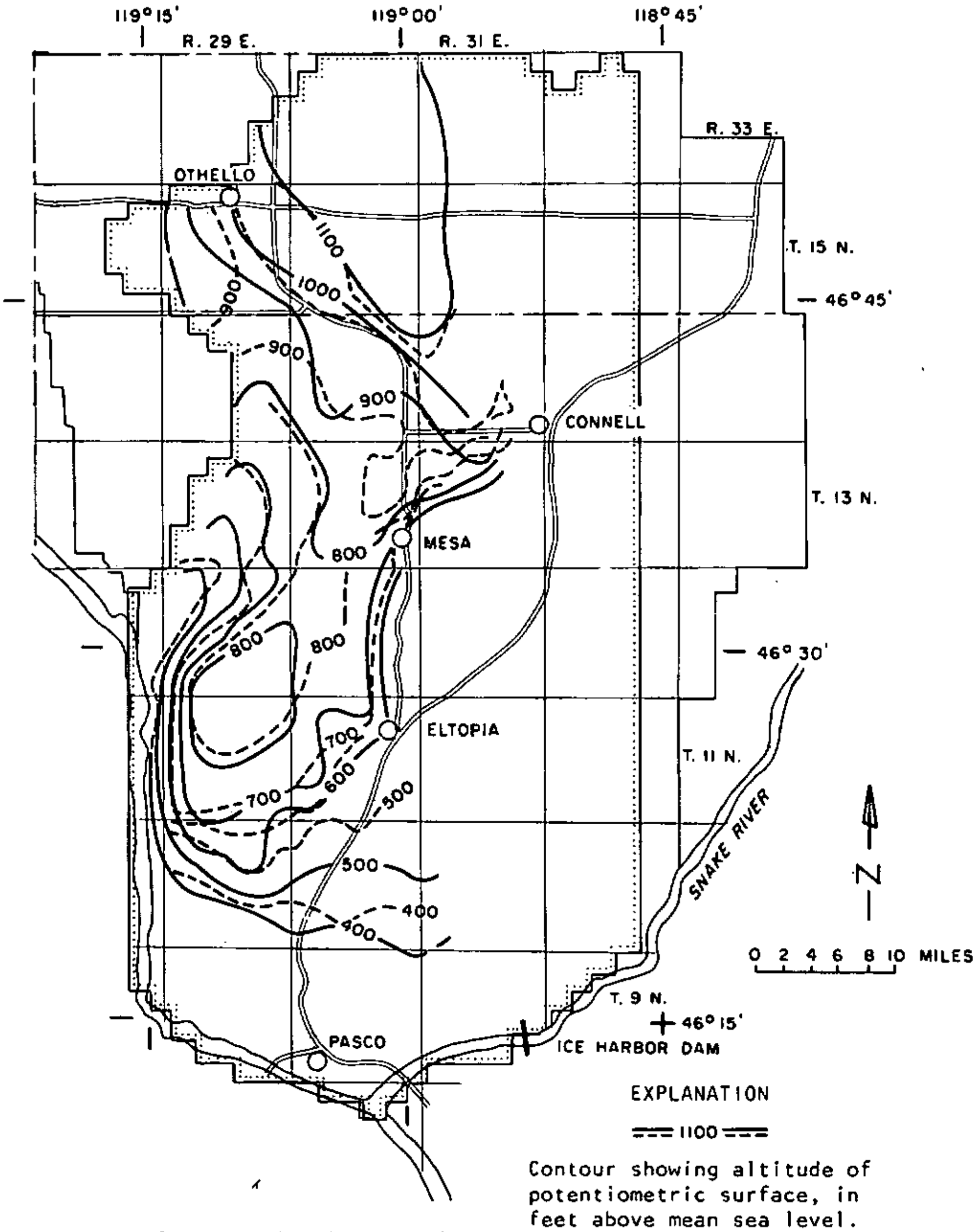

FIGURE 34.—Comparison of computed and measured contoured heads in the upper aquifer of the Pasco model in 1968.

The transient analysis simulated historical changes in water levels in the upper and lower aquifers as a result of irrigation. The storage in both aquifers and the hydraulic conductivity of the upper aquifer not verified during steady-state analysis were verified. Input parameters associated with irrigation were adjusted in the model in order to simulate contoured head maps based on measurements made in 1958, 1963, and 1968. Results of the transient analysis indicated that the cumulated storage of water between 1952-68 in the Quincy model was about 2.7 million acre-feet in the upper aquifer and about 29 thousand acre-feet in the lower aquifer; in the Pasco model it was about 3.8 million acre-feet in the upper aquifer and about 23 thousand acre-feet in the lower aquifer; in the Royal model, it was about 750 thousand acre-feet in the upper aquifer and about 14 thousand acre-feet in the lower aquifer.

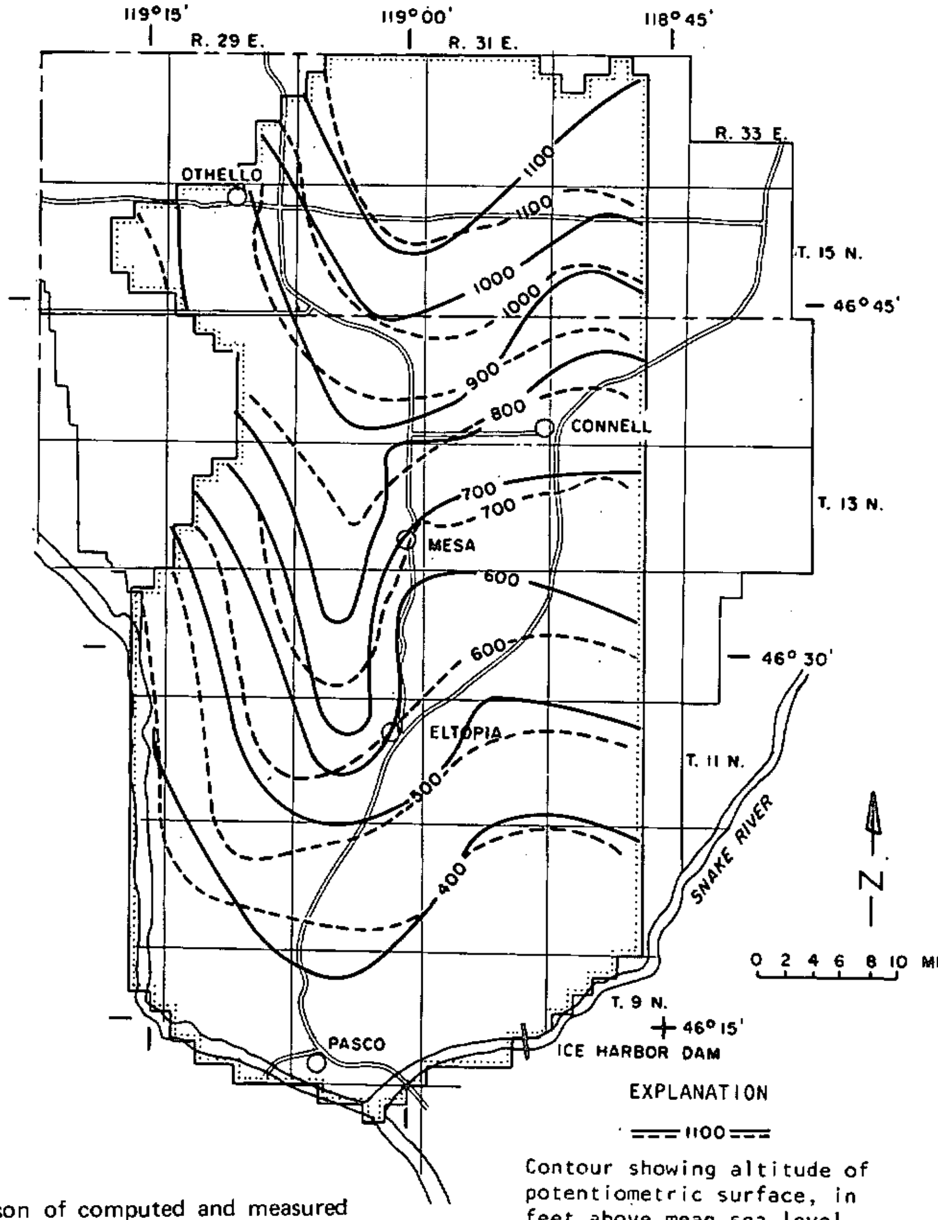

FIGURE 35.—Comparison of computed and measured contoured heads in the lower aquifer of the Pasco model in 1968.

It should be noted that a ground-water model is only as good as the data upon which it is based. A basic need during this study was for more water-level measurements from which to construct more accurate contoured-head maps. Except for parts of the Quincy Basin, the total number and distribution of reliable head measurements was not adequate for desired control in most of the project area, and good control was especially inadequate before 1952.

A valid contoured-head map based on reliable water-level measurement is important because the basic hydraulic characteristics of the model aquifer, boundary conditions, and all indeterminate hydrologic stresses imposed on the model are either determined or adjusted by simulating the head map during analyses for steady-state or transient conditions.

The real multilayered lower aquifer was simplified to a single-layered aquifer in the model. The composite

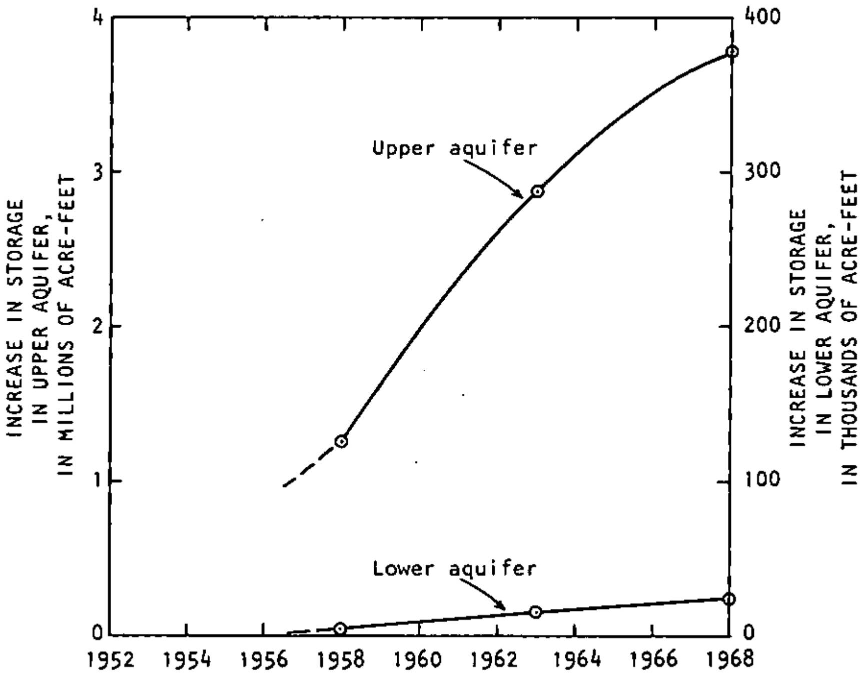

FIGURE 36.—Cumulative increases in storage of water in the upper and lower aquifers in the Pasco model, based on computations for 1958, 1963, and 1968.

head measured in the anisotropic, multilayered lower aquifer is largely controlled by the depth or number of interflow zones penetrated by the well, whereas the heads computed in the model are controlled only by the hydraulic characteristics of an isotropic, single-layered aquifer. This basic conceptual difference between the actual and modeled aquifer results in some difference between measured and computed heads in the lower aquifer.

The models were verified over a period of 16 years to respond in a manner similar to the aquifers they represent. However, because different combinations of data and aquifer characteristics would give similar solutions, model verification does not assure the uniqueness of the model data or results. Model results can be improved as more information on the physical and hydraulic characteristics of the aquifer become available and changes are made in the input data for the model.

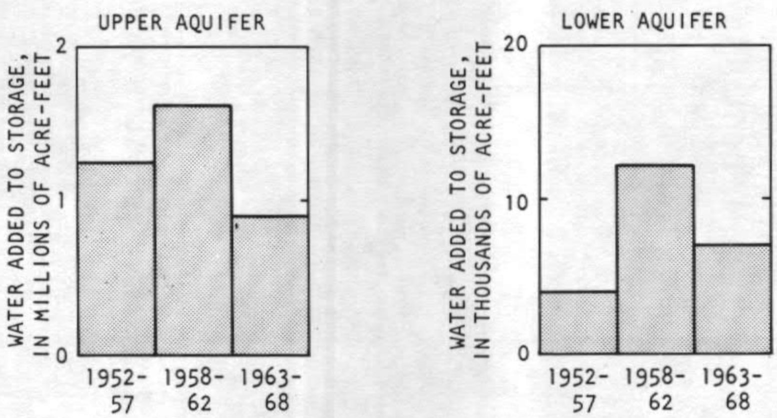

FIGURE 37.—Water added to the upper and lower aquifers of the Pasco model, during the periods 1952-58, 1958-63, and 1963-68.

The nature of the model's construction and the general deficiencies noted above preclude precise evaluation of the hydrology of any given point in the model. However, the general precision of the simulation over the 16-year period of verification strongly suggests that the interpretation and assumptions upon which the models are based is valid. The result is an effective tool for ground-water evaluation and management, with the potential for future refinement to increase accuracy when such precision may be required.

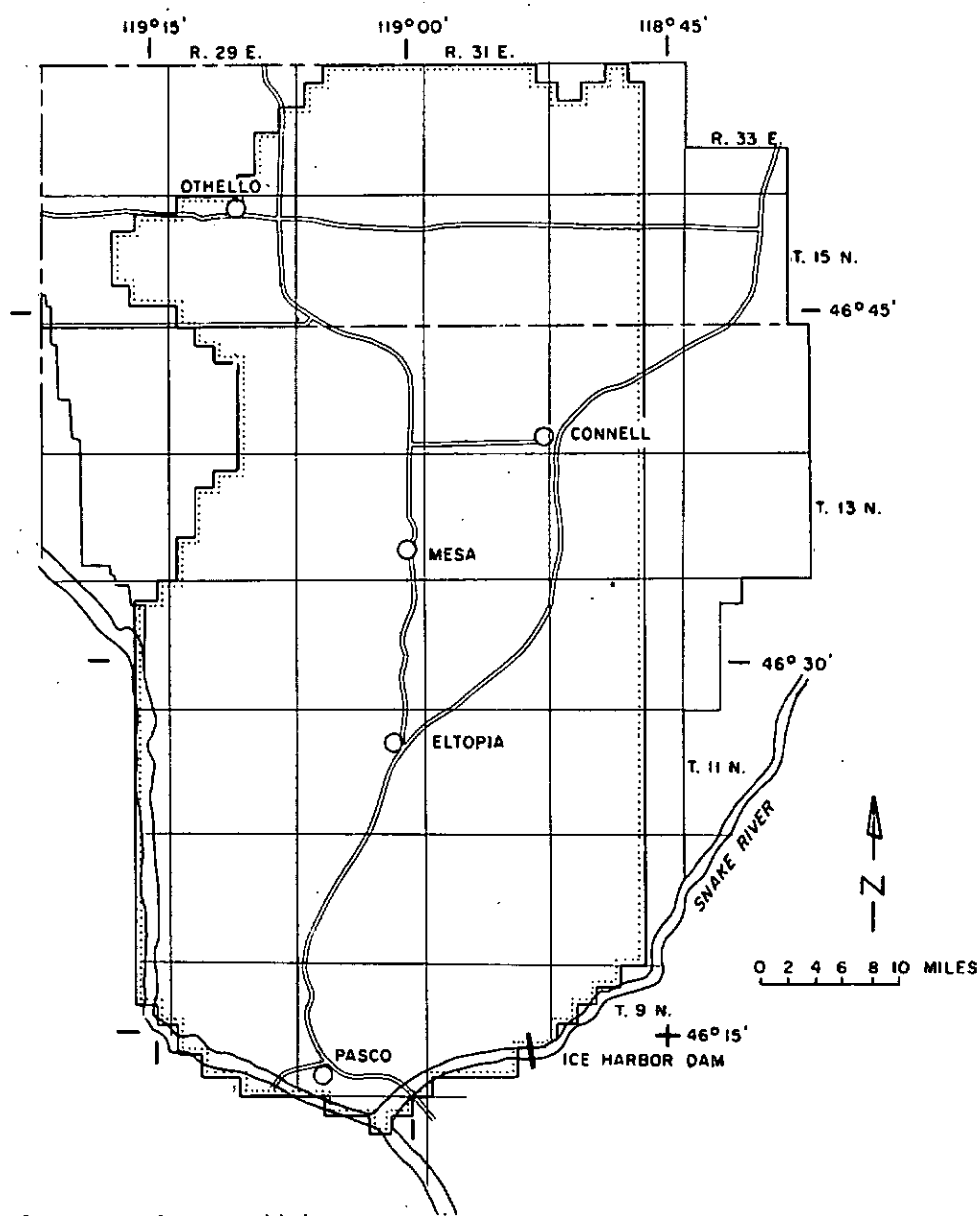

FIGURE 38.—Quantities of water added to storage in the upper aquifer of the Pasco model from 1952 to 1968.

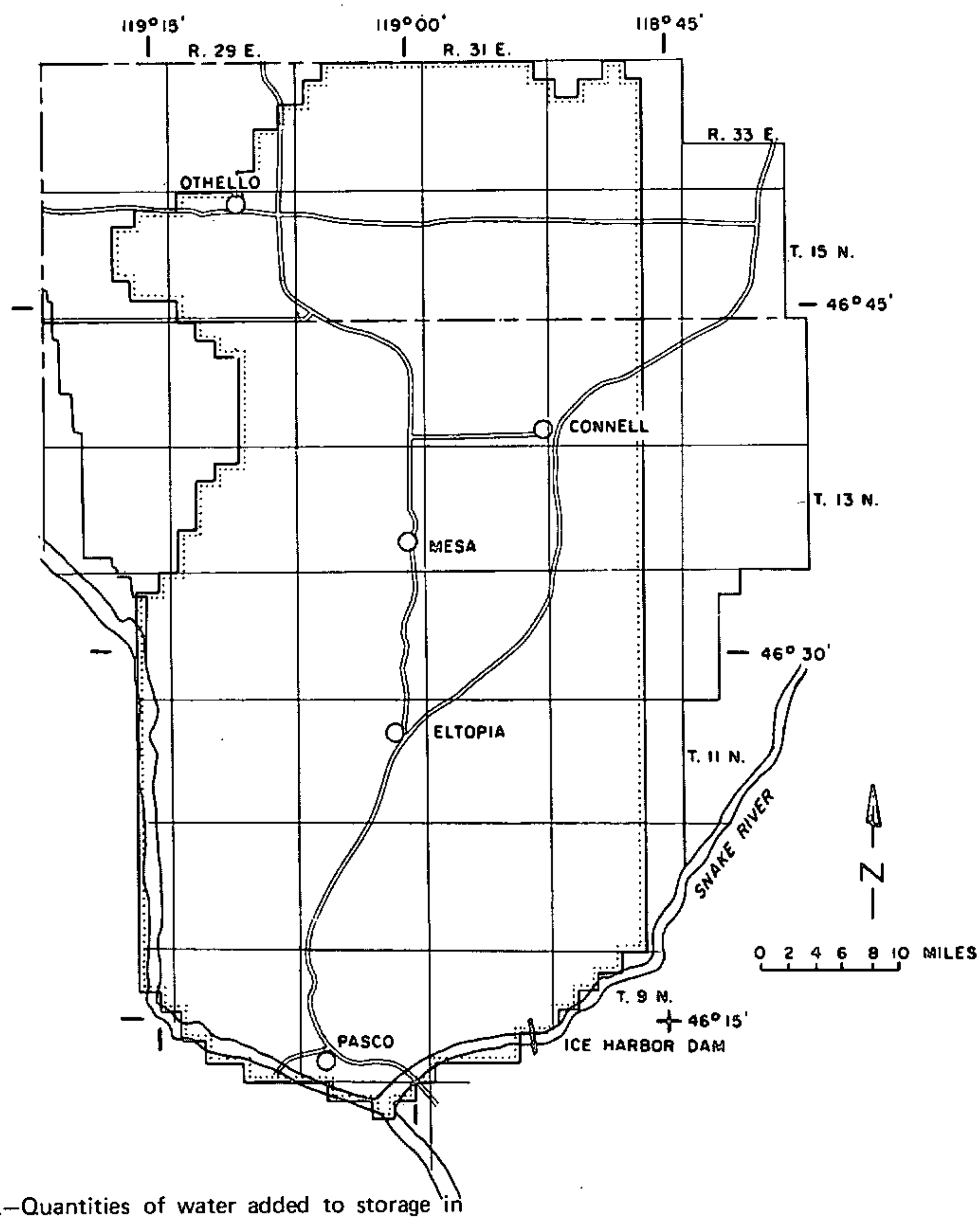

FIGURE 39.–Quantities of water added to storage in the lower aquifer of the Pasco model from 1952 to 1968.

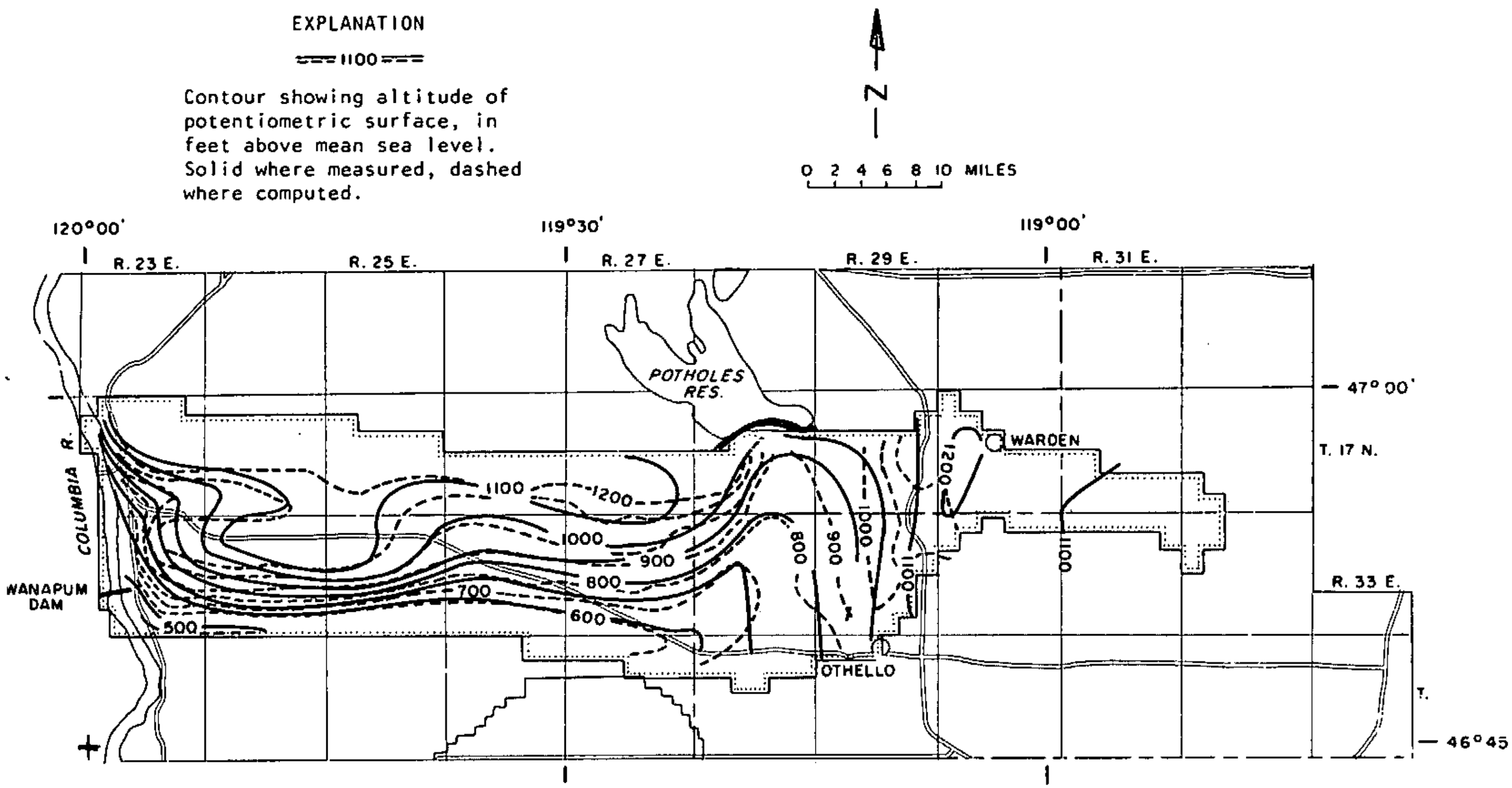

FIGURE 40.–Comparison of computed and measured contoured heads in the upper aquifer of the Royal model in 1968.

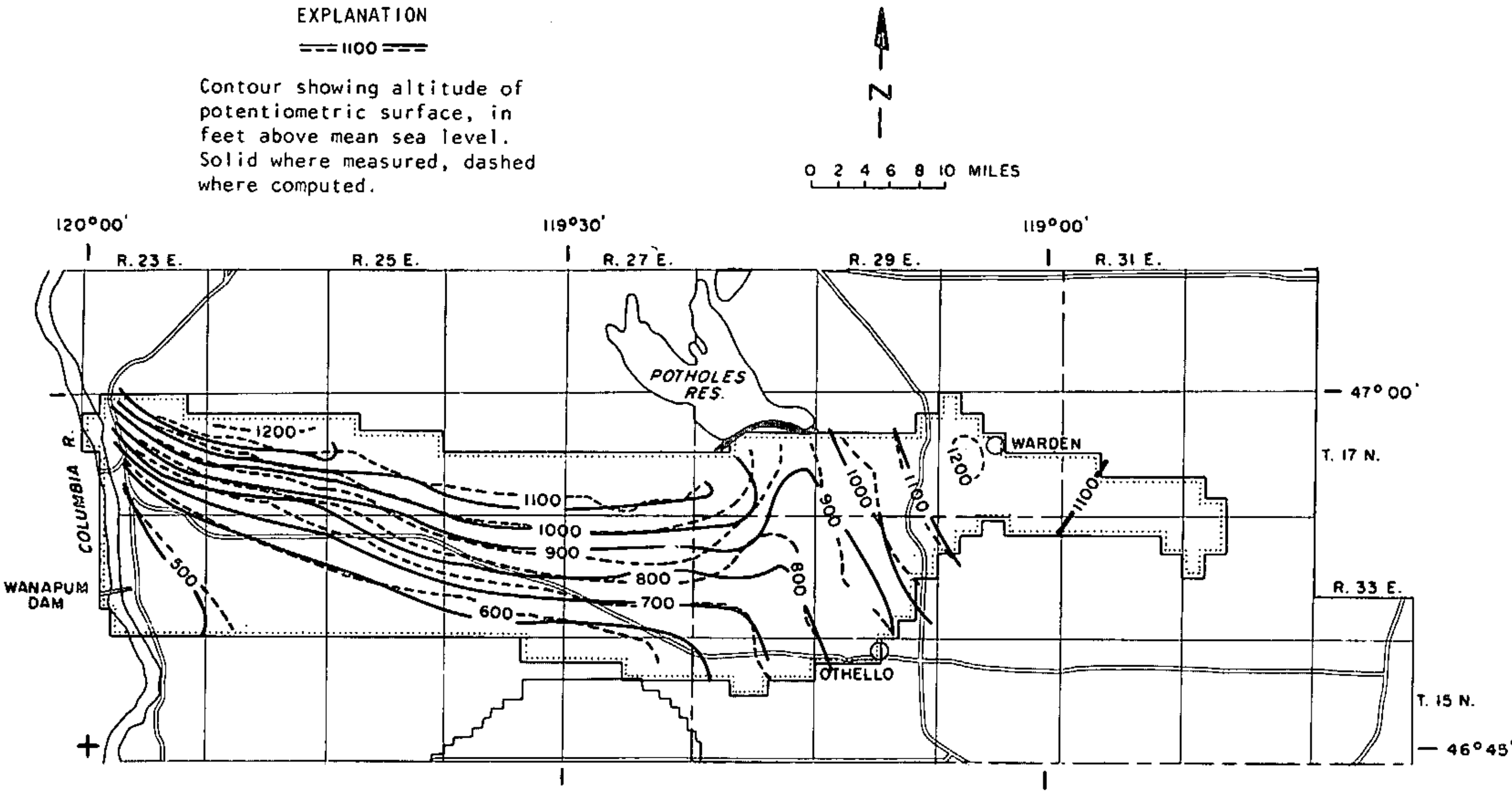

FIGURE 41.—Comparison of computed and measured heads in the lower aquifer of the Royal model in 1968.

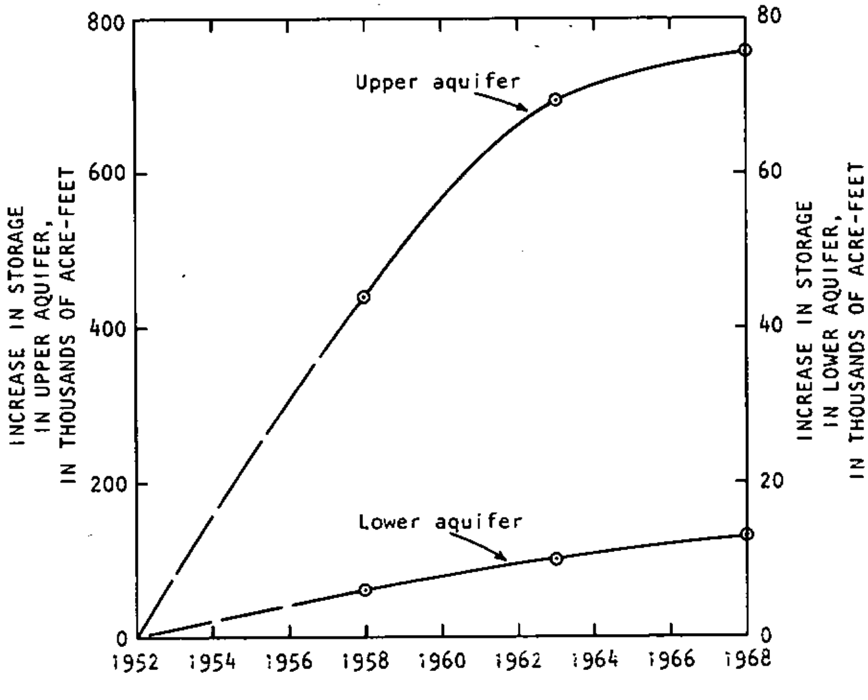

FIGURE 42.—Cumulative increase in storage of water in the upper and lower aquifers in the Royal model, based on computations for 1958, 1963, and 1968.

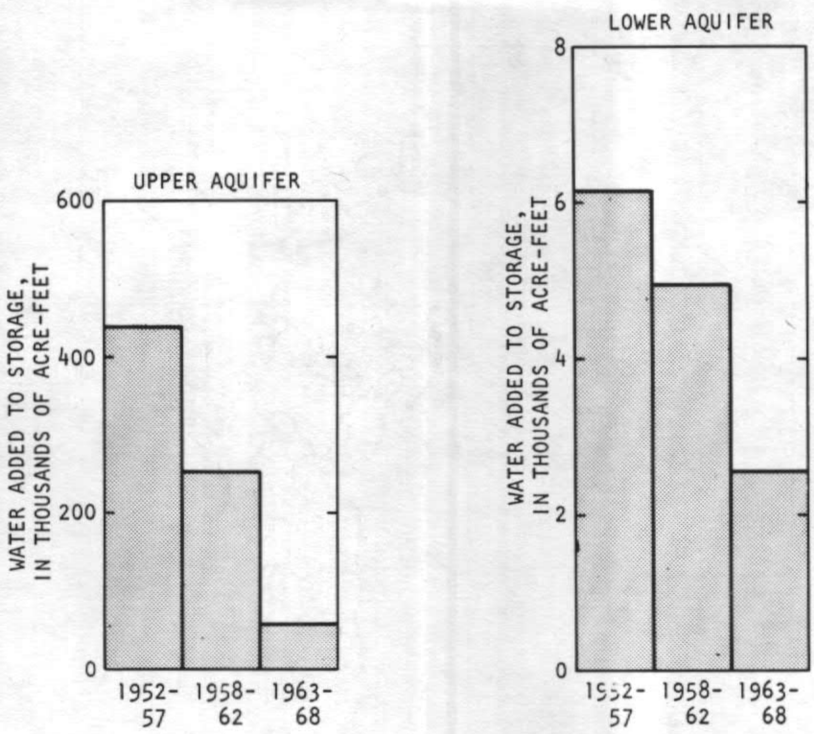

FIGURE 43.—Water added to the upper and lower aquifers of the Royal model, during the periods 1952-58, 1958-63, and 1963-68.

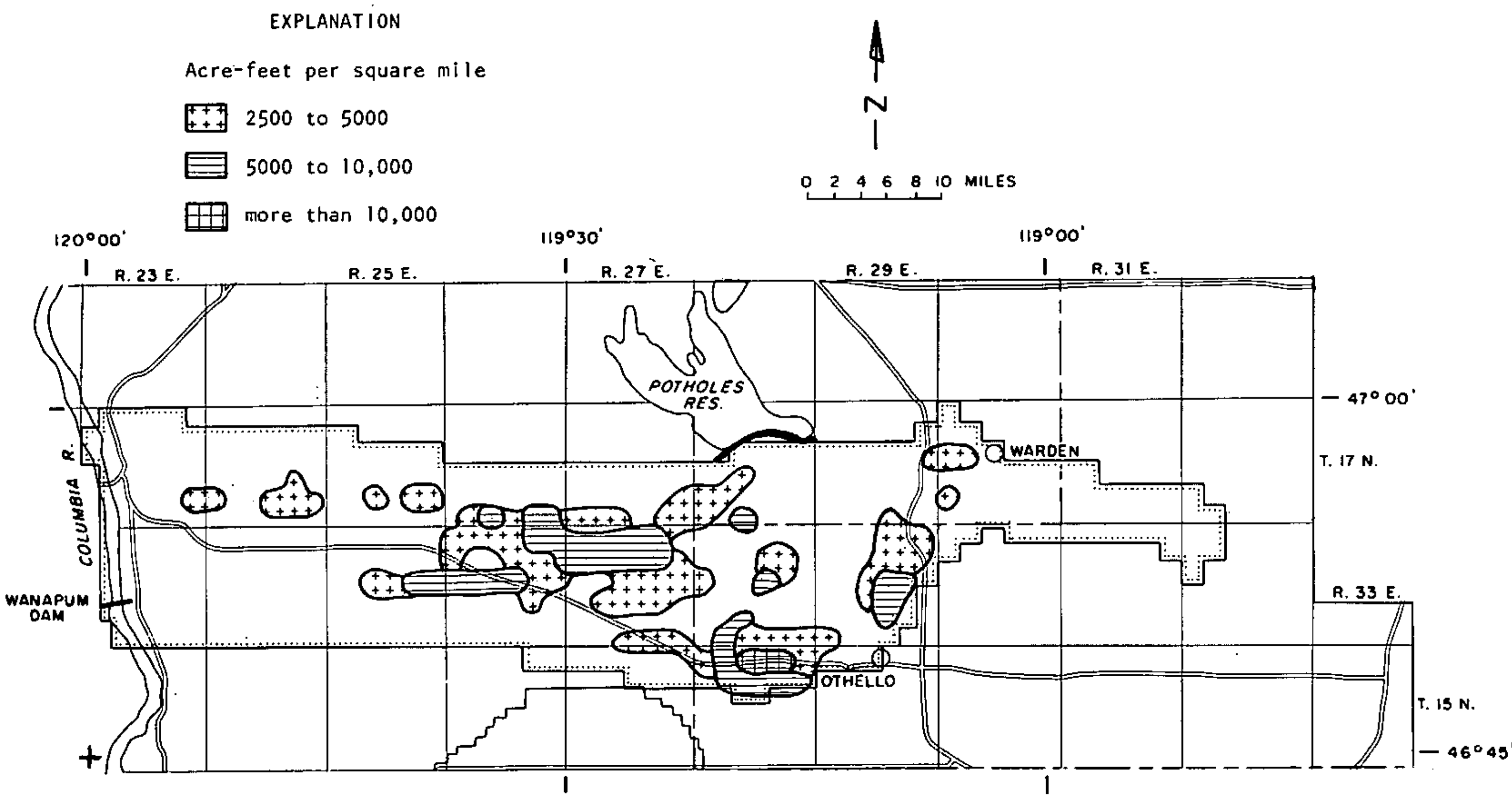

FIGURE 44.—Quantities of water added to storage in the upper aquifer of the Royal model from 1952 to 1968.

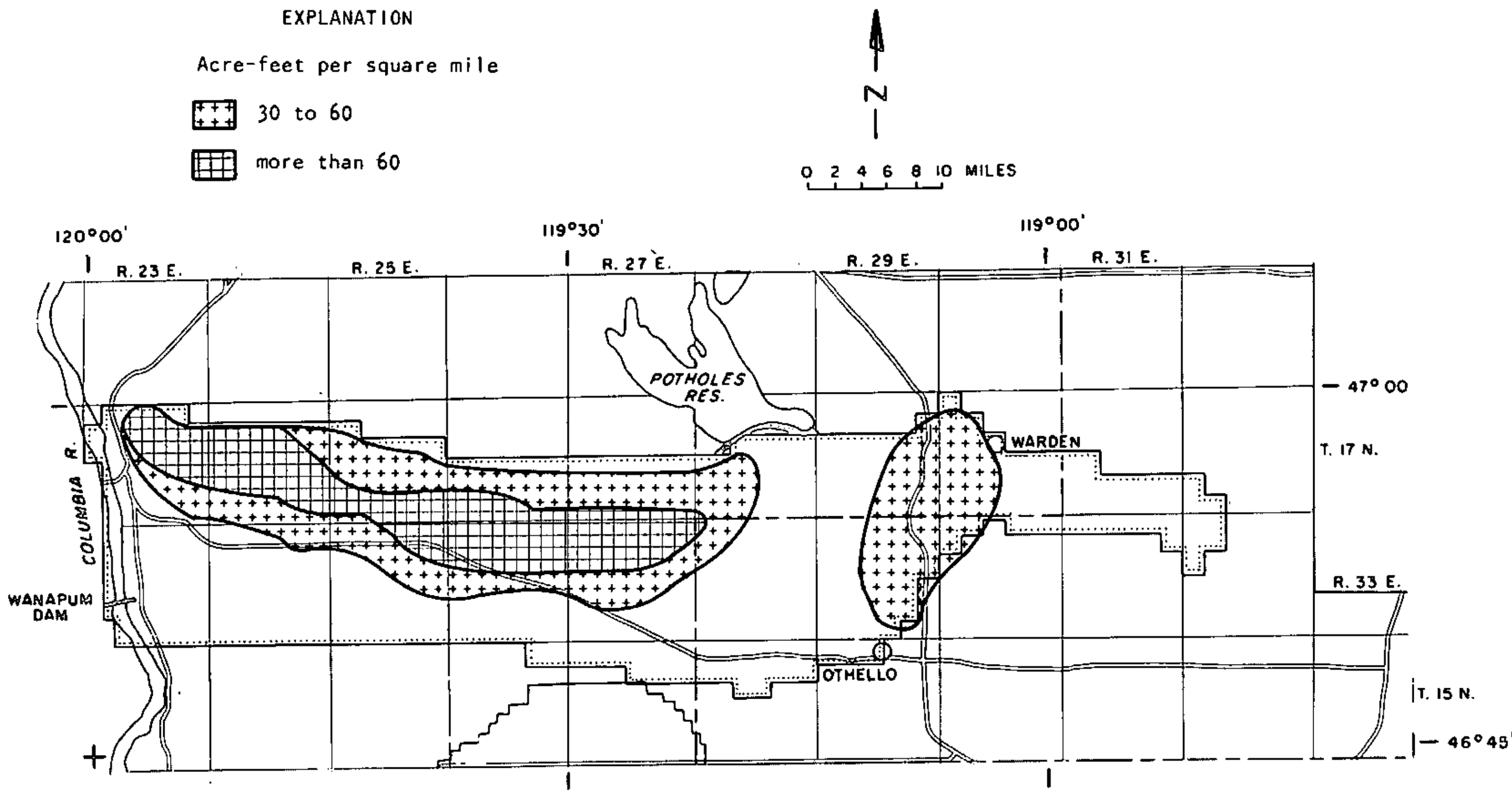

FIGURE 45.—Quantities of water added to storage in the lower aquifer of the Royal model, from 1952 to 1968.

REFERENCES CITED

Bierschenk, W.H., 1959, Aquifer characteristics and ground-water movement at Hanford: unclassified AEC Research and Development report, p. 33.

Blaney, H.F., and Criddle, W.D., 1950, Determining water requirements in irrigated areas from climatological and irrigation data: U.S. Dept. Agr. Soil Conserv. Serv. SCS-TP-96, 44 p.

Bredehoeft, J.D., and Pinder, G.F., 1970, Digital analysis of areal flow in multiaquifer ground-water systems: a quasi three-dimensional model: Water Resources Research, v. 6, No. 3, p. 883-888.

Bretz, J.H., 1930, Lake Missoula and the Spokane flood [abs.]: Geol. Soc. America Bull., v. 41, p. 92-93.

Grolier, M.J., and Bingham, J.W., 1971, Geologic map and sections of parts of Grant, Adams, and Franklin Counties, Washington: U.S. Geol. Survey Misc. Geol. Inv. Map I-589.

Kohler, M.A., Nordenson, T.J., and Baker, D.R., 1959, Evaporation maps for the United States: U.S. Weather Bur. Tech. Paper 37, 13 p.

Laird, L.B., and Walters, K.L., 1967, Municipal, industrial, and irrigation water use in Washington, 1965: U.S. Geol. Survey open-file report, 13 p.

Luzier, J.E., and Burt, R.J., 1973, Hydrology of basalt aquifers and depletion of ground water in east-central Washington: Washington Dept. Ecology Water-Supply Bull. p. (in press).

Mundorff, M.J., Reis, D.J., and Strand, J.R., 1952, Progress report on ground water in the Columbia Basin Project, Washington: U.S. Geol. Survey open-file report, 229 p.

Newcomb, R.C., Strand, J.R., and Frank, F.J., 1970, Geology and ground-water characteristics of the Hanford Reservation of the U.S. Atomic Energy Commission, Washington: U.S. Geol. Survey open-file report, 105 p.

Parker, G.G., Jr., 1971, Municipal, industrial, and irrigation water use in Washington, 1970: U.S. Geol. Survey open-file report, 21 p.

Pinder, G.F., and Bredehoeft, J.D., 1968, Application of digital computer for aquifer evaluation: Water Resources Research, v. 4, no. 5, p. 1069-1093.

Raymond, J.R., and Tillson, D.D., 1968, Evaluation of a thick basalt sequence in south-central Washington: AEC Research and Development Report, Pacific Northwest Laboratory, 120 p.

Schwennesen, A.T., and Meinzer, O.E., 1918, Ground water in Quincy Valley, Washington: U.S. Geol. Survey Water—Supply Paper 425-E, p. 131-161.

Taylor, G.C., Jr., 1941, Summary of ground-water conditions in parts of the Columbia Basin Project area with respect to development of domestic livestock water supplies: U.S. Geol. Survey open-file report, 8 p.

-------1944, Factual data pertaining to wells and springs in the Columbia Basin Project area, Washington: U.S. Geol. Survey open-file report, 85 p.

-------1948, Ground water in the Quincy Basin, Wahluke Slope, and Pasco Slope subareas of the Columbia Basin Project, Washington: U.S. Geol. Survey open-file report, 182 p.

Walters, K.L., and Grolier, M.J., 1960, Geology and ground-water resources of the Columbia Basin Project area, Washington: Washington Div. Water Resources Water-Supply Bull. 8, v. 1, 542 p.

Washington Division of Water Resources, 1955, Monthly and yearly summaries of hydrographic data: Washington Div. Water Resources Water Supply Bull. 6, 836 p.

NOTES:

NOTES:

NOTES:

NOTES: